U.PORTO

FEUP FACULDADE DE ENGENHARIA UNIVERSIDADE DO PORTO

# IMPLEMENTATION OF VISCOUS DAMPERS IN A LABORATORY STRUCTURE AIMING THE ATTENUATION OF ITS DYNAMIC RESPONSE

**ISABELLE IETKA**

Dissertation submitted for partial satisfaction of the requirements of the degree of

**MASTER IN CIVIL ENGINEERING STRUCTURES**

---

Advisor: Doctor Professor Carlos Manuel Ramos Moutinho

JULY 2020

**MASTER IN CIVIL ENGINEERING STRUCTURES 2019/2020**

DEPARTMENT OF CIVIL ENGINEERING

Tel. +351-22-508 1901

Fax +351-22-508 1446

✉ mestec@fe.up.pt

*Edited by*

FACULTY OF ENGINEERING OF UNIVERSITY OF PORTO

Rua Dr. Roberto Frias

4200-465 PORTO

Portugal

Tel. +351-22-508 1400

Fax +351-22-508 1440

✉ feup@fe.up.pt

http://www.fe.up.pt

To God.

*Whatever your task may be, put in your very best effort,*
*as something done for the Lord and not for men.*
*Colossians 3:23*

## ACKNOWLEDGMENT

First of all, I thank God for granting me the wisdom and commitment to carry out this work.

I would like to express my gratitude to my advisor Carlos Moutinho for directing me in the development of all my work, for not measuring efforts and always making himself available to all my needs in the progress of this study. Besides, I thank Professor Luis Guerreiro for the willingness to evaluate this research.

It would not be possible to elaborate this work if I did not have the people who supported me on this path by my side: my family, especially my parents Marcos and Haide.

I am also very grateful to my boyfriend, Henrique, who was always with me, giving me strength and persistence, encouraging me to do my best in all circumstances, and helping me in everything that was within his reach.

Finally, I thank my Masters teachers, for always doing their best to transmit their knowledge to us in the best possible way, making themselves available at all times to assist us during the entire academic period.

## ABSTRACT

Vibration problems in Civil Engineering structures are a current reality and must be studied. This type of disturbances which different types of buildings are submitted can have its effects mitigated through the use of vibration control systems. This study was developed on the passive systems to energy dissipation with the application of viscous dampers in structures.

The dynamic parameters of a 3-floor laboratory structure were calculated and its seismic response to seismic actions was numerically determinate, when considering both undamped and damped structure. Moreover, it was developed some comparison analysis through the determination of the seismic response of the structure following the Eurocode 8 recommendations, and comparing it to the numerical methods.

Sequentially, the framed structure was experimentally tested in a seismic table available in FEUP Structures Laboratory, by submitting it to sinusoidal actions and the same seismic actions that were initially simulated. Through these procedures, it was possible to compare the expected to the obtained results, as well as analyse the reduction of the achieved seismic response.

This study permitted to investigate that the dynamic parameters of a structure and its seismic response can be determined using different approaches, validating and comparing different methods. Besides, it was possible to numerically analyse different ways to apply damping devices in the framed structure, concluding that the installation on first and second floors provides the structure a more efficient behaviour than applying them in the three floors. Finally, the experimental dynamic tests allowed verifying the significant reduction that this type of vibration control system can provide in the seismic response of framed structures.


KEYWORDS: Vibration control systems, dynamic analysis, viscous dampers, seismic engineering, framed structures.

## RESUMO

Os problemas de vibração em estruturas de Engenharia Civil são uma realidade e necessitam ser estudados. Esse tipo de distúrbio a que diferentes tipos de construções são submetidos podem ter seus efeitos mitigados através do uso de sistemas de controlo de vibrações. Este trabalho foi realizado no contexto de sistemas passivos utilizados para dissipação de energia recorrendo a amortecedores viscosos em estruturas.

Os parâmetros dinâmicos de um pórtico estrutural laboratorial de 3 pisos foram calculados e a sua resposta a ações sísmicas foi numericamente determinada, considerando ambos os casos de estrutura não amortecida e amortecida. Além disso, foram desenvolvidas algumas análises comparativas através da determinação da resposta sísmica da estrutura, seguindo as recomendações do Eurocódigo 8, e comparando os resultados com os métodos numéricos utilizados.

Sequencialmente, o pórtico foi experimentalmente ensaiado numa mesa sísmica disponível no Laboratório de Estruturas da FEUP, submetendo-a a ações sinusoidais e ações sísmicas simuladas inicialmente. Através desses procedimentos, foi possível confrontar os resultados esperados com os obtidos, assim como analisar a redução da resposta sísmica alcançada.

Este estudo permitiu investigar que os parâmetros dinâmicos de uma estrutura e sua resposta sísmica podem ser determinados usando diferentes abordagens, validando e comparando diferentes métodos. Além disso, foi possível analisar numericamente diferentes maneiras de aplicar amortecedores na estrutura porticada, tendo-se concluido que a sua instalação no primeiro e segundo piso promovem um comportamento mais eficiente do que a aplicação nos três pisos. Finalmente, os testes experimentais dinâmicos permitiram verificar a significativa redução que esse tipo de sistema de controlo de vibração pode proporcionar à resposta sísmica de estruturas porticadas.


PALAVRAS-CHAVE: Sistemas de controlo de vibrações, análise dinâmica, amortecedores viscosos, engenharia sísmica, estruturas porticadas.

**GENERAL INDEX**

## FIGURES INDEX

## GRAPHICS INDEX

## TABLES INDEX

# 1

# INTRODUCTION

## 1.1 OBJECTIVES AND FRAMEWORK

Civil Engineering Structures may be submitted to several vibration problems. These situations may be divided in two principal categories: service problems and structural problems.

When the structural integrity is not concern, vibrations may become an adverse factor (in terms of human comfort, for example). In this category, there are several problems related to flexible slabs in habitation buildings, or industry, pedestrian and road bridges, among others.

On the other hand, the structural problems involve the concern with structural damage on buildings. This field is significantly connected to Wind Engineering and Seismic Engineering.

In many of these situations, the use of damping systems can greatly attenuate the vibrations, where the viscous dampers are a very used solution (and convenient for its simplicity). However, there are not many experimental works in this field, although the theory fundaments are well defined.

In this contest, the objectives of this work are:

- Describe the vibrations problems on structures and characterize practical cases of implementation of damping systems on structures;
- Identify the role of damping systems, especially the viscous ones, on the solutions of these problems;
- Study the analytic methods of damping design to introduce in a structure;
- Develop numerical simulations of different scenarios of seismic reinforcement;
- Experimentally characterize the different types of viscous dampers;
- Experimentally implement, in a medium size laboratorial building, one of the proposed solutions of viscous dampers and analyze the attenuation of its response. Furthermore, perform the comparison of the experimental results with the previous numerical ones.

## 1.2 ORGANIZATION OF THE THESIS

This document is divided in seven distinct chapters.

Initially, the main objectives of the work and its framework are summarized in the first chapter. In the second part, the most important vibration problems in structures are listed and explained, followed by the exposition of some of the most common vibration control systems. Also, on chapter 2, there is a description of the seismic simulations developed in this work, by the explanation of the available seismic table in terms of characteristics and dimensions.

The third chapter is composed of the analysis of dynamic systems, through the description of the damping calculation methodology of a framed structure. Initially, the characterization of the structure is described, in terms of the determination of mass, stiffness, natural frequencies and vibration modes. Then, the classical and non-classical damping matrixes determination methods are also explained. At the end of this section, the methods of determination of the modal damping are explained through the State Space Formulations and the Simplified Formulations used in FEMA 365 Code.

An application of the methodology presented on chapter 3 is developed on the next chapter. The fourth chapter consists of the study of a 3-floor laboratory structure, by the determination of all its dynamic parameters and modal damping matrixes. Moreover, in this section it is developed some simulations of the installation of different types of damping devices on the structure, with the determination of the modal damping factor of each case. Finally, it is also calculated the necessary damping coefficients that may be installed on the structure aiming to achieve different levels of damping factors.

In chapter 5, the seismic response of the structure is determinate through the comparison of the results between the State Space Formulation and the Eurocode 8 recommendations. In addition, the response determination was calculated based on non-classical methodologies and compared to the results of classical procedures.

Posteriorly, in the sixth chapter are presented the experimental results of some tests developed in FEUP Structure's Laboratory. These tests are divided into the dampers characterization and the dynamic tests. In this last case, the structure was submitted to random excitation tests, free vibration and seismic tests.

Finally, in chapter 7 the conclusions of this work are described.

# 2

# STATE-OF-THE-ART

## 2.1 VIBRATION PROBLEMS IN STRUCTURES

Many structures suffer from unwanted vibrations and, although careful analysis at the design stage can minimize these events, the vibration levels of many structures are excessive. Thus, the study of dynamic actions on Civil Engineering structures had become very significant and essential. Vibration induced by people, machinery-induced vibrations, wind and seism-induced vibrations, and vibration induced by traffic and construction activity can summarize the main source of vibration problems studied on structural design [16].

Vibrations caused by human body motions can significantly affect the structure by influencing its serviceability and its safety. Actions as walking, running, jumping, dancing (among others) are motions of great importance that can definitely influence the conduct of the structure when submitted to them, especially regarding pedestrian bridges, floors with walking people, floors for sports or dance activities and spectator galleries, for example.

Machinery equipment permanently fixed in structures may cause vibration problems. These equipments may cause effects that can be divided in direct and indirect dynamic effects. The first consists of effects on equipment and people in its proximity, on the other hand effects on the structure to which the machinery is attached, as well as the foundation it stands on. The indirect effects are related to the transmission of vibrations through foundations into other buildings and people living in them, or by propagating waves leading to structure-borne acoustic waves.

Basically, no civil engineering structure is safe from wind loading effects. Of critical importance are the non-stationary characteristics of wind and the dynamic proprieties of the structure exposed to [16]. This forced vibration can be caused in the wind direction due to gust actions (turbulence effects) and buffeting, or in the across-wind direction as vortex shedding (without “lock-in” effect). Besides, they can also be exposed to across-wind self-induced vibrations (aeroelasticity) due to vortex shedding (“lock in” effect), galloping and flutter (bridge flutter).

Besides, the structures can be submitted to seismic actions, which is one of the main topics studied in this work. The design process and considerations that must be taken for earthquake effects are very distinct and different from the calculations for wind forces. In earthquake design, the study elapses

regarding the random motion of the ground at the base of the structure, and this motion induces stresses caused by inertia forces.

There is also the vibrations induced by road and railway traffic. This type of loading can affect the serviceability of structures, while it can rarely cause problems related to structural safety. An example of the impact of traffic is when a heavy vehicle hits an irregularity in a road surface causing an impact load that generates significant vibrations.

All of the described vibration problems may be attenuated by implementing solutions to mitigate its consequences. In this work, it will be presented some alternatives to reduce the seismic response of a structure when submitted to this type of action, by using systems of structural control that can influence the building in different ways, as will be explained on the next chapter.

## 2.2 VIBRATION CONTROL SYSTEMS

The consequences due to seismic phenomenon can be catastrophic, causing loss of human lives and property. Unfortunately, it is not possible to avoid its occurrence, but currently the technologic development and the scientific advances in seismic engineering allow the mitigation of its effects [1]. Due to this preoccupation, the vibration control systems have been increasingly used in Civil Engineering structures.

The seismic behavior of structures can be improved through seismic protection systems by two distinct ways: the alteration of dynamic characteristics of the structure itself, or the increase of the structure's energy dissipation capacity.

The vibration control can be produced by techniques of passive, active or semi-active control systems (see Table 1). Besides that, there is the hybrid control technique, which results of an adequate combination of these techniques, where the most used is the combination of active or semi-active control with passive control [3].

Table 1 – Different types of vibration structural control, adapted from [12]

| | | | |
|---|---|---|---|
| Structural Control | · Passive | · Energy Absorbers | · Tuned Mass Dampers ("TMDs")<br>· Tunes Liquid Dampers ("TLDs") |
| | | · Energy Dissipation | · Viscous dampers<br>· Visco-elastic dampers<br>· Friction dampers<br>· Hysteretic dampers |
| | | · Energy Isolation | · Base isolation |
| | · Active | · Active mass dampers<br>· Active cables<br>· Active diagonals | |

- · Piezoelectric actuators
- · Semi-Active
  - · Variable stiffness devices
  - · Variable friction dampers
  - · Variable orifice viscous dampers
  - · Variable viscosity dampers
- · Hybrid

In Civil Engineering, the development and implementation of specific control system devices integrated on building structures started only from de 70's decade. Aiming to improve the process of energy dissipation inducted by the earthquake actions, on this decade the first applications of passive control using different types of dampers adapted to framed buildings has emerged. In fact, these devices work as local dissipation elements, relieving the sections of structural elements that singly perform this function through its resistance and ductility exploration [3].

Passive devices are the most implanted in Civil Engineering, particularly in Seismic Engineering. Passive control systems are defined by the utilization of devices that do not need any external energy source to promote the control action. For many reasons, it is important to always consider the use of passive systems in the implementation of any vibration control system. These devices promote a more interesting solution in terms of reliability, cost and maintenance. Moreover, they are prepared to deal with elevated amplitude forces and present a high capacity to dissipate energy [3].

In this work, the study will be developed around the application of fluid viscous dampers on framed structures, as in this chapter the focus will be on discussion and presentation of passive energy dissipation damper's use on Civil Engineering buildings. These devices are a great solution of rehabilitation because they can be installed on existing structures and have a reduced maintenance cost too. However, they present a disadvantage related to its only operation when the structure is already affected by the vibrations, not preventing its initial movement. The viscous dampers are devices where a damping force is generated in function of the relative or absolute velocity, depending on its assembly (they can be interposed between two spots of the structure or fixed on the exterior). They lead to simplified calculus and a very acceptable operation on most part of the cases that they are applied [2].

Originally developed for mechanical applications, fluid viscous dampers have successfully transitioned to the Civil Engineering community for use in protecting buildings, bridges and other structures worldwide. Fluid viscous dampers, or seismic dampers as they are sometimes referred to, are hydraulic devices that, when stroked, dissipate the energy placed on a structure by seismic or wind events. The concept is simple – the viscous dampers convert the kinetic energy of the structural movement into heat and then dissipate that energy into the air, thereby obeying the laws of physics through the conservation of energy [13]. On the presence of a seismic event and considering the deformability of the structure, the damper piston is pushed into the cylinder (where a compressible silicone fluid is found), and its displacement is done through small orifices in the piston head (see Figure 1), when the compression force is equal on both sides [8].

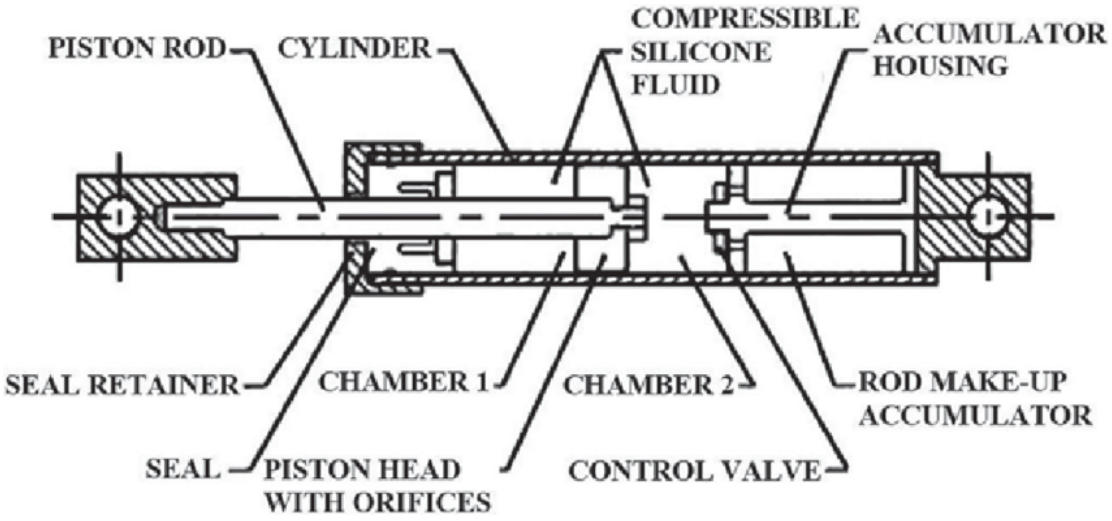


Figure 1 – A typical fluid viscous damper manufactured by Taylor Devices, Inc [20]

One example of application of fluid viscous dampers in buildings is the San Bernardino Justice Center (SBJC), built in San Bernardino County, California, which is one of the tallest seismically base-isolated buildings in the United States [14]. The devices installed on this structure absorb a significant amount of seismic energy, further reducing the story drift demands in the superstructure.

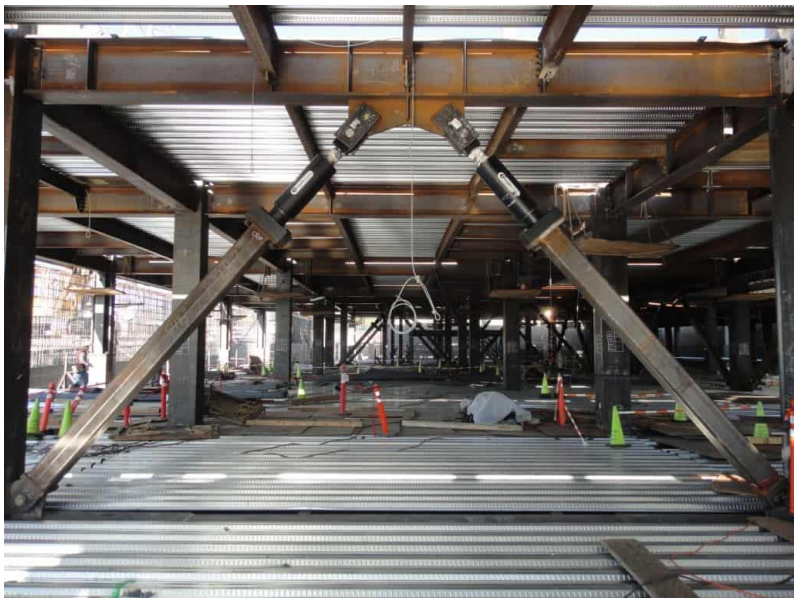

Figure 2 - Application of fluid viscous dampers on buildings: San Bernardino Justice Center (SBJC) – California, USA [13].

Another example is the Millennium London Footbridge, where a total of 37 viscous dampers were installed in order to remove the lateral vibrations of the bridge caused by sideways pedestrian loads exerted in the following way [15].

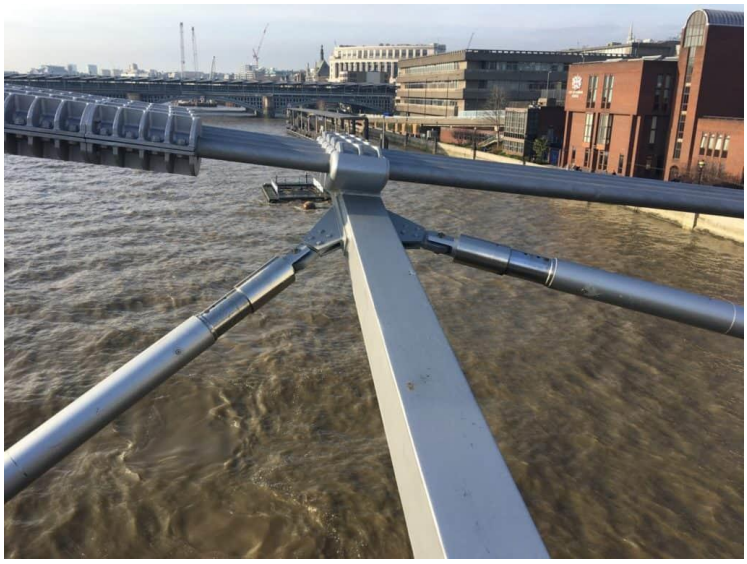

Figure 3 - Application of fluid viscous dampers on structures: Millennium London Footbridge [13].

## 2.3 SEISMIC SIMULATIONS IN SHAKING TABLES

Due to the frequent presence of seismic action on the design of Civil Engineering structures, the interest on studying its origin and caused damages arises. As human lives cannot be lost due to design mistakes, these researches intensify to make possible the attenuation of damages and allow the security of users.

The seismic tables provide the simulation of behavior of a seism and transmit it to the structure, where it is possible to analyze many parameters on study and perform tests on real structures. FEUP's seismic table is located on the Structure's Laboratory of the faculty, presents dimensions of 3.0 x 3.0 m² and a distance between the columns' fixation axis of 2.10, in both directions.

Referring to number of degrees of freedom, this table offers two degrees: the transversal and longitudinal movements of its deck. Besides, it allows the future installation of an additional axis that will provide one more degree of freedom in the vertical direction (only in one module of the table). For each one of the operating axis, there is a actuator that works separately and permits a simultaneous action of both axis. The maximum length of movement on each direction is 400mm and this allows significant displacements on the supported structure.


Figure 4 – Dynamic actuator for moving the seismic table

Regarding the system that induces the movement of the table, this consists of one Electro-Mechanical Cylinder (EMC) with a capacity of moving 3 tonnes (30 kN) on each axis. Each degree of freedom is connected to an independent EMC.

It is important to mention that the table was designed to provide a very high stiffness, and ensure a support the most closer of reality of a perfect fixed support. This structure presents regularity and symmetry on its design, aiming that different alternatives could be possible, from the assemblage of the framed on study to the assemblage of each attenuator.

Figure 5 – FEUP's seismic table.

The technical definitions of the seismic table are listed in Table 2.

Table 2 - Technical definitions of the seismic table – Adapted from [8].

| **Area** | **Mass capacity** | **Degrees of Freedom** | **Maximum Displacements / Velocities / Accelerations** | | **Frequency** |
|---|---|---|---|---|---|
| | | | x | y | |
| **3.0 x 3.0 m²** | 20 tonnes | 2 | 400 mm | - | 0 – 50 Hz (approximated) |
| | | | 0.37 m/s | - | |
| | | | 10 m/s² | - | |

# 3

# DAMPING CALCULATION METHODOLOGY

## 3.1 CHARACTERIZATION OF STRUCTURAL DYNAMIC PARAMETERS

The Vibration Modes of the system, the Natural Frequencies of each vibration mode and the respective Damping Coefficients define the dynamic parameters of a structure.

To know these parameters, it is essential to determine and verify the physical proprieties of the structure, such as mass, stiffness and natural damping. In this work, the study will be about a laboratory framed structure, comparing the results for the parameters when considering the structure with a flexible beams numerical model and a rigid beams numerical model**.**

In this chapter, there will be explained the methodology to obtain the dynamic parameters of an "n" degrees of freedom structure, where it is considerated one DOF per floor (thus, "n" also is the number of floors). In this work, the first degree of freedom is considered associated to the floor closest to the ground, and the "n"th DOF, to the last floor. It is relevant to consider that the studied structure has three floors, four columns and four beams on each floor.

### 3.1.1 MASS MATRIX DETERMINATION

As represented in the Figure 6, the calculation model of mass and stiffness matrix can be processed by the analysis of a mechanical system. Through this analysis, each degree of freedom is influenced only by its mass, and for this reason, the mass matrix is a diagonal matrix, where each value corresponds to the mass of each floor [6].

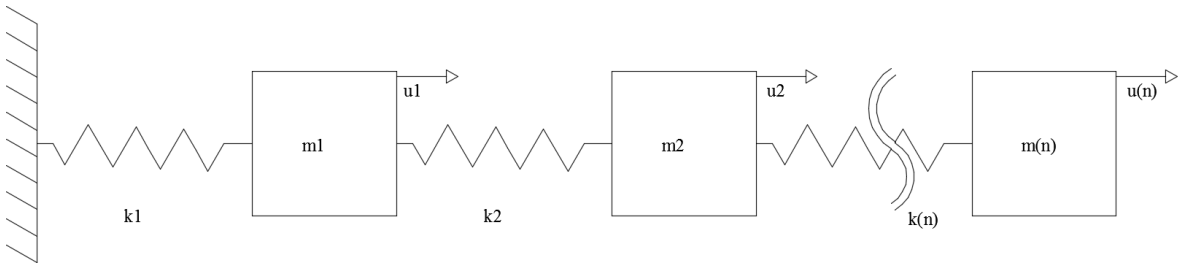


Figure 6 - Mechanical system with "n" DOF

Thus, the mass matrix has the following configuration:

$$M = \begin{bmatrix} m_1 & 0 & \cdots & 0 & 0 \\ 0 & m_2 & \cdots & 0 & 0 \\ \vdots & \vdots & \ddots & \vdots & \vdots \\ 0 & 0 & \ldots & m_{n-1} & 0 \\ 0 & 0 & \ldots & 0 & m_n \end{bmatrix} \quad (3.\ 1)$$

### 3.1.2 Stiffness Matrix Determination

The physical meaning of the stiffness coefficients represent the forces developed in the structure when a unit displacement corresponding to one degree of freedom is introduced and no other nodal displacements are permitted. They are numerally equal to the applied forces required to maintain the specified displacement condition [4].

In a structure design, it is ideal to consider that the connections between beams and columns are infinitely rigid and the rotation on the "beam-column" connections are not allowed or they can be considered ideally flexible, with a perfect hinge connection. The first one implies in a constant angle of the beam-column connection, but in the second case, this angle may vary, considering the technical features of the beam.

#### 3.1.2.1 Flexible beams Structure

When considering a flexible beams structure, the method adopted to determine the stiffness matrix is the Direct Method, by considering only the displacements on the considered floor (one displacement per floor) and applying on the structure a displacement set where one of them is unitary and the others, null [6]. This methodology can be observed in Figure 7, as an example, where it is presented the deformed shape resulted by a unitary displacement of the second floor (direction $\Delta_2$).

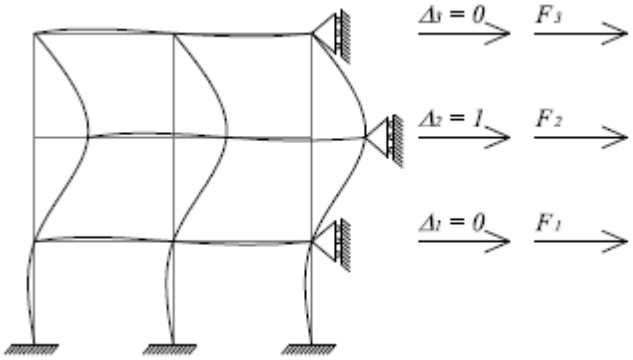


Figure 7 - Deformed shape by a unitary displacement on the 2nd floor [7]

The stiffness matrix is represented by de values "kij", where "i" represents the local in cause and "j" the local where the unitary displacement is applied. For example, "k12" means the force in the DOF 1 due to the displacement applied in the DOF 2. This matrix can be visualized below:

$$K = \begin{bmatrix} k_{i,i} & k_{i,j} & \cdots & \cdots & k_{i,n} \\ k_{j,i} & k_{j,j} & \cdots & \cdots & k_{j,n} \\ \vdots & \vdots & \ddots & \vdots & \vdots \\ \vdots & \vdots & \cdots & k_{n-1,n-1} & k_{n-1,n} \\ k_{n,i} & k_{j,n} & \cdots & k_{n,n-1} & k_{n,n} \end{bmatrix} \quad (3.\ 2)$$

These coefficients are positive when the direction of the applied force corresponds to a positive displacement and negative otherwise. Thereby, if a unitary displacement is applied in the last DOF (last floor), there is a positive force (with its value equal to its stiffness) in this DOF, and another negative force in the DOF below. If there is a unitary displacement applied in a DOF at a middle floor of the frame, there will be a positive force applied in this DOF (with its value equal to the sum of the stiffness of the two adjacent floors to the DOF), and two negative forces (one on the top due to the stiffness of the upper columns, and one below due to the stiffness of the bottom columns).

#### 3.1.2.2 Rigid Floor Structure

It is known that a column stiffness is significantly influenced by its base fixity [5]. In this section, the frame that will be studied can be considered with all columns connections fixed, as the beams are considered infinitely rigid and the rotation on the "beam-column" connections are not allowed. Thus, the stiffness coefficient can be written by:

$$k = \frac{12EI}{L^3} \quad (3.\ 3)$$

As the flexible beams method explained before, the coefficients are determined by applying a unitary displacement on each floor of the structure. However, now it will be considered that non-adjacent floors will not be deformed, as illustrated on Figure 8, and these stiffness coefficients on the matrix will be equal to zero. Consequently, the only values that will appear on the stiffness matrix are $k_1, k_2, \dots, k_n$, where $k_n$ is the stiffness of the column placed on the "n"th floor, calculated as explained in Equation 3.3.

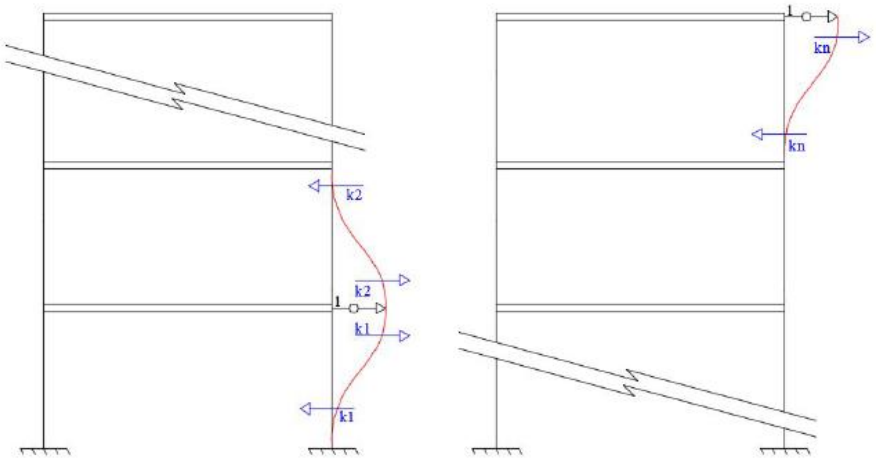


Figure 8 - Structure scheme to consider the stiffness on each DOF [8]

Accordingly, the stiffness matrix when considering a rigid floor structure, based in Equation 3.2**,** results in

$$K = \begin{bmatrix} k_1 & -k_1 & 0 & \cdots & 0 \\ -k_1 & k_1 + k_2 & \ldots & \ddots & \vdots \\ 0 & -k_2 & \ddots & -k_{n-2} & 0 \\ \vdots & \ddots & \ldots & k_{n-2} + k_{n-1} & -k_{n-1} \\ 0 & \ldots & 0 & -k_{n-1} & k_{n-1} + k_n \end{bmatrix} \quad (3.\ 4)$$

### 3.1.3 VIBRATION FREQUENCIES AND MODES CALCULATION

The vibration analysis consists of determining the conditions under which the equilibrium condition, considering a freely vibration undamped system:

$$M\ddot{\mathbf{v}} + C\dot{\mathbf{v}} + K\mathbf{v} = 0 \quad (3.\ 5)$$

In which 0 is a zero vector, C is the damping matrix that can be omitted for now, v are the displacements, $\dot{\mathbf{v}}$ are the velocity and $\ddot{\mathbf{v}}$, the accelerations in free vibration. Through some mathematic manipulations that can be verified in previously works [4], it can be affirmed that the finite-amplitude of free vibration are possible only when

$$\det\ (K - M \cdot \omega^2) = 0 \quad (3.\ 6)$$

Resolving this equation will give an algebraic equation of the Nth degree in the frequency parameter $\boldsymbol{\omega}$ for a system having N degrees of freedom. The N roots of this equation $(\boldsymbol{\omega_1}, \boldsymbol{\omega_2} \ldots, \boldsymbol{\omega_N})$ represent the frequencies of the N modes of vibration which are possible in the system. The vibration with the lowest frequency is called the first mode, the next higher frequency is the second mode, etc. The vector made up of the entire set of modal frequencies, arranged in sequence, will be called the frequency vector:

$$\omega = \begin{bmatrix} \omega_1 \\ \omega_2 \\ \vdots \\ \omega_{N-1} \\ \omega_N \end{bmatrix} \tag{3. 7}$$

$$f = \frac{\omega}{2\pi} \tag{3. 8}$$

Subsequently, when the natural frequencies $\boldsymbol{\omega}$ are determined, the natural modes of vibration ($\phi_N$) of each mode can be known by solving the equation above:

$$(K - M \cdot {\omega_N}^2) \cdot \phi_N = 0 \tag{3. 9}$$

The vector $\phi_N$ will be a "N" value vector:

$$\phi_N = \begin{bmatrix} \phi_{1,N} \\ \phi_{2,N} \\ \vdots \\ \phi_{N-1,N} \\ \phi_{N,N} \end{bmatrix} \tag{3. 10}$$

Corresponding to the N natural vibration frequencies $\boldsymbol{\omega}$ of a N-DOF system, there are N independent vectors $\phi_N$, witch are known as natural modes of vibration, or natural mode shapes of vibration [6].

However, the solution of Equation 3.9 leads to an indeterminate system because the values of the vectors are dependent on each other [2]. Thus, it is appropriate to arbitrate one of the values, and then it will be possible to determinate the others regarding this one.

In summary, a vibrating system with N-DOFs has N natural vibration frequencies $\omega_N$ $(n = 1, 2, \dots, N)$; corresponding natural periods $T_N$, and vibration modes $\phi_N$ [6]. They are called "natural" because they are natural proprieties of the structure in free vibration, depending only on its mass and stiffness proprieties.

Finally, the matrix of vibration modes $\phi$ is:

$$\phi = \begin{bmatrix} \phi_{1,1} & \phi_{1,2} & \cdots & \cdots & \phi_{1,N-1} & \phi_{1,N} \\ \phi_{2,1} & \phi_{2,2} & \cdots & \cdots & \phi_{2,N-1} & \phi_{2,N} \\ \vdots & \vdots & \ddots & \ddots & \vdots & \vdots \\ \vdots & \vdots & \ddots & \ddots & \vdots & \vdots \\ \vdots & \vdots & \ddots & \ddots & \vdots & \vdots \\ \phi_{N-1,1} & \phi_{N-1,2} & \cdots & \cdots & \phi_{N-1,N-1} & \phi_{N-1,N} \\ \phi_{N,1} & \phi_{N,2} & \cdots & \cdots & \phi_{N,N-1} & \phi_{N,N} \end{bmatrix} \tag{3. 11}$$

In this study, the vibration mode matrix will be used in its normalized form $\hat{\phi}$, regarding the mass propriety. This process is developed through the division of each vibration mode vector by its respective generalized mass [6].

The generalized mass of each vibration mode is calculated by a simple matrix multiplication, considering the respective mode vibration vector, as it is shown in Equation 3.12.

$$m^*_N = {\phi_N}^T \cdot M \cdot \phi_N \tag{3. 12}$$

Each normalized vibration mode vector $\hat{\phi}_N$ can be determined by Equation 3.13.

$$\hat{\phi}_N = \begin{bmatrix} \phi_{1,N} \\ \phi_{2,N} \\ \vdots \\ \phi_{N-1,N} \\ \phi_{N,N} \end{bmatrix} \cdot \frac{1}{\sqrt{m^*_N}} \tag{3. 13}$$

Consequently, the normalized vibration mode matrix $\hat{\phi}$ will have the same dimensions of the vibration mode matrix calculated before:

$$\hat{\phi} = \begin{bmatrix} \hat{\phi}_{1,1} & \hat{\phi}_{1,2} & \cdots & \cdots & \hat{\phi}_{1,N-1} & \hat{\phi}_{1,N} \\ \hat{\phi}_{2,1} & \hat{\phi}_{2,2} & \cdots & \cdots & \hat{\phi}_{2,N-1} & \hat{\phi}_{2,N} \\ \vdots & \vdots & \ddots & \ddots & \vdots & \vdots \\ \vdots & \vdots & \ddots & \ddots & \vdots & \vdots \\ \vdots & \vdots & \ddots & \ddots & \vdots & \vdots \\ \hat{\phi}_{N-1,1} & \hat{\phi}_{N-1,2} & \cdots & \cdots & \hat{\phi}_{N-1,N-1} & \hat{\phi}_{N-1,N} \\ \hat{\phi}_{N,1} & \hat{\phi}_{N,2} & \cdots & \cdots & \hat{\phi}_{N,N-1} & \hat{\phi}_{N,N} \end{bmatrix} \tag{3. 14}$$

### 3.1.4 Classical Damping Matrix

The natural damping of a structure is assumed as Classical Damping, where the only damping contribution is the genuine damping that the structure itself provides, without any extra damping system associated.

A classical damping matrix can be constructed with experimental data, considering the Rayleigh damping [6]:

$$C = \alpha \cdot M + \beta \cdot K \tag{3. 15}$$

If we apply the double product in Equation 3.15 and considering that the vector $\hat{\phi}_N$ is the normalized natural mode of vibration of the Nth vibration mode, it results in:

$${\hat{\phi}_N}^T \cdot \boldsymbol{C} \cdot \hat{\phi}_N = \boldsymbol{\alpha} \cdot {\hat{\phi}_N}^T \cdot \boldsymbol{M} \cdot \hat{\phi}_N + \boldsymbol{\beta} \cdot {\hat{\phi}_N}^T \cdot \boldsymbol{K} \cdot \hat{\phi}_N \tag{3. 16}$$

Thus, we have the equation with the generalized parameters:

$$c^*_N = \alpha \cdot m^*_N + \beta \cdot k^*_N \tag{3. 17}$$

Where $c^*_N$, $m^*_N$ and $k^*_N$ are the generalized damping coefficient, generalized mass and generalized stiffness, respectively, of the Nth vibration mode (determined following the same reasoning of Equation 3.12. To determine the modal damping factor $\xi_n$, it is necessary to know the critic modal damping coefficient $\boldsymbol{c^*_{N,crit}}$ that can be defined by:

$$c^*_{N,crit} = 2 \cdot m^*_N \cdot \omega_N \tag{3. 18}$$

Finally, the modal damping ratio $\boldsymbol{\xi_n}$ for each vibration mode is defined by Equation 3.19.

$$\xi_n = \frac{c^*_N}{c^*_{N,crit}} \tag{3. 19}$$

To simplify, we can substitute the Equation 3.17 and Equation 3.18 in Equation 3.19, resulting in:

$$\xi_n = \frac{1}{2} \cdot \left( \frac{\alpha}{\omega_N} + \beta \cdot \omega_N \right) \tag{3. 20}$$

The coefficients $\boldsymbol{\alpha}$ and $\boldsymbol{\beta}$ can be determined from estimated damping ratios $\boldsymbol{\xi_i}$ and $\boldsymbol{\xi_j}$ for the $i$th and $j$th modes, respectively [6]. Expressing Equation 3.20 for these two vibration modes in matrix form leads to:

$$\frac{1}{2} \cdot \begin{bmatrix} \frac{1}{\omega_i} & \omega_i \\ \frac{1}{\omega_J} & \omega_J \end{bmatrix} \cdot \begin{bmatrix} \alpha \\ \beta \end{bmatrix} = \begin{bmatrix} \xi_i \\ \xi_j \end{bmatrix} \tag{3. 21}$$

This means that two algebraic equations can be solved to determine the coefficients $\boldsymbol{\alpha}$ and $\boldsymbol{\beta}$.

In summary, the first step of the process is to arbitrate the damping ratios $\boldsymbol{\xi_i}$ and $\boldsymbol{\xi_j}$ (the modes usually used are the first and second mode), and by knowing the natural vibration frequencies $\boldsymbol{\omega_i}$ and $\boldsymbol{\omega_j}$, the matrix system (Equation 3.21) can be resolved. Thus, the classical damping matrix can be constructed (Equation 3.15), and consequently, the generalized and critic damping too. Lastly, the damping factor for each vibration mode is determined following the Equation 3.19.

## 3.2 NON CLASSICAL DAMPING MATRIX

The installation of extra damping system in the structure modifies the Damping Matrix determined previously. Two different contributions will influence this propriety: the classical damping matrix determined before (now termed as $C_0$) and the extra damping matrix ($C_d$).

By the superposition of these two matrix, the Non Classical Damping Matrix ($C$) is constructed. This matrix is also known as Effective Damping Matrix.

$$C = C_0 + C_d \tag{3. 22}$$

To determine the extra damping matrix ($C_d$), the study of a mechanical system of many DOF is necessary again, very similar to the process of the stiffness matrix determination, as represented in Figure 9.

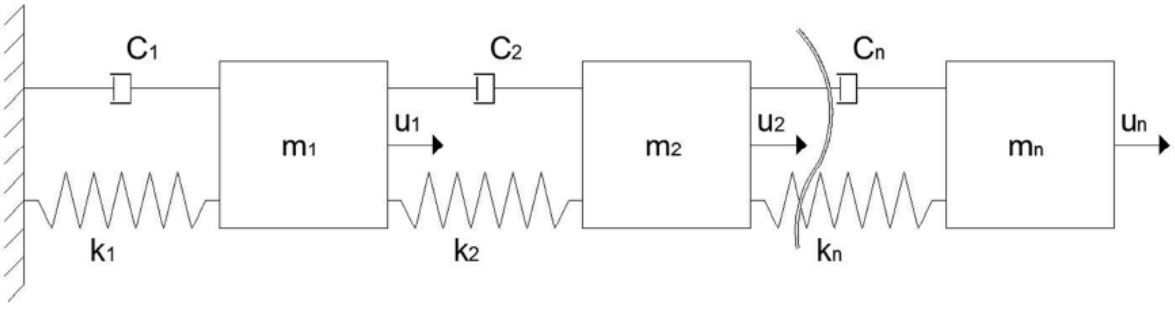


Figure 9 - Mechanical system with dampers, considering “n” DOF

In this study, the damping system added in the structure was installed in an “inverted V” configuration, as shown in Figure 10.

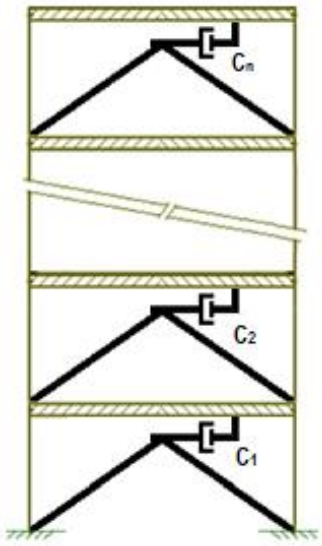


Figure 10 – Studied structure with viscous dampers installed in the “inverted V” configuration

The extra damping matrix in a rigid floor structure is defined as:

$$C_d = \begin{bmatrix} C_1 + C_2 & -C_2 & 0 & \cdots & 0 \\ -C_2 & C_2 + C_3 & \ldots & \ddots & \vdots \\ 0 & -C_3 & \ddots & -C_{n-1} & 0 \\ \vdots & \ddots & \ldots & C_{n-1} + C_n & -C_n \\ 0 & \ldots & 0 & -C_n & C_n \end{bmatrix} \times \cos^2\theta \quad (3.\ 23)$$

Where $C_n$ is the extra damping coefficient installed on the “N” DOF, and $\theta$ is the inclination angle of the positioned damper referring to the horizontal plane (considering it the same on all of the DOF). Thus, by the analysis of Equation 3.23, it can be observed that the inclination angle of the damper has a significant influence on the Extra Damping Matrix, and this matrix conditions the displacements of a structure.

Considering that the cosine of the inclination ($\cos\theta$) is always less than 1, unless it is horizontal, we can affirm that the structure will benefit more from the placement of dampers if they are placed horizontally. That is one of the reasons why the “K” configuration was chosen on the installation of the damping system on the studied structure, placing the viscous dampers on the horizontal position.

## 3.3 MODAL DAMPING DETERMINATION

In this subchapter, two possible methods of modal damping determination will be approached and described: the State Space Formulation and the Simplified Formulations from FEMA 356.

### 3.3.1 STATE SPACE FORMULATION

This method can be used to solve the equations of the dynamics equilibrium of a system. It can be used when the Damping Matrix is not diagonal, such as the case of this study. Besides, the State Space

Formulation is also used when the external force applied on the structure vary on discrete intervals over time, such as the influence of a seismic action [2].

The representation on Space State has three variables: the state variables, the input variables and the output variables [3]. These variables are characterized by the matrixes A, B and C, respectively. It is important to not confuse the damping matrix with the output matrix, even though they have the same designation. Matrixes A and B can be obtained by the mass, stiffness and damping matrixes, using the following relations:

$$A = \begin{bmatrix} 0 & I \\ -M^{-1} \times K & -M^{-1} \times C \end{bmatrix} \quad (3.\ 24)$$

$$B = \begin{bmatrix} 0 \\ M^{-1} \times J \end{bmatrix} \quad (3.\ 25)$$

Where M, K and C are the mass, stiffness and damping matrixes of the structure and I is the identity matrix with "n" x "n" dimensions. Thus, the A matrix will be a square matrix with dimensions "2n" x "2n".

J is the matrix of input variables location, with the number of lines equal to the number of DOF and the number of columns equal to the number of input variables of the system, where the unitary value represents the existence of a variable and "0", the inexistence. Therefore, B will be a "2n" x "m" matrix, where "m" represents the number of input variables.

The modal damping and the natural frequencies of a structure can be determined by the eigenvalues of the state matrix A, which is a very important propriety on the dynamic of structures. Each eigenvalue is composed of a real component, equal to the product of the structure's damping and its natural frequency, and an imaginary component, that represents the damping frequency of the structure.

$$v = \begin{cases} -\xi_1 \times \omega_1 \pm \omega_{d1} i \\ -\xi_2 \times \omega_2 \pm \omega_{d2} i \\ \vdots \\ -\xi_{n-1} \times \omega_{n-1} \pm \omega_{n-d1} i \\ -\xi_n \times \omega_n \pm \omega_{dn1} i \end{cases} \quad (3.\ 26)$$

The damping frequency $\omega_d$ depends on the modal damping and the natural frequency of the structure, as shown in Equation 3.27.

$$\omega_d = \omega \times \sqrt{1 - \xi^2} \quad (3.\ 27)$$

Each modal damping factor and respective natural frequency can be determined by solving a simple equation system formed by equating the real component to "x" and the imaginary component to "y" of the eigenvalues calculated, as represented in Equation 3.28.

$$\begin{cases} \xi_n \times \omega_n = x \\ \omega_n \times \sqrt{1 - {\xi_n}^2} = y \end{cases} \quad (3.\ 28)$$

Now, the determination of the modal damping factor of the structure is possible. The natural frequencies of each mode were already calculated before, so the determination of this parameter now can help on validating the previous calculus, as the values determined now should be the same as the previous ones.

Besides the Modal Damping Determination, the State Space Formulation can also determine the response of the structure due to the application of external forces.

When the mechanical system presents "n" DOF, its representation on State Space is done through the form of a system with "2n" equations of 1st order. This system is termed as "$x(t)$" and its formed by "n" displacements "$u(t)$" and "n" velocities "$\dot{u}(t)$" associated to the many DOF, as represented below.

$$x(t) = \begin{bmatrix} u_1(t) \\ u_2(t) \\ \vdots \\ u_{n-1}(t) \\ u_n(t) \\ \dot{u}_1(t) \\ \dot{u}_2(t) \\ \vdots \\ \dot{u}_{n-1}(t) \\ \dot{u}_n(t) \end{bmatrix} \tag{3. 29}$$

If there are external forces applied on the structure, there will be input variables that will be represented as a vector with "m" lines, symbolizing the "m" applied forces.

$$u(t) = \begin{bmatrix} F_1(t) \\ F_2(t) \\ \vdots \\ F_{n-1}(t) \\ F_n(t) \end{bmatrix} \tag{3. 30}$$

The variables of the system are calculates for a determined instant of time. This means that in another instant of time there will exist others state variables and input variables, working on a "step by step" method. The shorter increment of time, the more accurate system response determination. The matrix termed as E in this work depends exclusively on the state matrix A and on the time interval Δt, as it can be seen on Equation 3.31.

$$E = e^{\Delta t \times A} \tag{3. 31}$$

Therefore, E will be a "2n" x "2n" matrix, where "n" is the number of DOF.

On the other hand, G is a matrix that depends on the state matrix and on the time interval, as well as depends on the input matrix B:

$$\begin{aligned} G = \left( \int_0^{\Delta t} e^{\Delta t \times A} \, d\Delta t \right) \times B = \left[ A^{-1} \times e^{\Delta t \times A} \right]_0^{\Delta t} \times B = \left( A^{-1} \times e^{\Delta t \times A} - A^{-1} \right) \times B \\ = \left[ A^{-1} \times \left( e^{\Delta t \times A} - I \right) \right] \times B = \left[ A^{-1} \times (E - I) \right] \times B \end{aligned} \tag{3. 32}$$

It is assumed that the structure matrixes (mass, stiffness and damping) does not vary over time. That is why the state matrix A does not vary too, and consequently, neither does the matrix E. Besides, the input matrix B does not vary, thus, the matrix G does not vary too [2]. What is going to provide the system response are the input variables and the state variables in the previous instant.

With the constants E and G defined, the response of the system due to a determined external force can be finally calculated by a "step by step" method, using the following equation:

$$x(t + \Delta t) = E \times x(t) + G \times u(t) \tag{3. 33}$$

### 3.3.2 Simplified Formulation used in FEMA 356 Code

The method of calculation of the modal damping using the simplified formulation was extracted from the *Guidelines for the Seismic Rehabilitation of Buildings – FEMA 356* [9]. Following this documentation, the modal damping shall be calculate in accordance with Equation 3.34.

$$\xi_{eff} = \xi_0 + \frac{\sum W_g}{4\pi \cdot W_k} \tag{3. 34}$$

Where $\xi_0$ is the classical modal damping factor of the structure calculated in Equation 3.19, $W_g$ is the work done by the damping device "g" (Equation 3.35) and $W_k$, the maximum strain energy in the frame (Equation 3.36).

The work done by the damping device can be obtained by

$$\sum W_g = \sum \pi \cdot C_g \cdot {u_g}^2 \cdot \omega = \frac{2\pi^2}{T} \cdot \sum C_g \cdot {u_g}^2 \tag{3. 35}$$

Where T is the period of the vibration mode and $C_g$ is the damping coefficient of the viscous damper g. The maximum strain energy in the frame is equal to half of the sum of the relative displacements on the columns $\delta_i$ multiplied to its shear force $F_i$ [9].

$$W_k = \frac{1}{2} \cdot \sum F_i \cdot \delta_i \tag{3. 36}$$

It is known that the first vibration mode is the responsible for the most part of the total displacements on a structure [10]. Therefore, the work done $W_g$ and the strain energy in the frame $W_k$ will be determined using a modal analysis considering this mode only, as indicated in Equation 3.37 and 3.38.

$$\sum W_g = \frac{2\pi^2}{T} \cdot \sum C_g \cdot \left(\phi_{rg} \cdot \cos\theta_g\right)^2 = \frac{2\pi^2}{T} \cdot \sum C_g \cdot {\phi_{rg}}^2 \tag{3. 37}$$

(3. 38)

$$W_k = \frac{1}{2} \cdot {\phi_1}^T \cdot K \cdot \phi_1 = \frac{1}{2} \cdot {\phi_1}^T \cdot \omega^2 \cdot M \cdot \phi_1 = \frac{1}{2} \cdot \sum \omega^2 \cdot m_i \cdot {\phi_i}^2$$
$$= \frac{1}{2} \cdot \frac{4\pi^2}{T^2} \cdot \sum m_i \cdot {\phi_i}^2 = \frac{2\pi^2}{T^2} \cdot \sum m_i \cdot {\phi_i}^2$$

$\phi_{rg}$ and $\theta_g$ represent, respectively, the relative movement of the damper (equal to the relative movement between the DOF where the dampers are installed) and the inclination angle of the damper, that is equal to 0 in this work, as justified before. $m_i$ and $\phi_i$ are the mass and the modal component of the "i" floor, respectively [10]. By substituting Equations 3.37 and 3.38 in Equation 3.34, the effective modal damping factor of the framed structure is obtained:

(3. 39)

$$\xi_{eff} = \xi_0 + \frac{\frac{2\pi^2}{T} \cdot \sum C_g \cdot {\phi_{rg}}^2}{4\pi \cdot \frac{2\pi^2}{T^2} \cdot \sum m_i \cdot {\phi_i}^2} = \xi_0 + \frac{T \cdot \sum C_g \cdot {\phi_{rg}}^2}{4\pi \cdot \sum m_i \cdot {\phi_i}^2}$$

# 4

# STUDY OF A 3-FLOOR LABORATORY STRUCTURE

## 4.1 DYNAMIC PARAMETERS

Using the methodology explained in the previous chapters, the dynamic parameters of the laboratory structure analyzed in this work can be obtained. The frame studied in this work has been dimensioned and characterized in the references [7] and [8]. Thus, the data presented below was extracted from these studies.

The structure presents three floors, each one with a ceiling height of 1m, four columns and four beams per floor [8]. The horizontal distance between axes of the columns is 2.10m in both directions. It is illustrated in Figure 11 the general scheme of the structure.

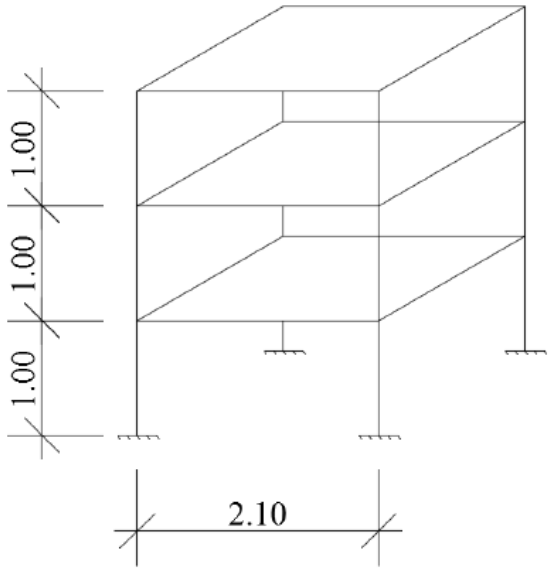


Figure 11 - General scheme of the analyzed structure [8]

### 4.1.1 MASS AND STIFFNESS MATRIX

In Table 3, the weights of slabs, columns and beams are represented [7]. It is important to notice that all beams and columns have its transversal sections defined by an IPE 100 (S 275) profile.

Table 3 - Weights of the structure's elements

| Elements | Quantity | 1 element weight (kN) | Total elements weight (kN) | 1 floor weight (kN) |
|---|---|---|---|---|
| Slab (2.10m x 2.10m x 0.085m) | 3 | 9.371 | 28.113 | 9.371 |
| Beam (2.10m) | 12 | 0.16681 | 2.00172 | 0.66724 |
| Column (1m) | 12 | 0.079434 | 0.953208 | 0.317736 |

By the analysis of the table above, the weight of one floor can be obtained, by the sum of the last column values. The result is 10.356 kN, that is equal to 1.055 tonnes, considering the gravity acceleration equal to 9.81 m/s². Thereby, it is possible now to construct the mass matrix of the structure:

$$M = \begin{bmatrix} 1.055 & 0 & 0 \\ 0 & 1.055 & 0 \\ 0 & 0 & 1.055 \end{bmatrix} ton \quad (4.\ 1)$$

Considering a flexible floor structure, the stiffness matrix was obtained with the support of the software Robot Structural Analysis, by applying concentrated loads on the level of each floor, aiming to induce a unitary displacement. Moreover, the other levels were fixed on the horizontal direction, through a support that restricts this movement. Thus, the force that originates the unitary displacement on the respective floor and the reactions originated on the other levels' supports are the values of the stiffness elements associated to the respective DOF.

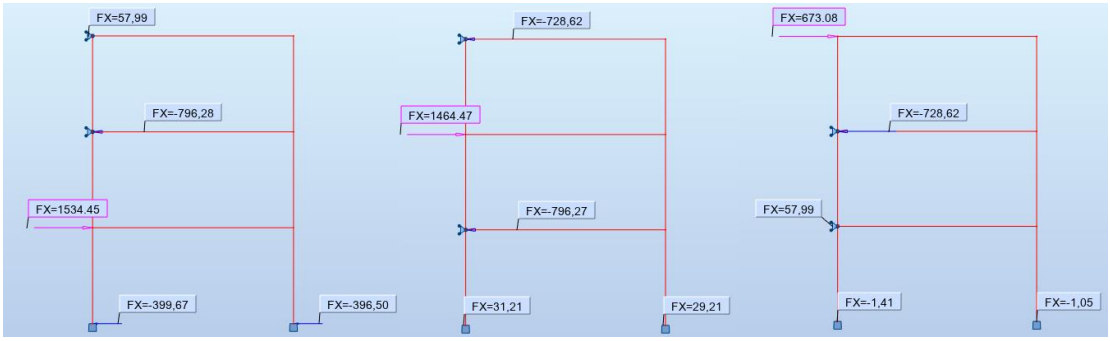


(a) (b) (c)

Figure 12 - Application of the Direct Method. (a) Unitary displacement in the first floor; (b) unitary displacement in the second floor; (c) unitary displacement in the third floor

As represented in the Figure 12, these reactions are referring to a system composed of one frame only. To determine the stiffness of the real structure, these values have to be multiplied for 2, as there are two frames on the analyzed direction. Accordingly, joining the different stiffness values associated to each DOF, the stiffness matrix is obtained, for the flexible floor structure:

$$K = \begin{bmatrix} 3068.9 & -1592.54 & 115.98 \\ -1592.56 & 2928.94 & -1457.24 \\ 115.98 & -1457.24 & 1346.16 \end{bmatrix} kN/m \quad (4.\ 2)$$

Differently from the methodology presented before, when it is considered that the structure presents rigid beams, the stiffness is calculated by another procedure, as explained on 3.1.2.2.

The moment of inertia **I** of the IPE 100 (S 275) profile, as informed on the *ARBED Sales Programme – Structural Shapes*, is 15.92 cm⁴. The elastic modulus **E** of the material is 210 GPa and, as described before, the height of each column is 1m. With this information, it is possible to determine the stiffness of each floor, following Equation 3.3.

$$k_1 = k_2 = k_3 = 4 \cdot \frac{12 \cdot 210 \cdot 10^6 \cdot 1.592 \cdot 10^{-7}}{1.0^3} = 1604.74 \frac{kN}{m} \tag{4. 3}$$

With each stiffness calculated, the stiffness matrix of the rigid floor system is obtained, as defined in Equation 3.4.

$$K = \begin{bmatrix} k_1 + k_2 & -k_2 & 0 \\ -k_2 & k_1 + k_2 & -k_2 \\ 0 & -k_2 & k_3 \end{bmatrix} = \begin{bmatrix} 3209.47 & -1604.74 & 0 \\ -1604.74 & 3209.47 & -1604.74 \\ 0 & -1604.74 & 1604.74 \end{bmatrix} kN/m \tag{4. 4}$$

### 4.1.2 Natural Frequencies and Vibration Modes

With the stiffness matrix determined, it is possible to calculate the natural vibration frequencies of the structure following Equations 3.6 to 3.8. By resolving the Equation 3.9 for each frequency, the vibration modes vectors are also calculated:

$$\omega = \begin{bmatrix} 15.44 \\ 45.07 \\ 68.50 \end{bmatrix} rad/s \tag{4. 5}$$

(a) Flexible beams

$$\omega = \begin{bmatrix} 17.36 \\ 48.63 \\ 70.28 \end{bmatrix} rad/s$$

(b) Rigid beams

$$f = \begin{bmatrix} 2.46 \\ 7.17 \\ 10.90 \end{bmatrix} Hz \tag{4. 6}$$

(a) Flexible beams

$$f = \begin{bmatrix} 2.76 \\ 7.74 \\ 11.18 \end{bmatrix} Hz$$

(b) Rigid beams

$$\phi = \begin{bmatrix} 1 & 1 & 1 \\ 1.950 & 0.523 & -1.145 \\ 2.491 & -0.811 & 0.495 \end{bmatrix} \tag{4. 7}$$

(a) Flexible beams

$$\phi = \begin{bmatrix} 1 & 1 & 1 \\ 1.802 & 0.445 & -1.247 \\ 2.247 & -0.802 & 0.555 \end{bmatrix}$$

(b) Rigid beams

The generalized masses $m^*_1$, $m^*_2$ and $m^*_3$ are shown in

Table 4, to the both models. Normalizing the vibration modes regarding to the mass, the corresponding vibration modes matrixes are represented in Equation 4.8:

Table 4 – Generalized masses

| | Flexible beams Structure | Rigid beams Structure |
|---|---|---|
| $\boldsymbol{m^*_1}$ (tones) | 11.614 | 9.807 |
| $\boldsymbol{m^*_2}$ (tones) | 2.037 | 1.942 |
| $\boldsymbol{m^*_3}$ (tones) | 2.697 | 3.021 |

$$\hat{\phi} = \begin{bmatrix} 0.293 & 0.701 & 0.609 \\ 0.572 & 0.366 & -0.697 \\ 0.731 & -0.568 & 0.301 \end{bmatrix} \qquad \hat{\phi} = \begin{bmatrix} 0.319 & 0.718 & 0.575 \\ 0.575 & 0.319 & -0.718 \\ 0.718 & -0.575 & 0.319 \end{bmatrix} \tag{4. 8}$$

(a) Flexible beams (b) Rigid beams

The normalized vibration modes are represented on Figure 13.

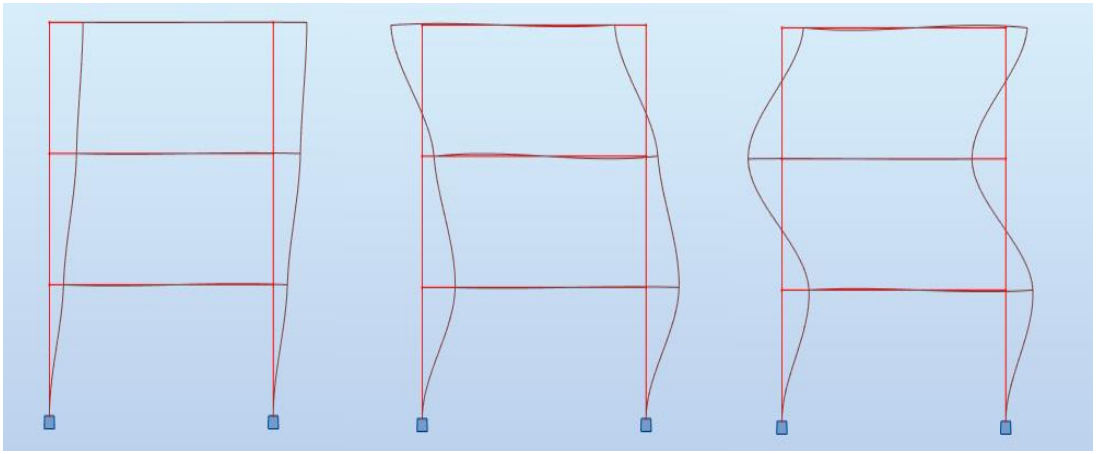

(a) (b) (c)

Figure 13 - Normalized vibration modes. (a) 1st mode; (b) 2nd mode; (c) 3rd mode

### 4.1.3 Classical Damping Matrix

Using the Rayleigh Damping Method, first it is necessary to arbitrate the damping factor to the 1st and 2nd modes. In this work, these factors were initially arbitrated as 1% for both modes. Thus, by using the modal frequencies $\omega_1$ and $\omega_2$ in Equation 3.21, the resulting values of α and β are the ones represented below.

Table 5 – Rayleigh coefficients

| | Flexible beams method | Rigid beams method |
|---|---|---|
| **α** | 0.230 | 0.256 |
| **β** | 0.000331 | 0.000303 |

Now, using Equation 3.15 it is possible to calculate the natural damping matrix for the flexible and the rigid floor structure:

**Flexible beams**

$$C = 0.230 \cdot M + 0.000331 \cdot K = \begin{bmatrix} 1.258 & -0.527 & 0.038 \\ -0.527 & 1.212 & -0.482 \\ 0.038 & -0.482 & 0.688 \end{bmatrix} \quad (4.\ 9)$$

**Rigid beams**

$$C = 0.256 \cdot M + 0.000303 \cdot K = \begin{bmatrix} 1.242 & -0.486 & 0 \\ -0.486 & 1.242 & -0.486 \\ 0 & -0.486 & 0.756 \end{bmatrix} \quad (4.\ 10)$$

Following the procedure explained in the subchapter 3.1.4, the natural damping factors $\xi_1$, $\xi_2$ and $\xi_3$ can be determined, as shown in Table 6. The results for the 1st and 2nd mode were already expected (1%) due to its initially arbitration.

Table 6 - Rayleigh damping ratios

| | Vibration Mode | Generalized mass (ton) | Generalized stiffness (kN/m) | Generalized damping (kN.s/m) | Critic damping coefficient (kN.s/m) | Damping ratio |
|---|---|---|---|---|---|---|
| **Flexible beams Structure** | 1 | 11.614 | 2769.27 | 3.588 | 358.669 | 1% |
| | 2 | 2.037 | 4136.19 | 1.838 | 183.568 | 1% |
| | 3 | 2.697 | 12654.40 | 4.809 | 369.485 | 1,3% |
| **Rigid beams Structure** | 1 | 9.807 | 2954.58 | 3.404 | 340.447 | 1% |
| | 2 | 1.942 | 4594.33 | 1.889 | 188.937 | 1% |
| | 3 | 3.021 | 14917.40 | 5.293 | 424.528 | 1,2% |

## 4.2 NON CLASSICAL DAMPING DETERMINATION

The classical damping matrix calculated before, using the Rayleigh Method, is now designed as $C_0$.

$$C_0 = \begin{bmatrix} 1.258 & -0.527 & 0.038 \\ -0.527 & 1.212 & -0.482 \\ 0.038 & -0.482 & 0.688 \end{bmatrix} kN.\frac{s}{m} \quad C_0 = \begin{bmatrix} 1.242 & -0.486 & 0 \\ -0.486 & 1.242 & -0.486 \\ 0 & -0.486 & 0.756 \end{bmatrix} kN.\frac{s}{m} \quad (4.\ 11)$$

(a) Flexible beams (b) Rigid beams

The extra damping matrix $C_d$ is composed of the damping coefficients of the installed dampers in the structure:

$$C_d = \begin{bmatrix} C_1 + C_2 & -C_2 & 0 \\ -C_2 & C_2 + C_3 & -C_2 \\ 0 & -C_2 & C_3 \end{bmatrix} \quad (4.\ 12)$$

In this work, it will be developed different numerically simulations pointing the determination of the modal damping of the structure by using diverse dampers (with different damping coefficients), aiming the best use of the dampers available on the laboratory.

Moreover, it will be presented some ideal scenarios, with the calculus of the necessary damping coefficients to be installed on the structure to achieve modal damping goals of 10, 15 and 20%.

Initially, four dampers per floor were considered, installed on the three floors of the structure. Among these four devices, two of them presents a damping coefficient of 400 N.s/m (*Taylor Devices* – REF 27-5) and the other two, 900 N.s/m (*Taylor Devices* – REF 20-5), resulting on a damping coefficient of 2600 N.s/m per floor.

$$C_1 = C_2 = C_3 = 2 \cdot 400 + 2 \cdot 900 = 2600\ N.\frac{s}{m} = 2.6\ kN.\frac{s}{m} \tag{4. 13}$$

Thus, the extra damping matrix is

$$C_d = \begin{bmatrix} 5.2 & -2.6 & 0 \\ -2.6 & 5.2 & -2.6 \\ - & -2.6 & 2.6 \end{bmatrix} kN.\frac{s}{m} \tag{4. 14}$$

Finally, the non-classical damping matrix is obtained by the sum of the classical and the extra damping matrixes:

$$C = \begin{bmatrix} 6.458 & -3.127 & 0.0384 \\ -3.127 & 6.412 & -3.082 \\ 0.0384 & -3.082 & 3.288 \end{bmatrix} kN.\frac{s}{m} \quad C = \begin{bmatrix} 6.442 & -3.086 & 0 \\ -3.086 & 6.442 & -3.086 \\ 0 & -3.086 & 3.356 \end{bmatrix} kN.\frac{s}{m} \tag{4. 15}$$

(a) Flexible beams (b) Rigid beams

## 4.3 EFFECTIVE MODAL DAMPING EVALUATION

The results of modal damping using the State Space Formulation and Simplified Formulation are exposed below, to compare and validate the values.

### 4.3.1 STATE SPACE FORMULATION

Following the methodology explained on the subchapter 3.3.1, first is essential to obtain the state matrix A, using the mass, stiffness and damping matrixes (Equation 3.24).

**Flexible beams**

$$A = \begin{bmatrix} 0.000 & 0.000 & 0.000 & 1.000 & 0.000 & 0.000 \\ 0.000 & 0.000 & 0.000 & 0.000 & 1.000 & 0.000 \\ 0.000 & 0.000 & 0.000 & 0.000 & 0.000 & 1.000 \\ -2908.910 & 1509.517 & -109.934 & -6.122 & 2.964 & -0.036 \\ 1509.536 & -2776.246 & 1381.270 & 2.964 & -6.078 & 2.922 \\ -109.934 & 1381.270 & -1275.981 & -0.036 & 2.922 & -3.117 \end{bmatrix} \tag{4. 16}$$

**Rigid beams**

$$A = \begin{bmatrix} 0.000 & 0.000 & 0.000 & 1.000 & 0.000 & 0.000 \\ 0.000 & 0.000 & 0.000 & 0.000 & 1.000 & 0.000 \\ 0.000 & 0.000 & 0.000 & 0.000 & 0.000 & 1.000 \\ -3042.154 & 1521.077 & 0 & -6.107 & 2.925 & 0 \\ 1521.077 & -3042.154 & 1521.077 & 2.925 & -6.107 & 2.925 \\ 0 & 1521.077 & -1521.077 & 0 & 2.925 & -3.181 \end{bmatrix} \quad (4.17)$$

Using the *Mat Lab* Software, it was possible to calculate the eigenvalues of the A matrix:

$$\boldsymbol{v = -x \pm yi}$$

$$v = \begin{cases} -0.400 \pm 15.437\, i \\ -2.370 \pm 45.002\, i \\ -4.888 \pm 68.322\, i \end{cases} \qquad v = \begin{cases} -0.418 \pm 17.352 i \\ -2.402 \pm 48.574 i \\ -4.877 \pm 70.108 i \end{cases} \quad (4.18)$$

(a) Flexible beams (b) Rigid beams

Now, it is possible to solve the equation systems following Equation 3.28. The damping ratios and damping frequencies of the structure with the dampers installed are listed below:

**Flexible beams** (4.19)

$$\xi_1 = 2.59\% \qquad \omega_{g1} = 15.442\, rad/s$$
$$\xi_2 = 5.26\% \qquad \omega_{g2} = 45.065\, rad/s$$
$$\xi_3 = 7.14\% \qquad \omega_{g3} = 68.497\, rad/s$$

**Rigid beams** (4.20)

$$\xi_1 = 2.41\% \qquad \omega_{g1} = 17.358\, rad/s$$
$$\xi_2 = 4.94\% \qquad \omega_{g2} = 48.633\, rad/s$$
$$\xi_3 = 6.94\% \qquad \omega_{g3} = 70.278\, rad/s$$

### 4.3.2 Simplified Formulation

In accordance with Equation 3.39, it is important to define now the relative displacements of each floor of the framed structure, on its respective vibration mode. Considering the normalized vibration mode matrix determined on section 4.1.2, the total and relative displacements are shown in Table 7.

Table 7 - Total and relative displacements on the structure

| | Vibration Mode | Floor | Total Displacement (m) | Relative Displacement (m) |
|---|---|---|---|---|
| **Flexible beams Structure** | 1 | 1 | 0,293 | 0,293 |
| | 1 | 2 | 0,572 | 0,279 |
| | 1 | 3 | 0,731 | 0,159 |
| | 2 | 1 | 0,701 | 0,701 |
| | 2 | 2 | 0,366 | -0,335 |
| | 2 | 3 | -0,568 | -0,934 |
| | 3 | 1 | 0,609 | 0,609 |

| | | | | |
|---|---|---|---|---|
| | 3 | 2 | -0,697 | -1,306 |
| | 3 | 3 | 0,301 | 0,998 |
| | | | | |
| **Rigid beams Structure** | 1 | 1 | 0,319 | 0,319 |
| | 1 | 2 | 0,575 | 0,256 |
| | 1 | 3 | 0,718 | 0,143 |
| | 2 | 1 | 0,718 | 0,718 |
| | 2 | 2 | 0,319 | -0,399 |
| | 2 | 3 | -0,575 | -0,894 |
| | 3 | 1 | 0,575 | 0,575 |
| | 3 | 2 | -0,718 | -1,293 |
| | 3 | 3 | 0,319 | 1,037 |

Finally, it is possible to determine each effective modal damping. The calculus are detailed above.

**Flexible beams**

$$\xi_{eff,1} = 0.01 + \frac{0.407 \cdot 2.6 \cdot (0{,}293^2 + 0{,}279^2 + 0{,}159^2)}{4\pi \cdot 1.055 \cdot (0{,}293^2 + 0{,}572^2 + 0{,}731^2)} = 2{,}59\% \quad (4.\ 21)$$

$$\xi_{eff,2} = 0.01 + \frac{0.139 \cdot 2.6 \cdot (0{,}701^2 + 0{,}335^2 + 0{,}934^2)}{4\pi \cdot 1.055 \cdot (0{,}701^2 + 0{,}366^2 + 0{,}568^2)} = 5{,}26\%$$

$$\xi_{eff,3} = 0.012 + \frac{0.092 \cdot 2.6 \cdot (0{,}609^2 + 1{,}306^2 + 0{,}998^2)}{4\pi \cdot 1.055 \cdot (0{,}609^2 + 0{,}697^2 + 0{,}301^2)} = 7{,}13\%$$

**Rigid beams**

$$\xi_{eff,1} = 0.01 + \frac{0.362 \cdot 2.6 \cdot (0.319^2 + 0.256^2 + 0.143^2)}{4\pi \cdot 1.055 \cdot (0.319^2 + 0.575^2 + 0.718^2)} = 2{,}41\% \quad (4.\ 22)$$

$$\xi_{eff,2} = 0.01 + \frac{0.129 \cdot 2.6 \cdot (0{,}718^2 + 0{,}399^2 + 0{,}894)}{4\pi \cdot 1.055 \cdot (0{,}718 + 0{,}319^2 + 0{,}575^2)} = 4{,}94\%$$

$$\xi_{eff,3} = 0.012 + \frac{0.089 \cdot 2.6 \cdot (0{,}575^2 + 1{,}293^2 + 1{,}037^2)}{4\pi \cdot 1.055 \cdot (0{,}575^2 + 0{,}718^2 + 0{,}319^2)} = 6{,}89\%$$

Through the analysis of the obtained results, and comparing the damping factors of the flexible beams model to the rigid floor model, it can be concluded that the values resulted approximate. The use of a flexible floor model can be considered as a more complex and laborious procedure, but provides more accurate results and closer to reality. However, the rigid floor model offers results significantly approximate from the other model, as it can be a great alternative to determine the dynamic parameters and modal damping of a structure.

Another conclusion that can be taken through this study is that the FEMA simplified formulations are considerably reliable, when comparing its results to the ones provided by the State Space Formulation. This can be affirmed because the damping factor obtained when using the simplified formulation for the

first and second vibration modes resulted the same values of the State Space formulation's results, and for the third mode the values got really approximate.

### 4.4 OTHER SCENARIOS

In order to achieve a higher effective damping and a most efficient behavior of the structure, other different settings of the damped structure were simulated. These simulation were done considering all the available devices in the laboratory and some unavailable ones but with ideal damping coefficients to reach goals of 10, 15 and 20%, that could be hereafter installed on the framed structure. In this section, it will be presented only the results for each simulation, as the methodology were already explained and exemplified on the previous sections.

To guarantee most reliable results and closer to the reality, in these simulations, the dynamic parameters of the structure were utilized considering that it presents a flexible floor system, despite the values between the both considerations resulted in Sections 4.1 to 4.3 were quite approximate.

Moreover, as the effective damping ratios calculated on Section 4.3 using the State Space Formulation and the Simplified Formulations resulted expressively approximate too, in this subchapter the simplified formulation method will be used.

Initially, to evaluate the influence of the damping installation on each floor, it was simulated situations where the same devices presented on Section 4.3 were applied only on the first floor, on the first and second floor and lastly the results were compared to the previous simulation (devices installed on the three floors).

The effective damping factors were calculated only for the first vibration mode, as this mode is the most significant. The results are available on Table 8.

Table 8 – Effective damping considering different situations (2.6 kN.s/m per floor)

| Location of damping devices | Floor | Damping coefficient installed (N.s/m) | Effective Damping |
|---|---|---|---|
| First floor only | 1 | 2600 | 1.72 % |
| | 2 | 0 | |
| | 3 | 0 | |
| First and second floor | 1 | 2600 | 2,38 % |
| | 2 | 2600 | |
| | 3 | 0 | |
| First, second and third floor | 1 | 2600 | 2,59 % |
| | 2 | 2600 | |
| | 3 | 2600 | |

From these results, it can be observed that the difference of damping between the second and the third case is minimum. If we could replace the 2.6 kN.s/m installed on the third floor to the first and second

floors, adding 1.3 kN.s/m on each one, or 2.6 kN.s/m in one of them, the following results would be obtained:

Table 9 – Redistribution of damping devices on the structure

| Location of damping devices | Floor | Damping coefficient installed (N.s/m) | Effective Damping |
|---|---|---|---|
| First and second floor | 1 | 2600+1300=3900 | 3.07 % |
| | 2 | 2600+1300=3900 | |
| | 3 | 0 | |
| First floor only | 1 | 2600+2600=5200 | 2.45 % |
| | 2 | 0 | |
| | 3 | 0 | |
| Second floor only | 1 | 0 | 2.31 % |
| | 2 | 2600+2600=5200 | |
| | 3 | 0 | |

Thus, the conclusion that can be obtained is that the structure can provide a most efficient behavior when the damping coefficient in the first and second floors is increased, as these two are most influential on achieving a higher effective damping factor on the structure.

The experimental test developed on the structural frame were done applying 4 devices per floor, by using the available devices that present the higher damping coefficients. These experimental results are shown in sub-chapter 6.2, and they were performed applying the devices initially only on the first floor, and secondly on the first and second floor.

In order to compare the response of the structure determined by the formulations and by experimental tests, the theoretical results are shown below.

Table 10 - Effective damping considering four devices per floor, on 1st floor only

| Location of damping devices | Amount of Devices | Device's Damping Coefficient (N.s/m) | Total Damping Coefficient (N.s/m) | Effective Damping |
|---|---|---|---|---|
| First floor | 2 | 1852.18 | 5098 | 2.42% |
| | 2 | 696.79 | | |

Table 11 - Effective damping considering four devices per floor, on 1st and 2nd floor

| Location of damping devices | Amount of Devices | Device's Damping Coefficient (N.s/m) | Total Damping Coefficient (N.s/m) | Effective Damping |
|---|---|---|---|---|
| First floor | 2 | 1852.18 | 5098 | 3.18% |
| | 2 | 696.79 | | |
| Second floor | 4 | 753.4 | 3014 | |

It is important to note that in this simulation, the calculus was proceeded considering the damping coefficients determined through the damping characterization tests (sub-chapter 6.1), and not the coefficients provided by the manufacturer, aiming results closer to reality.

To reach the goals of 10, 15 and 20%, the inverse calculus was done. Considering that it would be installed the same damping coefficient on each floor, the Equation 3.39 was adapted to determine the coefficient needed to achieve the three damping ratios (Equation 4.23). Again, the devices were considered installed on the first and second floors only.

$$C_g = (\xi_{eff} - \xi_0) \cdot \frac{4\pi \cdot \sum m_i \cdot \phi_i{}^2}{T \cdot \sum \phi_{rg}{}^2} \quad (4.\ 23)$$

The results of the damping coefficients needed on each floor are exposed on Table 12.

Table 12 – Damping coefficient needed (same coefficients on each floor)

| Effective Damping Goal $\xi_{eff}$ | Floor | Damping coefficient needed (N.s/m) - $C_g$ | Proposed solution |
|---|---|---|---|
| 10 % | 1 | 17000 | 4 devices x 4.25 kN.s/m |
| | 2 | 17000 | 4 devices x 4.25 kN.s/m |
| | 3 | 0 | - |
| 15 % | 1 | 26500 | 4 devices x 6.70 kN.s/m |
| | 2 | 26500 | 4 devices x 6.70 kN.s/m |
| | 3 | 0 | - |
| 20 % | 1 | 36000 | 4 devices x 9.00 kN.s/m |
| | 2 | 36000 | 4 devices x 9.00 kN.s/m |
| | 3 | 0 | - |

Besides the solutions presented to achieve the effective damping (10, 15 and 20%), infinite other possible solutions can be defined through different attempts, now considering that the total damping coefficients installed on first and second floor are different from each other. Aiming devices with coefficients between 2 to 6 kN.s/m, some solutions are exposed on Table 13.

Table 13 - Damping coefficient needed (different coefficients on each floor)

| Effective Damping Goal $\xi_{eff}$ | Floor | Damping coefficient needed (N.s/m) - $C_g$ | Proposed solution |
|---|---|---|---|
| 10 % | 1 | 20000 | 8 devices x 2.5 kN.s/m |
| | 2 | 14000 | 4 devices x 3.5 kN.s/m |
| | 3 | 0 | - |
| 15 % | 1 | 30000 | 8 devices x 3.75 kN.s/m |
| | 2 | 22500 | 4 devices x 5.70 kN.s/m |
| | 3 | 0 | - |
| 20 % | 1 | 40000 | 8 devices x 5.00 kN.s/m |

| | | | |
|---|---|---|---|
| | 2 | 31500 | 8 devices x 4.00 kN.s/m |
| | 3 | 0 | - |

# 5

# SEISMIC RESPONSE DETERMINATION

## 5.1 COMPARISON BETWEEN THE STATE SPACE FORMULATION AND THE EC-8 RECOMMENDATIONS (1 DEGREE-OF-FREEDOM STRUCTURE)

As explained on section 3.3.1, besides of the modal damping determination, the State Space Formulation can determine the response of a structure due to the application of external forces, as a seismic action, for example.

In this work, a comparative analysis was developed through the determination of the response of a structure considering different levels of damping applied on the laboratory frame, using the state space formulation. After that, the results were compared to the ones obtained by using the formulation presented on Eurocode 8 (EC-8).

The European Regulation (EC-8) affirms that the spectrum of horizontal elastic response can be defined by using the following equations:

$$0 \leq T \leq T_B:\ S_e(T) = a_g \times S \times \left[1 + \frac{T}{T_B} \times (\eta \times 2.5 - 1)\right] \quad (5.\ 1)$$

$$T_B \leq T \leq T_C:\ S_e(T) = a_g \times S \times \eta \times 2.5 \quad (5.\ 2)$$

$$T_C \leq T \leq T_D:\ S_e(T) = a_g \times S \times \eta \times 2.5 \times \left[\frac{T_C}{T}\right] \quad (5.\ 3)$$

$$T_D \leq T \leq 4s:\ S_e(T) = a_g \times S \times \eta \times 2.5 \times \left[\frac{T_C \times T_D}{T^2}\right] \quad (5.\ 4)$$

Where:

- $S_e(T)$ is the elastic response spectrum;

- $T$ is the vibration period of a linear single-degree-of-freedom system;
- $a_g$ is the design ground acceleration;
- $T_B$ is the lower limit of the period of the constant spectral acceleration branch;
- $T_C$ is the upper limit of the period of the constant spectral acceleration branch;
- $T_D$ is the value defining the beginning of the constant displacement response range of the spectruln;
- $S$ is the soil factor;
- $\eta$ is the damping correction factor with a reference value of $\eta$ = 1 for 5% viscous dampingThe design ground acceleration "$a_g$" is adopted accordingly to the seismic zone, being determined using the following equation.

$$a_g = \gamma_I \times a_{gR} \tag{5. 5}$$

The advisable values of "$a_{gR}$" to be used are listed in the National Annex of the EC-8, and are divided by seismic zones, to the 2 types of seismic actions (type 1 or 2). The factor $\gamma_I$ is usually used equal to 1, but it depends on the structure importance.

According to the regulation, the values of the periods $T_B$, $T_C$, $T_D$ and the soil factor $S$ that describe the form of the response spectrum depends on the ground type (A, B, C, D or E) and the type of seismic action. The recommended values to use are also all listed in the document.

Finally, it is needed to determine de damping correction factor $\eta$, that can be fixed using the following formulation, described on the EC-8:

$$\eta = \sqrt{\frac{10}{5 + \xi}} \tag{5. 6}$$

$\xi$ is the viscous damping on the structure, expressed in percentage. As mentioned before, the value of $\eta$ is equal to 1 when the damping is 5%.

To proceed the comparison of responses, it was numerically generated 10 different earthquakes with 4096 points each one. By multiplying the accelerations to the mass of the structure, it was determined the external forces applied on the structure to each time interval, on each generated earthquake.

The response spectrum method is adequate for a single DOF systems, thus, the response was evaluated using a 1 DOF structure, considering its mass equal to 1 tonne and its stiffness equal to 1000 kN/m. It is important to mention that the extra damping of the structure ($C_d$) was considered null, consequently, the Damping Matrix "C" of the structure was classical, composed exclusively by the structure's natural damping ($C_0$).

Making the natural damping factor vary between 1 to 30%, the response of the single DOF structure was determined to each one of the 10 seisms. Posteriorly, there was calculated de average maximum displacement on the structure between the 10 simulations considering each level of structure damping. This calculation procedure in MatLab language is available on Annex 4.

The EC-8 informs that when the response to a 5% damping is known ($\eta$=1), the response to any other level of damping can be determined by multiplying the 5% response to the damping factor of the respective damping level.

Thus, the response of the structure was determined in the time domain using the State Space Formulation to damping levels of 1 to 30% and all these results were compared with the ones using the simplified method mentioned before (EC-8). The results are shown in Table 14, and the difference between the results of the both methods was calculated considering as the base value the displacement resulted through the State Space Formulation method. Thus, when the difference results positive, it means that the medium displacement calculated by the State Space Formulation is higher than the one calculated by EC-8 method, and when the difference is negative, the displacement calculated by the EC-8 method is higher, in other words, is more conservative than the State Space Formulation.

It was also generated a *Damping Factor x Medium Displacement* curve to each method, which is shown in Graphic 1.

Table 14 – Seismic response results (1-DOF system)

| **Damping Factor** | **State Space Formulation** | **EC-8 Method** | | **Difference** |
|---|---|---|---|---|
| | Medium displacement (m) | Medium displacement (m) | $\eta$ | |
| **1%** | 0,00842 | 0,00642 | 1,291 | 23,82% |
| **2%** | 0,00690 | 0,00594 | 1,195 | 13,90% |
| **3%** | 0,00600 | 0,00556 | 1,118 | 7,32% |
| **4%** | 0,00542 | 0,00524 | 1,054 | 3,42% |
| **5%** | 0,00497 | 0,00497 | 1,000 | 0,00% |
| **6%** | 0,00460 | 0,00474 | 0,953 | -3,10% |
| **7%** | 0,00431 | 0,00454 | 0,913 | -5,16% |
| **8%** | 0,00410 | 0,00436 | 0,877 | -6,32% |
| **9%** | 0,00394 | 0,00420 | 0,845 | -6,55% |
| **10%** | 0,00380 | 0,00406 | 0,816 | -6,90% |
| **11%** | 0,00367 | 0,00393 | 0,791 | -7,10% |
| **12%** | 0,00356 | 0,00381 | 0,767 | -7,13% |
| **13%** | 0,00347 | 0,00370 | 0,745 | -6,77% |
| **14%** | 0,00339 | 0,00361 | 0,725 | -6,25% |
| **15%** | 0,00332 | 0,00351 | 0,707 | -5,74% |
| **16%** | 0,00326 | 0,00343 | 0,690 | -5,30% |
| **17%** | 0,00319 | 0,00335 | 0,674 | -4,95% |
| **18%** | 0,00313 | 0,00328 | 0,659 | -4,66% |
| **19%** | 0,00307 | 0,00321 | 0,645 | -4,43% |

| | | | | |
|---|---|---|---|---|
| **20%** | 0,00301 | 0,00314 | 0,632 | -4,25% |
| **21%** | 0,00296 | 0,00308 | 0,620 | -4,12% |
| **22%** | 0,00291 | 0,00302 | 0,609 | -4,03% |
| **23%** | 0,00286 | 0,00297 | 0,598 | -3,98% |
| **24%** | 0,00281 | 0,00292 | 0,587 | -3,95% |
| **25%** | 0,00276 | 0,00287 | 0,577 | -3,84% |
| **26%** | 0,00272 | 0,00282 | 0,568 | -3,65% |
| **27%** | 0,00268 | 0,00278 | 0,559 | -3,50% |
| **28%** | 0,00265 | 0,00274 | 0,550 | -3,36% |
| **29%** | 0,00261 | 0,00270 | 0,542 | -3,24% |
| **30%** | 0,00258 | 0,00266 | 0,535 | -3,13% |

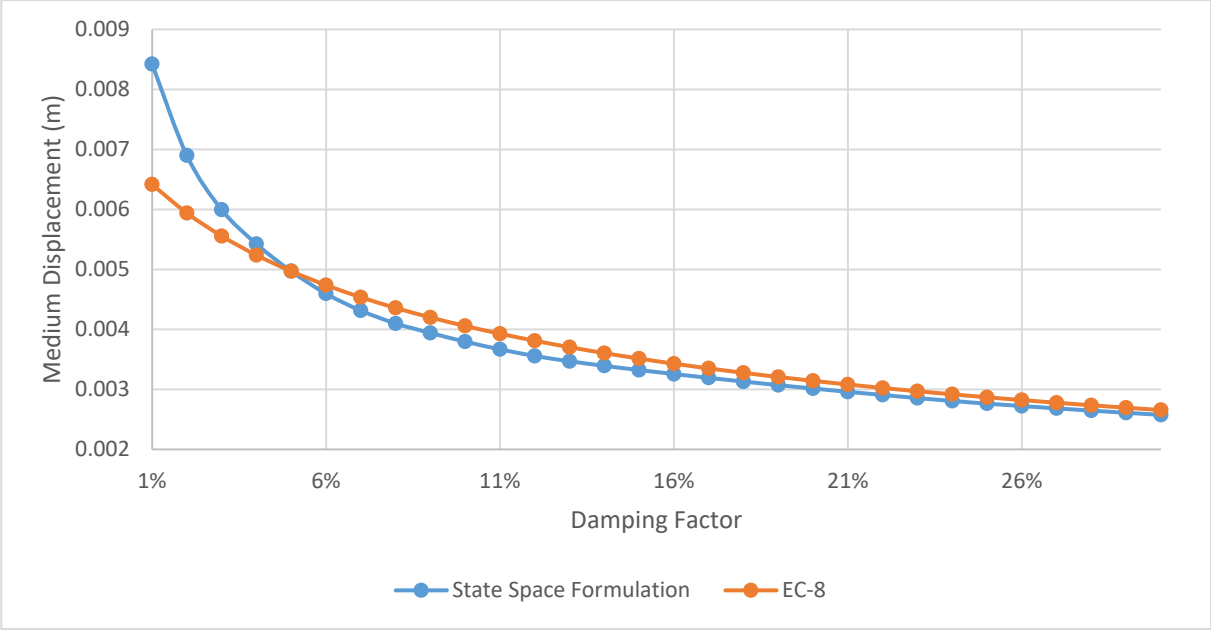


Graphic 1 – Damping Factor *versus* Medium Displacement curves (1-DOF system)

By the analysis of the results shown above, it can be noted that the difference between both methods can be considered low when a damping factor higher than 5%, as these difference are not superior to 8%.

Besides that, it can be highlighted that when the structure's damping factor is lower than 5%, the method recommended on the Eurocode 8 is not most conservative, as the displacements obtained using the State Space Formulation are higher than the displacements calculated using the damping correction factor suggested on the regulation. However, when the damping factor is higher than 5%, the EC-8 formulation can be accepted as a conservative method, resulting on displacements that exceeds the ones determined by the State Space Formulation.

## 5.2 STRUCTURAL RESPONSE BASED ON NON-CLASSICAL AND CLASSICAL DAMPING

To determine the seismic response of the 3 DOF structure studied on this work, the State Space Formulation was used. Considering null the natural damping of the structure, the response was determined to different levels of damping coefficients applied on each floor of the structure (always considering the same coefficients on the three floors), varying from 1 to 40 kN.s/m.

When applying on the structure damping coefficients on each floor, the damping matrix of the structure turns to be a non-classical matrix, constructed as explained on Section 3.2, but now composed only by the extra damping ($C_d$), as the natural damping of the structure ($C_0$) is considered null.

The damping factors of the structure associated to each vibration mode ($\xi_1$, $\xi_2$ and $\xi_3$) were calculated as explained on Section 3.3.1, considering the different damping coefficient imposed to the structure (Table 15). Moreover, the average displacements on the 3rd floor were calculated among the displacements for all the 10 earthquakes (Table 16). This calculation procedure in MatLab language can be consulted on Annex 5.

Table 15 – Damping factors associated to different damping coefficients

| C (kN.s/m) | ξ – 1ST mode | ξ – 2nd mode | ξ – 3rd mode |
|---|---|---|---|
| 1,0 | 0,6% | 1,6% | 2,2% |
| 2,0 | 1,2% | 3,3% | 4,5% |
| 3,0 | 1,8% | 4,9% | 6,7% |
| 4,0 | 2,4% | 6,6% | 9,0% |
| 5,0 | 3,1% | 8,2% | 11,2% |
| 6,0 | 3,7% | 9,8% | 13,5% |
| 7,0 | 4,3% | 11,5% | 15,7% |
| 8,0 | 4,9% | 13,1% | 18,0% |
| 9,0 | 5,5% | 14,7% | 20,2% |
| 10,0 | 6,1% | 16,4% | 22,4% |
| 11,0 | 6,7% | 18,0% | 24,7% |
| 12,0 | 7,3% | 19,6% | 26,9% |
| 13,0 | 8,0% | 21,3% | 29,2% |
| 14,0 | 8,6% | 22,9% | 31,4% |
| 15,0 | 9,2% | 24,6% | 33,7% |
| 16,0 | 9,8% | 26,2% | 35,9% |
| 17,0 | 10,4% | 27,8% | 38,2% |
| 18,0 | 11,0% | 29,5% | 40,4% |
| 19,0 | 11,6% | 31,1% | 42,7% |
| 20,0 | 12,2% | 32,7% | 44,9% |
| 21,0 | 12,9% | 34,4% | 47,1% |
| 22,0 | 13,5% | 36,0% | 49,4% |
| 23,0 | 14,1% | 37,7% | 51,6% |
| 24,0 | 14,7% | 39,3% | 53,9% |

| | | | |
|---|---|---|---|
| 25,0 | 15,3% | 40,9% | 56,1% |
| 26,0 | 15,9% | 42,6% | 58,4% |
| 27,0 | 16,5% | 44,2% | 60,6% |
| 28,0 | 17,1% | 45,8% | 62,9% |
| 29,0 | 17,7% | 47,5% | 65,1% |
| 30,0 | 18,4% | 49,1% | 67,4% |
| 31,0 | 19,0% | 50,7% | 69,6% |
| 32,0 | 19,6% | 52,4% | 71,9% |
| 33,0 | 20,2% | 54,0% | 74,1% |
| 34,0 | 20,8% | 55,6% | 76,4% |
| 35,0 | 21,4% | 57,3% | 78,6% |
| 36,0 | 22,0% | 58,9% | 80,9% |
| 37,0 | 22,6% | 60,6% | 83,2% |
| 38,0 | 23,2% | 62,2% | 85,4% |
| 39,0 | 23,9% | 63,8% | 87,7% |
| 40,0 | 24,5% | 65,5% | 89,9% |

The Damping Coefficient *versus* the Damping Factor of each vibration mode can be analyzed in Graphic 2.

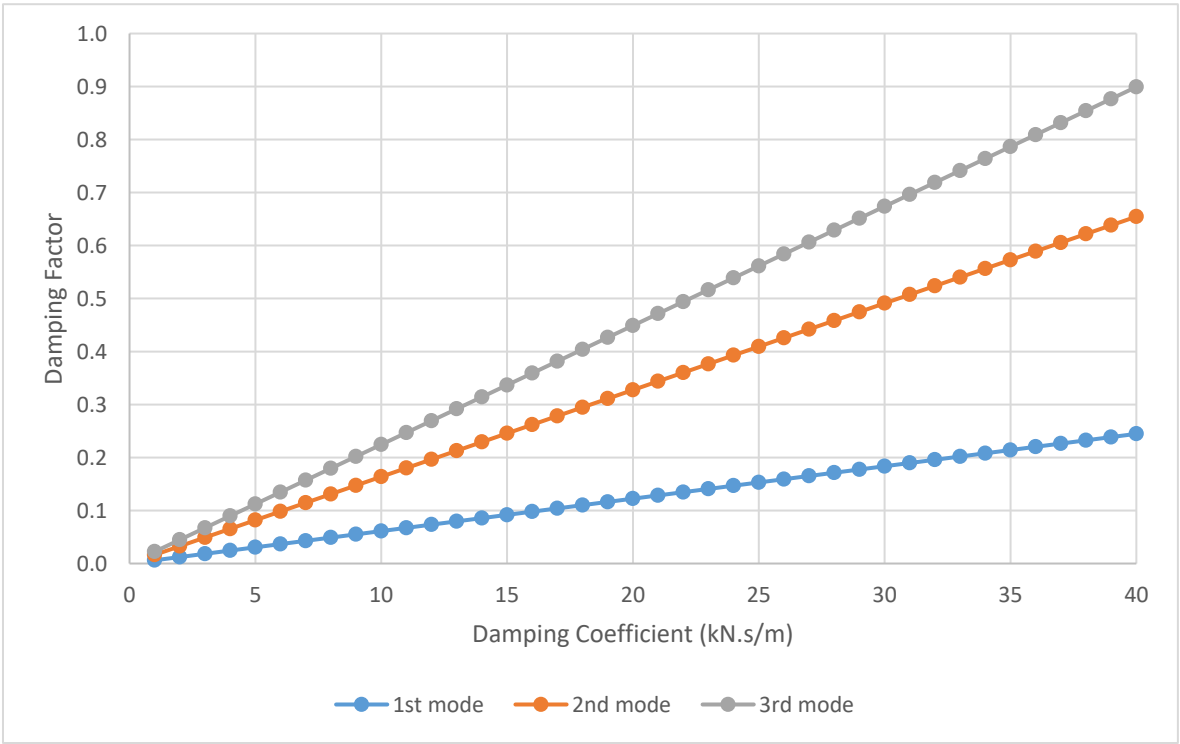


Graphic 2 - Damping Factors *versus* Damping Coefficients graphic (3-DOF system)

Now, the response of the structure was determined assuming a classical damping, in order to compare these results with the previously ones assuming non-classical damping (Table 16).

The "conversion" of the non-classical camping matrix ($C_d$) to a classical matrix was conducted through the use of the Rayleigh method explained in Section 3.1.4. When the damping factors and the natural

frequencies are known, it is possible to determine the parameters α and β (Equation 3.21), that will be used to construct the classical damping matrix, using Equation 3.15. This "conversion" procedure in MatLab language is available on Annex 6.

Finally, using the classical damping matrix, the same calculus routine is used to determine the average maximum displacements on the 3rd floor associated to each damping coefficient applied on the structure. In Table 16, the average displacements are listed side-by-side, considering the non-classical damping matrix and its "conversion" to a classical damping matrix.

Table 16 – Seismic Response comparing non-classical and classical damping

| C (kN.s/m) | Medium displacement (m) | | Difference |
|---|---|---|---|
| | Non-Classical Damping | Classical Damping | |
| 1,0 | 0,045835 | 0,045836 | 0,002% |
| 2,0 | 0,038698 | 0,038699 | 0,003% |
| 3,0 | 0,034897 | 0,034898 | 0,003% |
| 4,0 | 0,032323 | 0,032324 | 0,003% |
| 5,0 | 0,030250 | 0,030251 | 0,003% |
| 6,0 | 0,02855 | 0,028551 | 0,004% |
| 7,0 | 0,027199 | 0,027201 | 0,007% |
| 8,0 | 0,025966 | 0,025968 | 0,008% |
| 9,0 | 0,024837 | 0,024840 | 0,012% |
| 10,0 | 0,023804 | 0,023807 | 0,013% |
| 11,0 | 0,022878 | 0,022881 | 0,013% |
| 12,0 | 0,022023 | 0,022027 | 0,018% |
| 13,0 | 0,021275 | 0,021279 | 0,019% |
| 14,0 | 0,020645 | 0,020649 | 0,019% |
| 15,0 | 0,020116 | 0,020121 | 0,025% |
| 16,0 | 0,019616 | 0,019620 | 0,020% |
| 17,0 | 0,019163 | 0,019168 | 0,026% |
| 18,0 | 0,018735 | 0,018741 | 0,032% |
| 19,0 | 0,01833 | 0,018336 | 0,033% |
| 20,0 | 0,017942 | 0,017950 | 0,045% |
| 21,0 | 0,017574 | 0,017582 | 0,046% |
| 22,0 | 0,017225 | 0,017234 | 0,052% |
| 23,0 | 0,016926 | 0,016936 | 0,059% |
| 24,0 | 0,016649 | 0,016659 | 0,060% |
| 25,0 | 0,016384 | 0,016395 | 0,067% |
| 26,0 | 0,016132 | 0,016143 | 0,068% |
| 27,0 | 0,01589 | 0,015902 | 0,076% |
| 28,0 | 0,015657 | 0,015670 | 0,083% |
| 29,0 | 0,015433 | 0,015446 | 0,084% |
| 30,0 | 0,015215 | 0,015229 | 0,092% |
| 31,0 | 0,015006 | 0,015020 | 0,093% |
| 32,0 | 0,014804 | 0,014820 | 0,108% |

| | | | |
|---|---|---|---|
| 33,0 | 0,014612 | 0,014628 | 0,109% |
| 34,0 | 0,014426 | 0,014443 | 0,118% |
| 35,0 | 0,014246 | 0,014263 | 0,119% |
| 36,0 | 0,014073 | 0,014090 | 0,121% |
| 37,0 | 0,013905 | 0,013922 | 0,122% |
| 38,0 | 0,013741 | 0,013759 | 0,131% |
| 39,0 | 0,013581 | 0,013600 | 0,140% |
| 40,0 | 0,013425 | 0,013445 | 0,149% |

It can be observed that the average displacement resulted very approximate between the both considerations, showing differences lower than 0.15%, as the Damping Factor *versus* Medium Displacement curves resulted superimposed (Graphic 3).

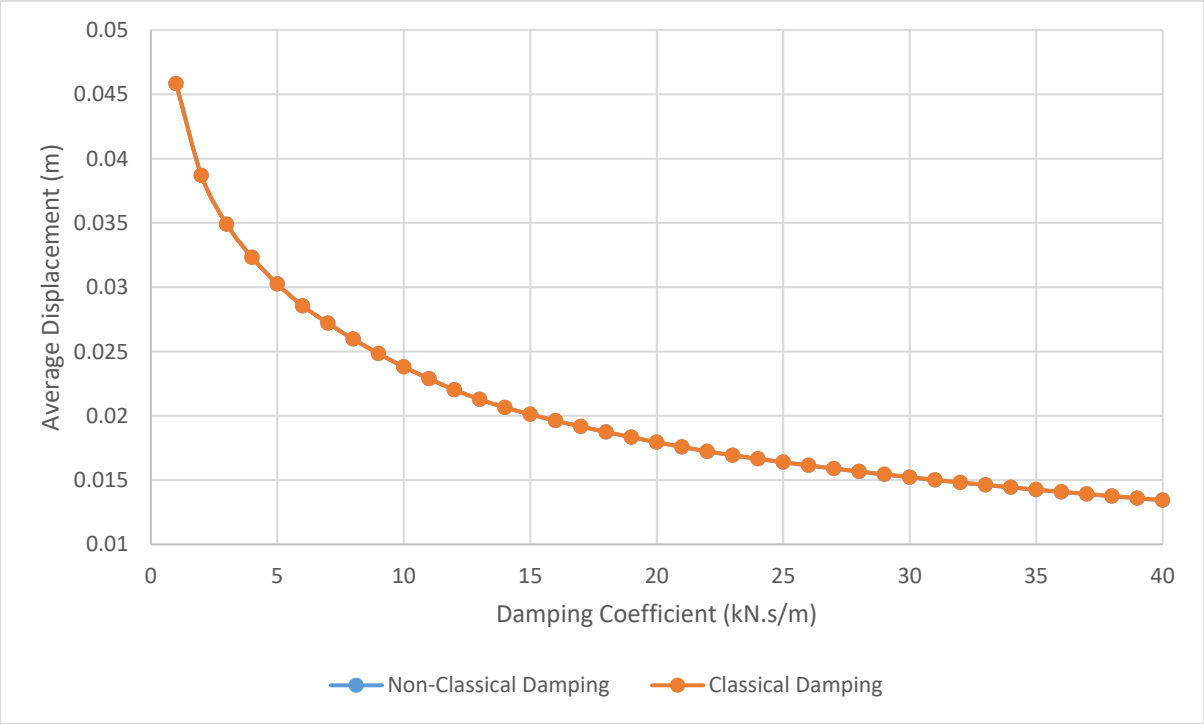


Graphic 3 – Damping Factor *versus* Medium Displacement curves considering Non-Classical and Classical damping (3-DOF system)

This comparative analysis was developed to verify and confirm the validity of the classical methods on the seismic design of damped structures, as the response of damped structures is based on a non-classical damping, but the traditional methods assume classical damping.

Thus, it can be affirmed that a conventional modal analysis can be used on the determination of seismic response of viscous damped structures.

# 6

# EXPERIMENTAL TESTS

## 6.1 TESTS WITH DAMPERS

First, it is necessary to characterize the different types of available dampers to determine each damping coefficient, before applying them in the laboratory structure. Each damper was positioned in an equipment that applies sinusoidal forces (Figure 14) and submitted to different levels of force amplitudes. Dampers with a total stroke of 50mm and 100mm were tested in frequencies of 0,5 to 3 Hz.


Figure 14 – Equipment that applies sinusoidal force

This equipment provides the ection of the relevant data, which are displacement (mm) and velocity (mm/s). Besides these values, it is also important to extract the load that is applied on the damper when it is being tested (Figure 15 and Figure 16). This measurement turns possible with the use of a load cell.

In this work, the dampers characterization tests were performed with two load cells with different load capacities shown in Table 17. First, it was necessary to perform a calibration test on the cell to convert its output on Voltage to Newton, by charging a known mass in the cell and measuring the electrical voltage output.

Table 17 – Load cells capacities

| Load Cell | HT Sensor – Model TAL220 | HT Sensor – Model TAS501 |
|---|---|---|
| Load Capacity | 10 kg | 200 kg |

To better illustrate and facilitate the understanding, the damping characterization tests are shown below. The load cell “1” was used on the first tests (TAL220) and cell “2” on the second tests (TAS501). Moreover, in the second tests, it was also used a displacement sensor, indicated as “3”. This displacement sensor was calibrated using the same procedure as the load cell calibration tests. Thus, in the second tests, the displacement data were provided by the displacement sensor, and not by the equipment output. In this case, the velocity was posteriorly determined by a numerical derivative method.

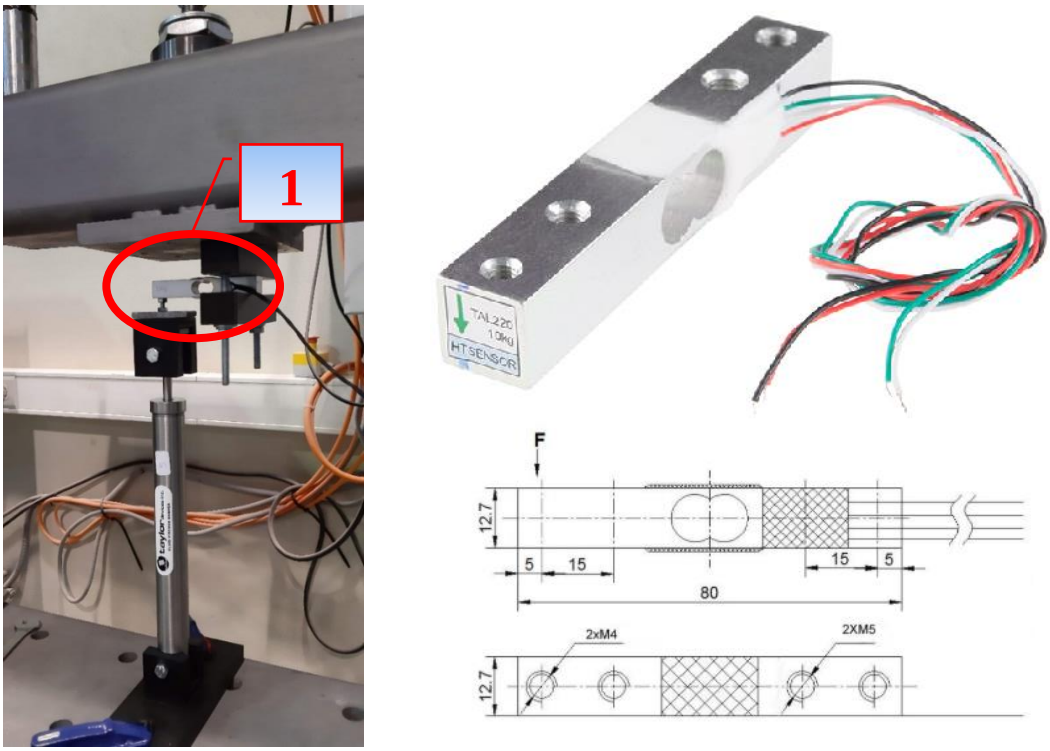


Figure 15 - Dampers Characterization Tests: Load Cell “1” details

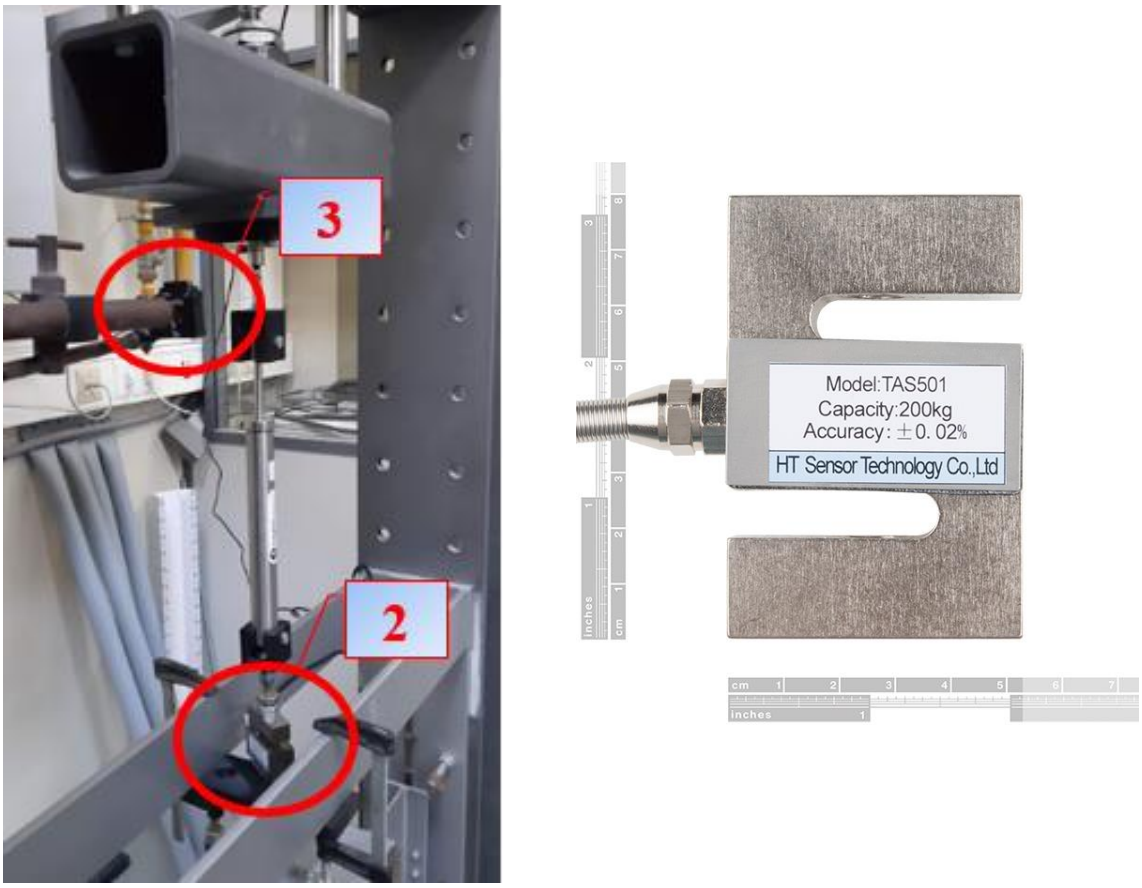


Figure 16 - Dampers Characterization Tests: Load Cell “2” details

With the information provided by the equipment and the load cell, the velocity *versus* force graphic can be plotted, and through this graphic, its tendency line can be defined. By knowing the equation of the tendency line, the damping coefficient (N.s/m) is determined because it is equal to its angular coefficient. Each calculated damping coefficient was compared with the provided by the manufacturer. The graphics velocity *versus* force and displacement *versus* force graphics of each performed tests can be visualized in Annex 1 and Annex 2.

On the first tests, in order to avoid high stresses and risk of damage of the dampers, the amplitude of motion for the 100m dampers was limited to ±40mm (using 80mm of its total stroke), and for the 50mm dampers, limited to ±20mm (using 40mm of its total stroke). This test was performed with the application of forces on a much different scale than the reading range of the cell, which caused a visible residue on the results provided, making them inaccurate.

As an alternative to match the reading range of the cell and the scale of the applied load, the second tests were needed. Now with an appropriate load cell that reads the results with more accuracy, as its load capacity reading is more approximate of the applied load.

The second tests were performed only with the damper devices that would be used in the structural frame. Considering that the frame can receive at most four devices per floor, and they would be applied

only on the first and second floor, the eight devices with the highest coefficients (considering the coefficients provided by the manufacturer) were applied to the structure, as explained on Section 4.4. These devices' references are: 20-5, 19-5 and 25-30.

The devices were all submitted to frequencies of 2.5 Hz with variable amplitude of motion. The devices 19-5 and 25-30 were tested five times, with the amplitude ranging from 5 to 25mm, every 5mm. The device 20-5 was tested three times with amplitudes of 5, 10 and 15mm.

Considering the results of all the tests of each tested damper, it can be observed that the damping coefficient obtained is not a constant value, but there is a tendency for the damping coefficient to decline when increasing the maximum speed (Graphic 4). Thus, the damping coefficient of each device was determined by the average of the coefficients determined on the tests with different amplitudes.

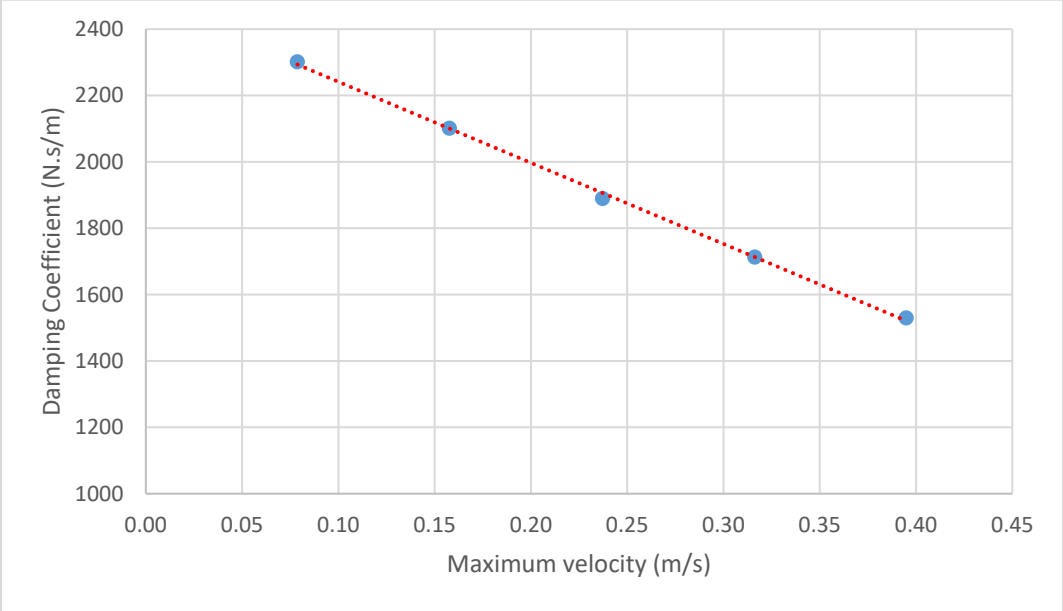


Graphic 4 – Damping Coefficient *versus* Maximum Velocity results of device 25-30 (decay trend of the coefficient values)

The results of the second tests are listed on Table 18. These obtained damping coefficients were used on the numerical simulations of the structural frame.

Table 18 - Results of dampers characterization

| Reference | Total stroke (mm) | Damping Coefficient (N.s/m) |
|---|---|---|
| 20-5 | 50.0 | 753.40 |
| 19-5 | 100.0 | 696.79 |
| 25-30 | 100.0 | 1852.18 |

## 6.2 DYNAMIC TESTS

The laboratory structure described and characterized in the previous chapters was experimentally tested to evaluate its response and behavior when submitted to sinusoidal and seismic actions.

To compare the different responses, the structure was initially tested with no additional damping, then with damping devices only on the first floor, and finally with damping devices installed in the first and second floors, as shown in Figure 17.

(a) (b) (c)

Figure 17 – Structural framed. (a) Without extra damping; (b) With extra damping on 1st floor; (c) With extra damping on 1st and 2nd floors.

The damping devices were installed in parallel, two on each vertical plan of each floor, as represented in Figure 18 and Figure 19.

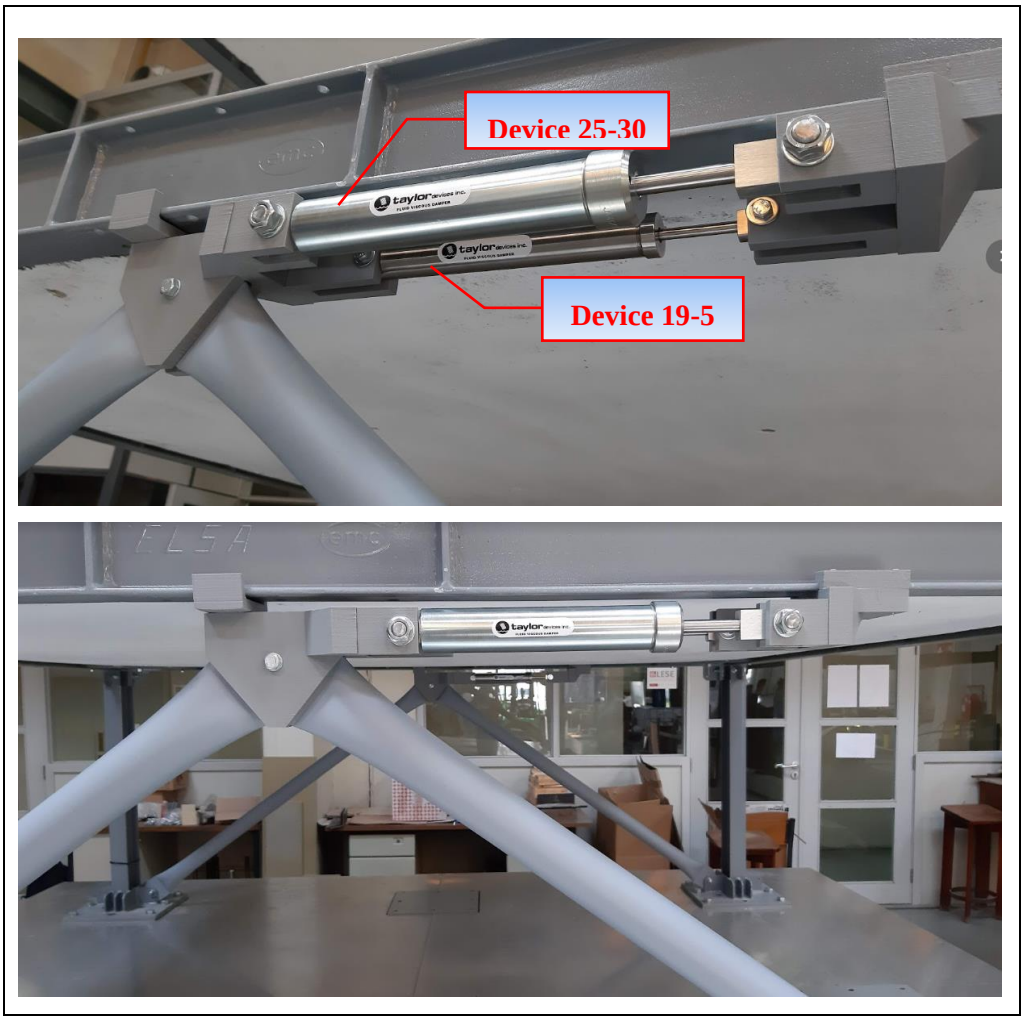


Figure 18 - Damping devices positioned on 1st floor

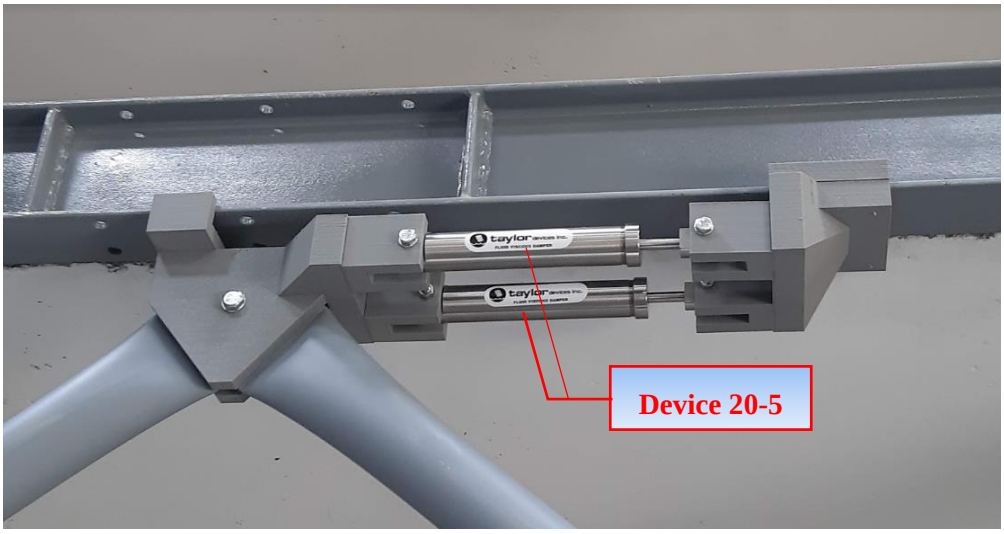


Figure 19 - Damping devices positioned on 2nd floor

The experimental part of this work can be divided on three distinct parts: the frequency tests, free-vibration tests and seism tests. Each one will be explained in Sections 6.2.1, 6.2.2 and 6.2.3.

### 6.2.1 FREQUENCY TESTS

Initially, the structure without any damping devices was submitted to a generated white noise signal, aiming at reaching the natural frequencies of the frame. This test allowed the determination of the three natural frequencies.

A random function with 30,000 points was created, with an amplitude ranging from -1 to 1 over a frequency range of 0-25 Hz, and an average equal to zero. The generated displacement function is represented on Graphic 5.

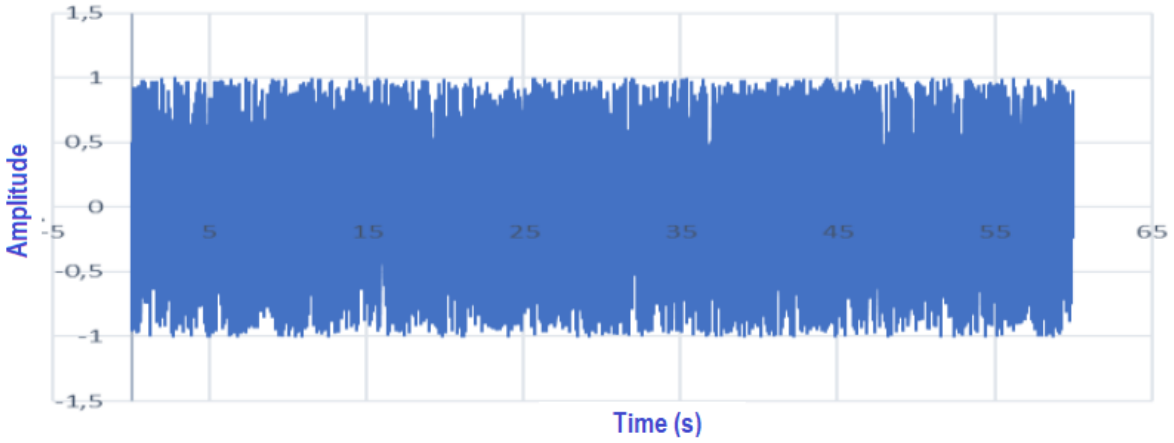


Graphic 5 - White noise spectrum

To extract the data, an accelerometer was installed on the top of a column located in the third floor of the structure. The average frequency spectrum of the structure response is represented Figure 20.

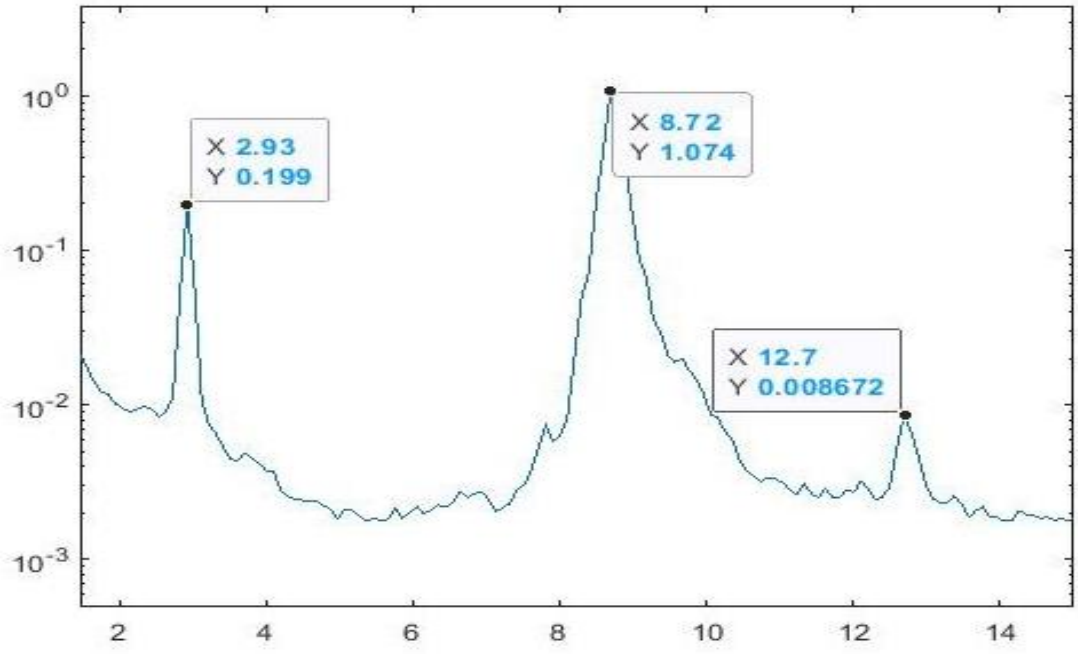


Figure 20 – Spectral density function of the white noise response (normalized medium spectrum)

This measurement was made only on the top of the third floor, since this spot is distinctly affected by the contribution of different resonant modes in the direction of lower inertia. With the experimental results obtained of the natural frequencies, it is possible to compare them to the frequencies previously calculated (Table 19).

Table 19 – Frequency test results

| Vibration Mode | Calculated Natural Frequency (Hz) | Obtained Natural Frequency (Hz) |
|---|---|---|
| 1 | 2.46 | 2.93 |
| 2 | 7.17 | 8.72 |
| 3 | 10.90 | 12.70 |

By the comparison between the expected and obtained frequencies, it can be confirmed that the tests results achieved higher values than the previously calculated ones, but they can still be considered approximate.

### 6.2.2 FREE VIBRATION TEST

The free vibration tests were performed aiming the determination of the modal damping factors of the structure considering the three cases of study: when the framed have none extra damping installed, when the damping devices are installed on the first floor only, and finally when they are installed on the first and second floors.

When the modal damping factors of each case are known the structure's response attenuation can be analyzed. Moreover, the comparison of the experimental results with the previous theoretical results (Chapter 4) is possible.

This experiment was developed by positioning and fixing the structure on a seismic table that was subjected the sinusoidal actions. The test were performed three times for each case of study: applying three different resonant excitation frequencies and, by suddenly stopping the shaking table, leaving the structure in free vibration.

The accelerometer positioned on the structure provides the acceleration on the point that it is installed, and by the extraction of the structure response is possible to obtain the time *versus* acceleration graphic of its free decay. The decay curve is an exponential function defined as

$$y(x) = A \cdot e^{b \cdot x} \tag{6. 1}$$

Where A and b are constant values. On a dynamic analysis, the decay curve of a structure that is submitted to a sinusoidal force can be defined as

$$a(t) = A \cdot e^{-\xi \cdot \omega \cdot t} \tag{6. 2}$$

Where $a(t)$ is the acceleration on a determined instant of time "t", $\xi$ is the modal damping factor and $\omega$ is the natural frequency of the sinusoidal action. Thus, the damping factor of each vibration mode can be determined by matching the constant value "b" that is multiplying the variable "x" on the equation to the product of "$-\xi \cdot \omega$" of each mode:

$$b = -\xi \cdot \omega \quad \Rightarrow \quad \xi = -\frac{b}{\omega} \tag{6. 3}$$

The natural frequencies of each vibration mode were calculated through the frequencies obtained in the frequency test, following the Equation 3.8. The results are shown in Table 20.

Table 20 – Natural Frequencies (ω)

| Vibration mode | Natural Frequency (rad/s) |
|---|---|
| 1 | 18.41 |
| 2 | 54.79 |
| 3 | 79.80 |

The results of the experimental tests related to the first case of study (no damping devices applied on the structure) are detailed on Graphic 6, Graphic 7, Graphic 8 and Table 21.

The first mode test was performed by placing the accelerometer in the top of the third floor, limiting the amplitude of displacement of the sinusoidal action to 0.50 mm. The excitation frequency was set to 2.93 Hz.

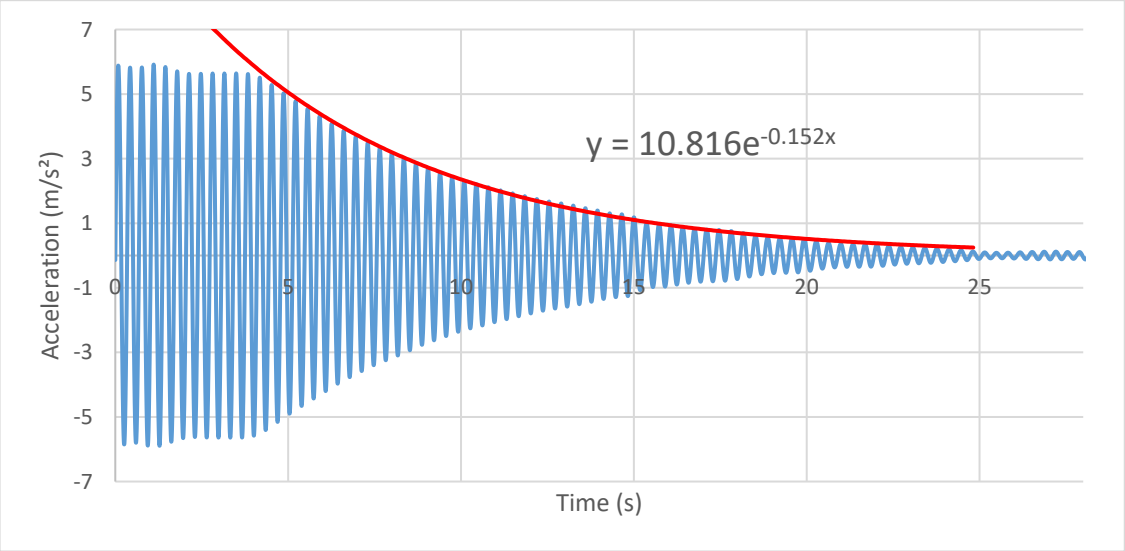


Graphic 6 - Decay curve of the 1st vibration mode (no extra damping applied on the structure) – 2.93 Hz

The second and third mode tests were performed with vibration frequencies of 8.72 and 12.70 Hz, respectively. They were performed by placing the accelerometer in the second floor, and limiting the amplitude of displacement of the sinusoidal action on 0.25 mm.

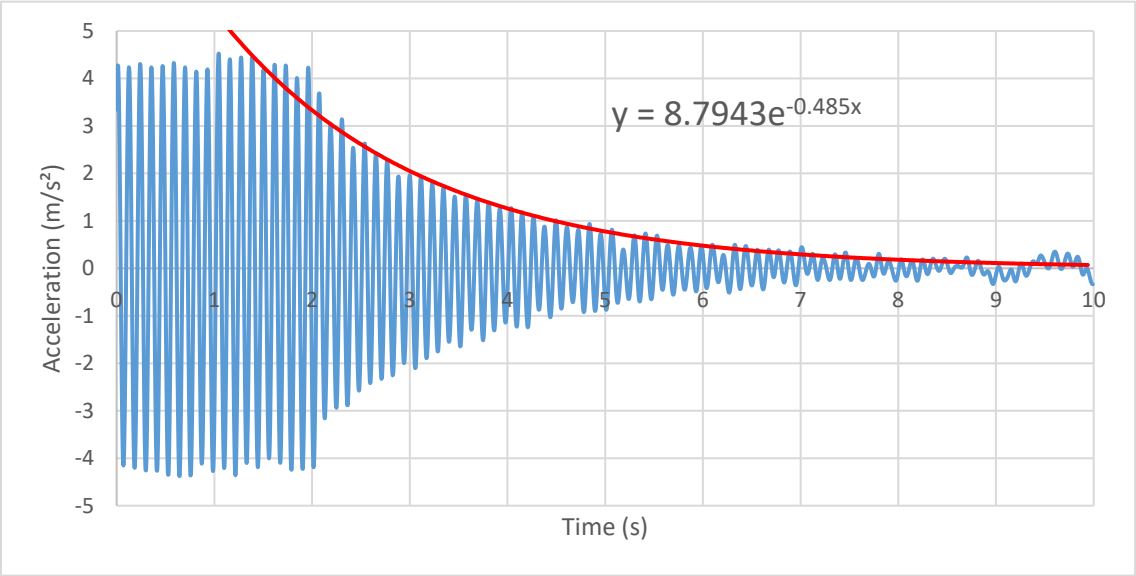


Graphic 7 - Decay curve of the 2nd vibration mode (no extra damping applied on the structure) – 8.72 Hz

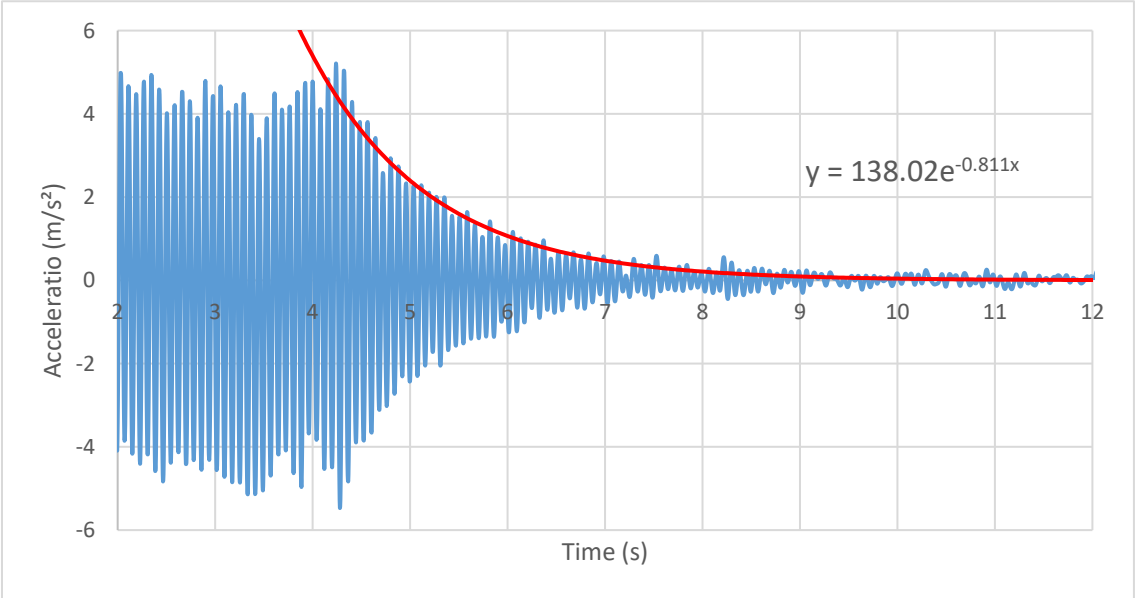


Graphic 8 - Decay curve of the 3rd vibration mode (no extra damping applied on the structure) – 12.70 Hz

Table 21 – Experimental results of first case of study (no extra damping applied on the structure)

| Vibration Mode | $\xi \cdot \omega$ | $\xi$ (obtained) | $\xi$ (calculated) (Table 6) |
|---|---|---|---|
| 1 | 0.152 | 0.83% | 1.00% |
| 2 | 0.485 | 0.89% | 1.00% |
| 3 | 0.811 | 1.02% | 1.30% |

The second and third cases of study (damping devices on the first floor only and damping devices on the first and second floor) were tested under the same conditions of the first case, with the same positions of the accelerometer, displacement amplitudes and vibration frequencies. The results of the second case test are exposed on Graphic 9, Graphic 10, Graphic 11 and Table 22. The results of the last case are visible on Graphic 12, Graphic 13, Graphic 14 and Table 23.

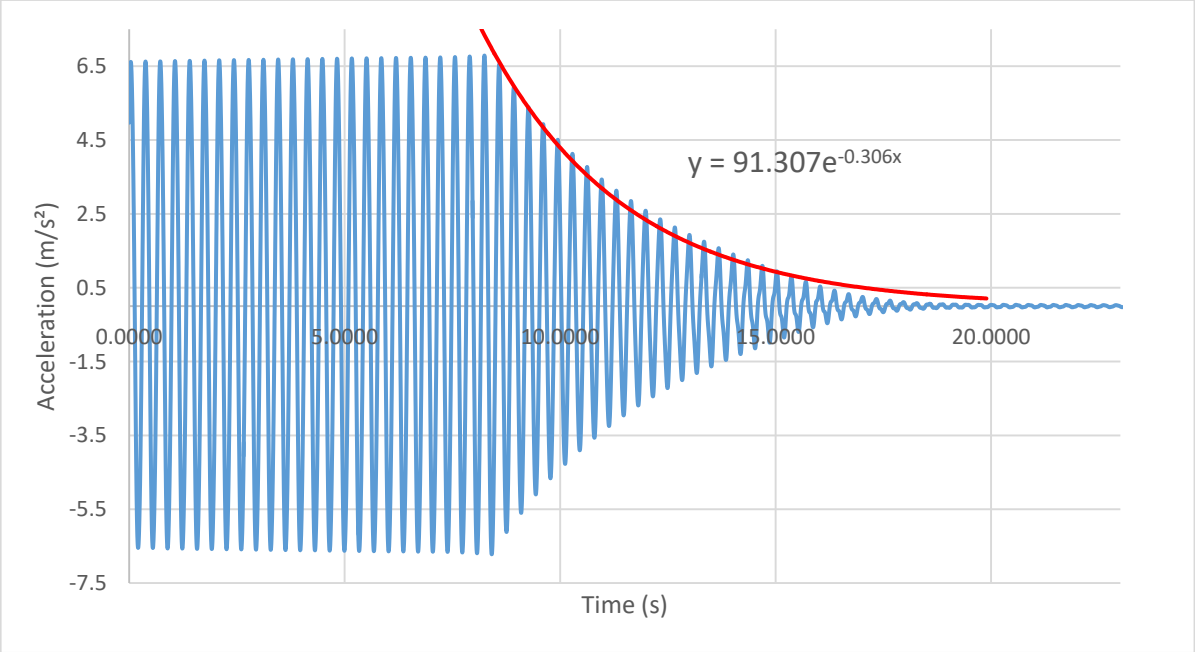


Graphic 9 - Decay curve of the 1st vibration mode (damping devices applied on first floor only) – 2.93 Hz

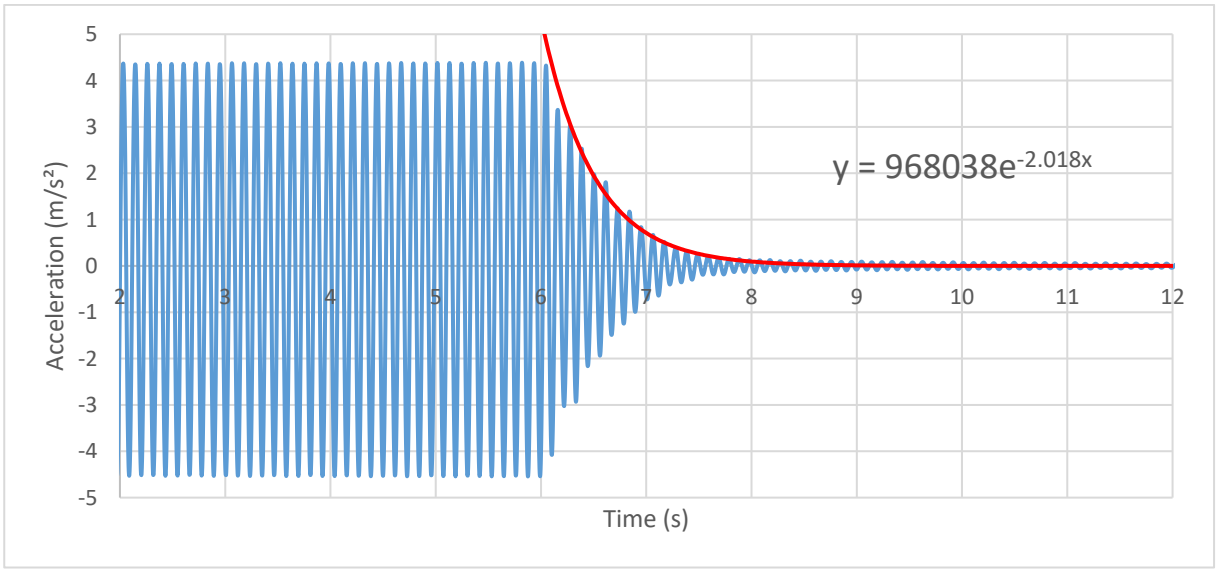


Graphic 10 - Decay curve of the 2nd vibration mode (damping devices applied on first floor only) – 8.72 Hz

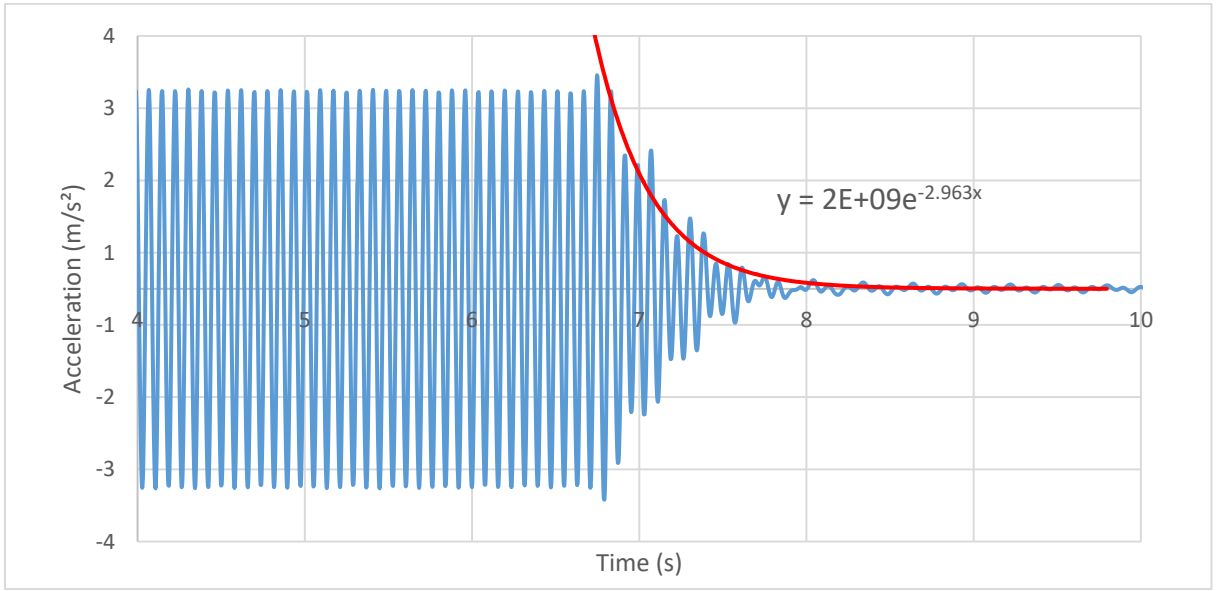


Graphic 11 - Decay curve of the 3rd vibration mode (damping devices applied on first floor only) – 12.70 Hz

Table 22 - Experimental results of second case of study (damping devices applied on first floor only)

| Vibration Mode | $\xi \cdot \omega$ | $\xi$ (obtained) | $\xi$ (calculated) |
|---|---|---|---|
| 1 | 0.306 | 1.66% | 2.42% |
| 2 | 2.018 | 3.68% | 3.78% |
| 3 | 2.963 | 3.71% | 2.68% |

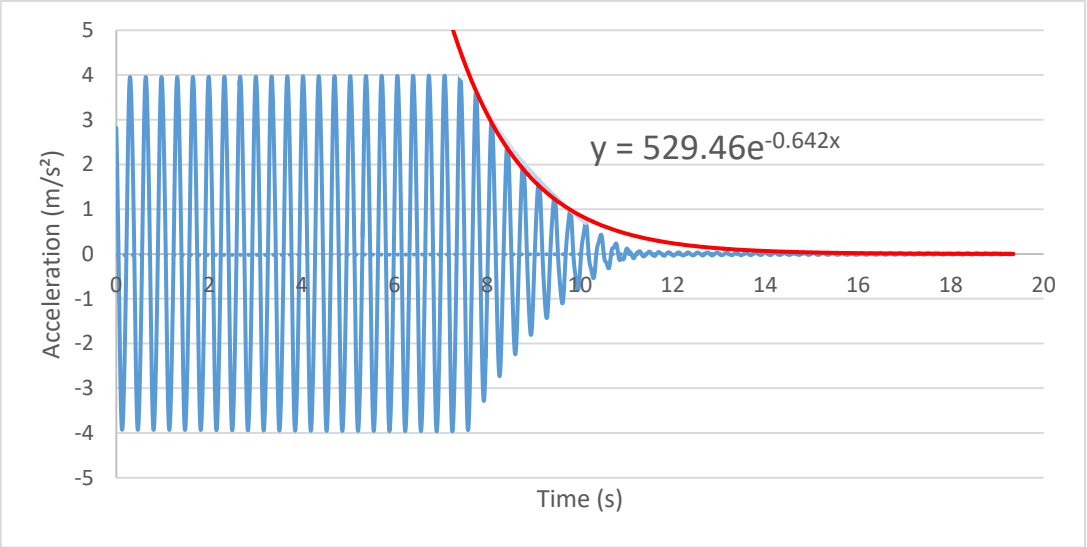


Graphic 12 - Decay curve of the 1st vibration mode (damping devices applied on first and second floors) – 2.93 Hz

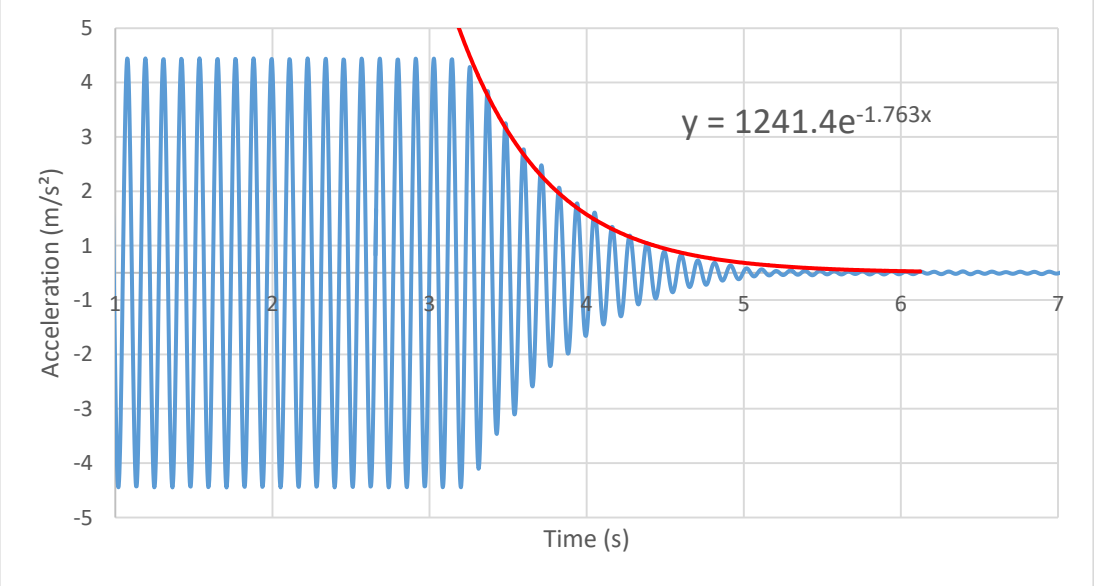


Graphic 13 - Decay curve of the 2nd vibration mode (damping devices applied on first and second floors) – 7.82 Hz

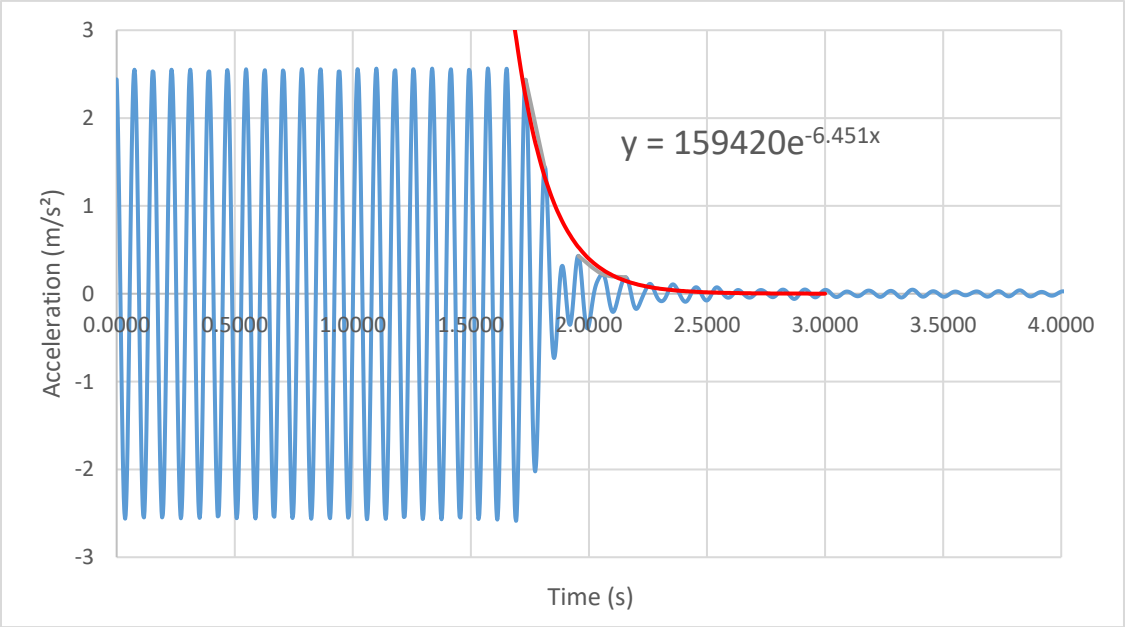


Graphic 14 - Decay curve of the 3rd vibration mode (damping devices applied on first and second floors) – 12.70 Hz

Table 23 - Experimental results of third case of study (damping devices applied on first and second floors)

| Vibration Mode | $\xi \cdot \omega$ | $\xi$ (obtained) | $\xi$ (calculated) |
|---|---|---|---|
| 1 | 0.6420 | 3.49% | 3.18% |
| 2 | 1.7630 | 3.22% | 4.15% |
| 3 | 6.4510 | 8.08% | 6.43% |

A brief comparative of the results of the three cases can be visualized on Graphic 15.

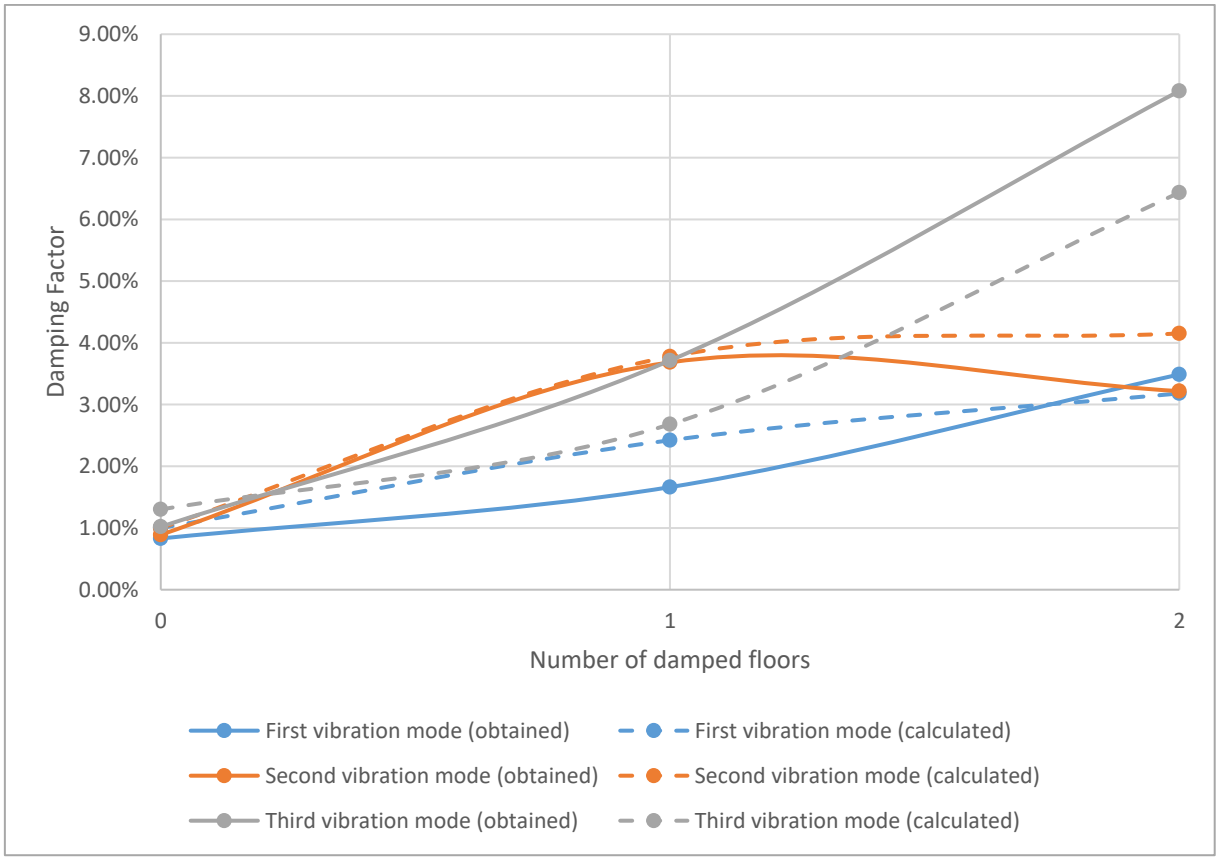


Graphic 15 – Comparative of obtained and expected damping factors

Through the analysis of the obtained results from the free vibration tests, and comparing them to the previously calculated damping factors, some conclusions can be taken. For the first vibration mode, the obtained damping factor exceeded the calculated only when the structure was damped on the first and second floors, as in the other cases the expected factor was higher.

In the second vibration mode, although the damping factors on the first and second case resulted significantly close, none of the three cases' obtained values achieved the expected damping factors. Moreover, the obtained damping factor of the third case of study (2 damped floors) resulted lower than the obtained factor of the second case (1 damped floor), differently from all the other cases in the three vibration modes.

However, the third vibration mode presented almost the opposite of the second vibration mode, as in exception of the first case (undamped structure), the obtained damping factors resulted higher than the expected values.

### 6.2.3 SEISMIC TEST

The laboratory structure was submitted to 10 different types of numerically generated earthquakes, all of them with the same peak acceleration. These tests were performed twice: initially with the structure without any damper device, and then with the devices installed on the first and second floors.

In each test, the acceleration on the top of the columns of the third floor was measured and compared with the results of the numerical simulations developed using the State Space Formulation. Since this formulation provides only the displacement and velocity on each floor and instant of time, the acceleration was obtained through the numerical derivation of velocity as a function of time.

The graphic results of the test and numerical simulations of the Seism 1 are shown in Graphic 16 and Graphic 17. The results of the remaining seisms (2 to 10) are shown in Annex 3. The horizontal axis of the graphics are referring to the time (s), and the vertical axis to the acceleration (m/s²).

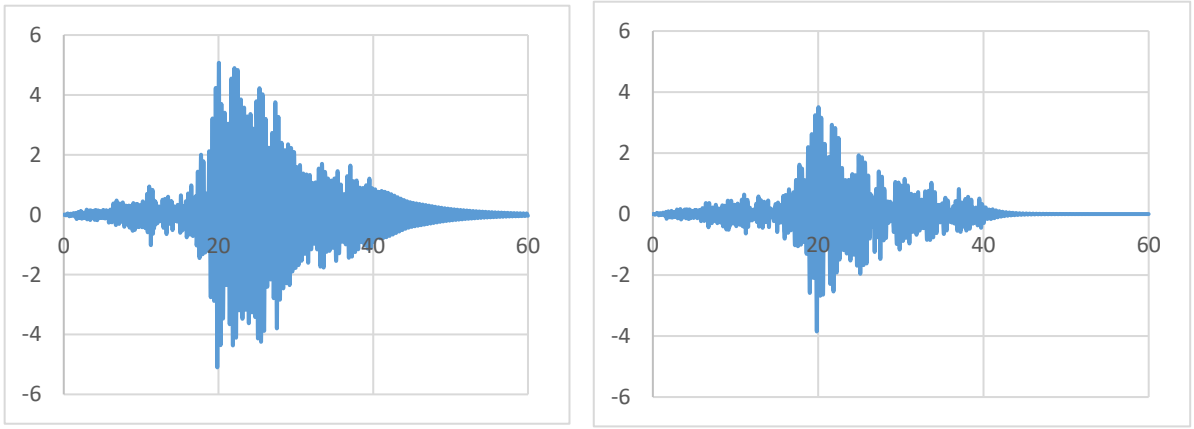


(a) (b)

Graphic 16 – State Space Formulation Results: Time (s) *versus* Acceleration (m/s²) graphic of Seism 1.
(a) Un-damped structure; (b) Damped structure

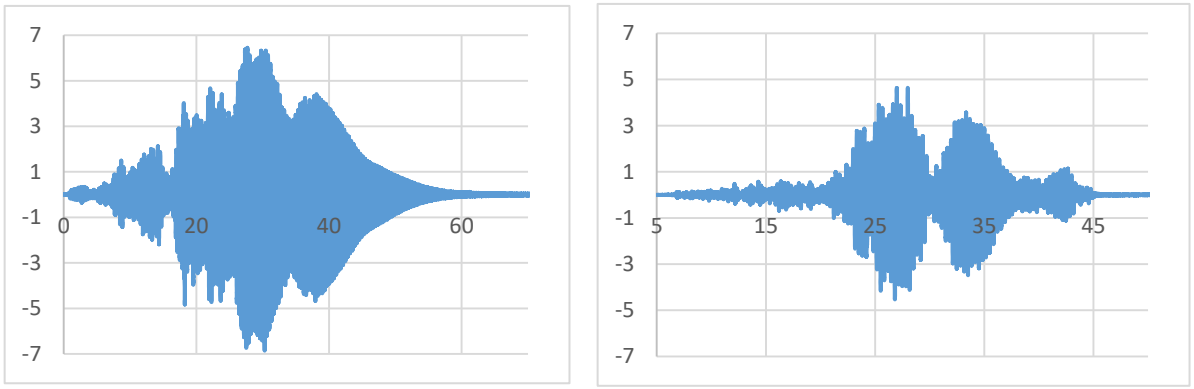


(a) (b)

Graphic 17 – Simulation Test Results: Time (s) *versus* Acceleration (m/s²) graphic of Seism 1.
(a) Un-damped structure; (b) Damped structure

Graphic 16 and all the State Space Formulation graphics in Annex 3 are expressed in terms of relative acceleration to the ground, while Graphic 17 and the simulation tests graphics in Annex 3 are represented in terms of absolute acceleration.

The maximum accelerations achieved in the simulation tests were compared to the maximum accelerations obtained in the numerical simulations determined through the State Space Formulation, and the results are listed on Table 24 and Table 25.

The response attenuation ($\Delta_a$) was determined using the following equation:

$$\Delta_a = \frac{a_D - a_{UD}}{a_{UD}} \times 100 \quad (6.\ 4)$$

Where $a_D$ is the maximum acceleration on the 3rd floor of the damped structure and $a_{UD}$ is the maximum acceleration on the 3rd floor of the un-damped structure.

Table 24 - State Space Formulation results: Maximum Acceleration on the 3rd floor

| Seism | Maximum Acceleration on the 3rd floor (m/s²) | | Response attenuation |
|---|---|---|---|
| | Un-damped structure | Damped structure | |
| 1 | 5.10 | 3.85 | -24.51% |
| 2 | 4.41 | 3.31 | -24.96% |
| 3 | 5.46 | 3.73 | -31.62% |
| 4 | 5.09 | 4.03 | -20.91% |
| 5 | 5.57 | 3.76 | -32.55% |
| 6 | 6.32 | 3.42 | -45.92% |
| 7 | 3.54 | 3.65 | 3.15% |
| 8 | 7.34 | 4.40 | -39.96% |
| 9 | 4.24 | 3.93 | -7.38% |
| 10 | 3.91 | 3.21 | -24.51% |
| | | **Medium response attenuation** | **-24.26%** |

Table 25 – Simulation Tests results: Maximum Acceleration on the 3rd floor

| Seism | Maximum Acceleration on the 3rd floor (m/s²) | | Response attenuation |
|---|---|---|---|
| | Un-damped structure | Damped structure | |
| 1 | 6.85 | 4.64 | -32.36% |
| 2 | 5.45 | 3.49 | -35.98% |
| 3 | 5.24 | 3.22 | -38.50% |
| 4 | 6.21 | 4.38 | -29.58% |
| 5 | 6.14 | 3.33 | -45.66% |
| 6 | 4.62 | 3.64 | -21.34% |
| 7 | 5.16 | 2.50 | -51.44% |

| | | | |
|---|---|---|---|
| 8 | 4.47 | 3.45 | -22.81% |
| 9 | 5.75 | 3.92 | -31.91% |
| 10 | 4.98 | 2.96 | -40.45% |
| | | **Medium response attenuation** | **-35.00%** |

It is curious to observe that in the numerical simulations in the case of seism 7 and 9 the damping system did not produce any significant effect. This is probably due to the main frequencies of these signals be away of the natural frequencies of the structure, and so, the structure response is not so conditioned by the damping of the vibration modes. Taking out these two cases, the results obtained from the numerical simulations using the State Space Formulation presented an average response attenuation of 30.62%, becoming closer to the experimental tests results, with an average attenuation response of 35%. This difference can be explained by the additional damping, beyond the damping provided by the viscous damping devices, that was noticed in the experimental tests as a friction damping. The diagonal bars and connections that were installed on the structure to receive and guide the devices may induce friction in the frame, which provided extra damping that was not considered in the numerical model.

# 7

# CONCLUSIONS

The development of this study aimed at the analysis of the seismic response of a 3-floor laboratory structure. The results provided important conclusions that will be commented in this section.

Initially, with the determination of the dynamic parameters of the structure it was possible to compare two different numerical models, by considering it with flexible and rigid beams. Although the rigid floor model is simplified and presents less accuracy than the flexible model, its results leaded to values significantly closed to the parameters determined with the flexible one. Moreover, this analysis also permitted to conclude that the FEMA simplified approach is reliable to determine the structure's damping factors, as it presents the same results obtained with the use of the State Space Formulation, with exception of the third vibration mode, which still showed a very approximate result.

Furthermore, the comparison of different scenarios of the damped structure allowed noticing that it can present a most efficient behavior with the installation of damping devices in the first and second floors than by installing them in the three floors. The damping factor of the structure with only two damped floors resulted slightly lower than the factor of the structure with three damped floors, as it can be considered that is not worth applying the devices on the third floor.

In chapter 5, the analysis permitted the validation of the Eurocode 8 method to determine the structure's response by using the correction factor $\eta$, as its simulations achieved values very close to the State Space Formulation, when considering different levels of damping added to the structure. Besides, through this investigation, it was possible to notice that when the structure presents a damping factor greater than 5%, the Eurocode method can be considered a more conservative alternative to determinate the response, as it presented higher medium displacements on the top of the structure. In addition, the determination of the structure response based on non-classical damping and its comparison with the assumption of classical damping allowed to confirm that a conventional modal analysis can be used to provide the seismic response of viscous damped structures.

With the free vibration tests, it was possible to confront the expected damping factors determined previously with the experimental results. This comparison resulted differently between the analyses of the three vibration modes. When evaluating the first mode, the expected factor was higher when the structure was undamped and with one damped floor, but when two floors were damped, the obtained factor exceeded the calculated one. The second vibration mode presented values lower than the expected

for the tree cases (undamped structure, one damped floor and two damped floors). Lastly, the obtained results of the third mode achieved higher results than the expected, with exception of the simulation considering the undamped structure, which presented approximate damping factors.

Finally, the seismic tests allowed evaluating the reduction of the structure's response when applying damping devices on two floors of the structure and comparing it with the undamped structure. In the numerical calculations, the use of this type of passive system control using viscous dampers permitted to decrease the maximum accelerations on the top of the structure in 30%, which is close to the experimental result of a decrease of 35%. This difference may the attributed to the existence of additional friction damping in the structural connections observed during the tests, which was not considered in the numerical simulations.

## REFERENCES

[1] Gonçalves, M. *Estimativa do amortecimento equivalente em edifícios com dissipadores viscosos.* Master Dissertation, Instituto Superior Técnico of University of Lisbon, 2017.

[2] Chaves, S. *Atenuação da Resposta Sísmica de Estruturas de Edifícios Utilizando Amortecedores Viscosos.* Master Dissertation, Faculty of Engineering of University of Porto, 2010.

[3] Moutinho, C. *Controlo de Vibrações em Estruturas de Engenharia Civil.* Doctorate Dissertation, Faculty of Engineering of University of Porto, 2007.

[4] Clough, R., Penzien, J. *Dynamics of Structures*. Computers & Structures, Berkeley, 2003.

[5] Eröz, M., White, D., DesRoches, R. *Direct Analysis and Design of Steel Frames Accounting for Partially Restrained Column Base Conditions*. Journal of Structural Engineering, September 1st 2008, 1508-1517, ASCE.

[6] Chopra, A. *Dynamics of Structures: Theory and Applications to Earthquake Engineering*. Prentice Hall, New Jersey, 1995.

[7] Falcão, J. *Análise Dinâmica Experimental do Comportamento de uma Estrutura Tridimensional de Média Dimensão em Plataforma Vibratória*. Master Dissertation, Faculty of Engineering of University of Porto, 2018.

[8] Moreira, N. *Estudo da Atenuação da Resposta Sísmica de um Pórtico Metálico Tridimensional Utilizando Sistemas Passivos*. Master Dissertation, Faculty of Engineering of University of Porto, 2016.

[9] ASCE – American Society of Civil Engineers. Seismic Rehabilitation of Existing Buildings (FEMA 356). 2000.

[10] Hwang, J. *Seismic Design of Structures with Viscous Dampers.* International Training Programs for Seismic Design of Building Structures, National Center for Research on Earthquake Engineering (NCREE), 2003.

[11] Eurocode 8: Design of structures for earthquake resistance - Part 1: General rules, seismic actions and rules for buildings (EN 1998-1). European Committee for Standardization (CEN), 2004.

[12] Barros, J. *Utilização de TMDs de Grandes Dimensões no Controlo da Resposta Dinâmica de Estruturas de Edifícios.* Master Dissertation, Faculty of Engineering of University of Porto, 2010.

[13] https://www.taylordevices.com/products/fluid-viscous-dampers/. June 2020.

[14] Sarkisian, M., Lee, P., Hu, L., Tsui, A. *Tempering Tremors.* Modern Steel Construction, February 2016, American Institute of Steel Construction, Chicago.

[15] Fitzpatrick, T., Smith, R. *Stablishing the London Millennium Bridge.* Ingenia Magazine, 2001, 18-22, Royal Academy of Engineering, London.

[16] Bachmann, H., et al. *Vibration Problems in Structures: Practical Guidelines.* Birkhauser, Basel, 1995.

[17] Murty, C., Goswami, R., Vijayanarayanan, A., Mehta, V. *Some Concepts in Earthquake Behaviour of Buildings.* Gujarat State Disaster Management Authority, Government of Gujarat,

2012.

[18] Hunaidi, O. *Traffic Vibrations in Buildings*, Construction Technology Update, No. 39, 1-6, January 2000.

[19] Svinkin, M. *Soil and Structure Vibrations from Construction and Industrial Sources*. International Conference on Case Histories in Geotechnical Engineering, 2008, Arlington.

[20] Agrawal, A., Amjadian, M. *Seismic component devices*. Innovative Bridge Design Handbook, 2016, 531-553, Elsevier, Boston.

## ANNEX

Annex 1: Damping Characterization Tests – Velocity (m/s) *versus* Force (N) graphics

Annex 2: Damping Characterization Tests – Displacement (mm) *versus* Force (N) graphics

Annex 3: Seism Tests Results – Time (s) *versus* Acceleration ($m/s^2$) graphics

Annex 4: Calculus Procedure for the Response Determination of a 1-DOF Structure with a Variable Damping Natural Factor

Annex 5: Calculus Procedure for the Response Determination of a 3-DOF Structure with a Variable Extra Damping Coefficient

Annex 6: Calculus Procedure for the "Conversion" of a Non-Classical Damping Matrix to a Classical Damping Matrix and Respective Response Determination

## ANNEX 1: DAMPING CHARACTERIZATION TESTS – VELOCITY (M/S – HORIZONTAL AXIS) VERSUS FORCE (N – VERTICAL AXIS) GRAPHICS

DAMPING DEVICE 19-5 – FREQUENCY: 2.5 HZ

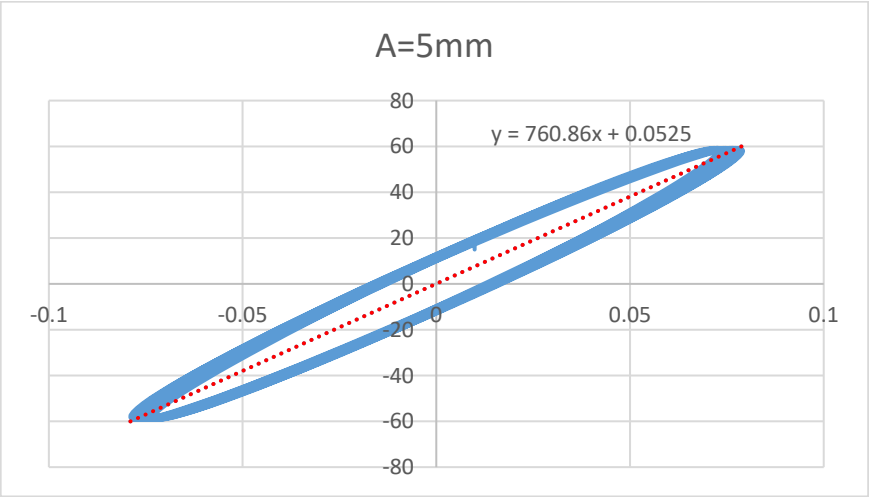


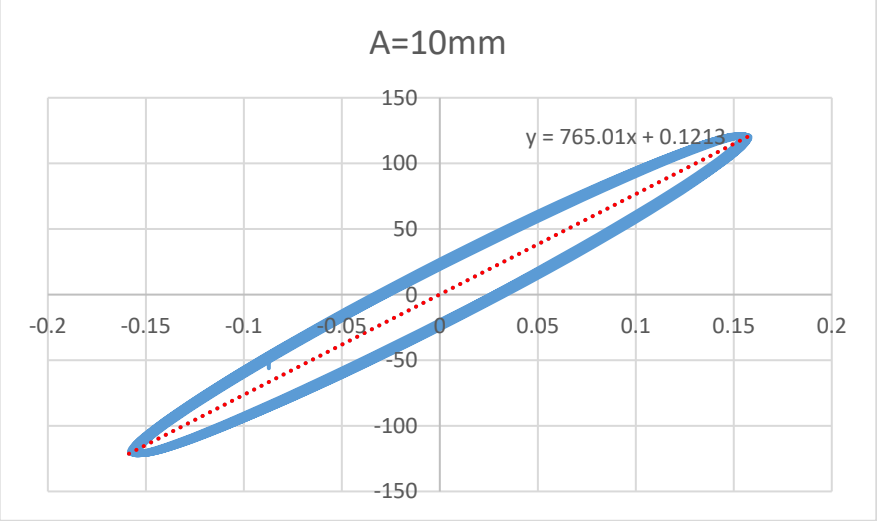

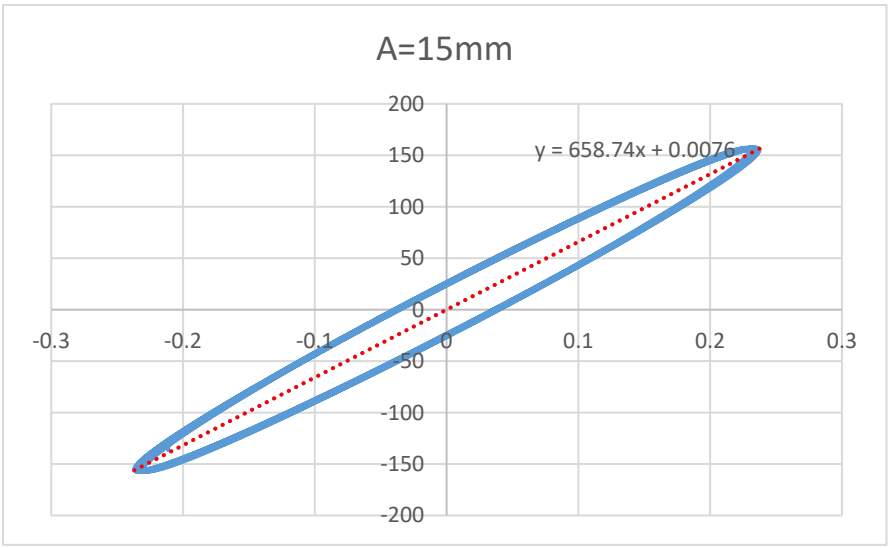
A=15mm
y = 658.74x + 0.0076
200
150
100
50
0
-50
-100
-150
-200
-0.3
-0.2
-0.1
0
0.1
0.2
0.3

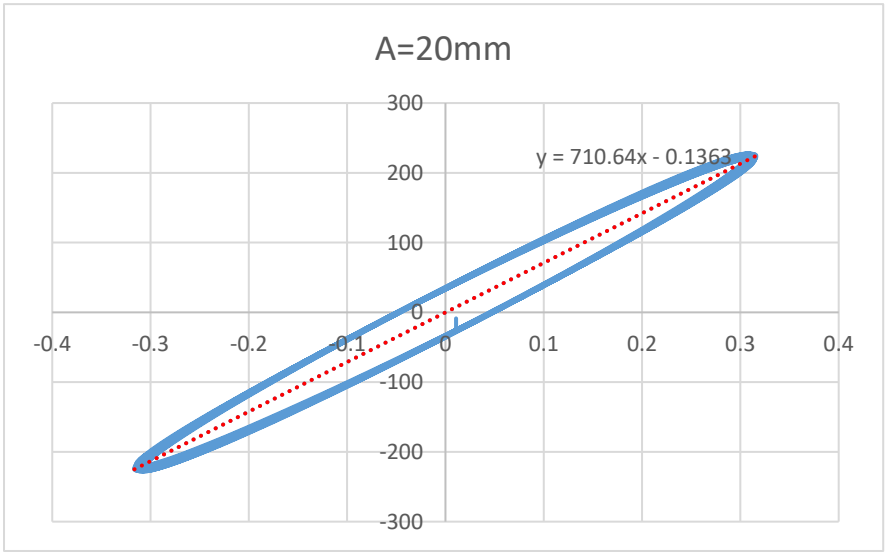
A=20mm
y = 710.64x - 0.1363
300
200
100
0
-100
-200
-300
-0.4
-0.3
-0.2
-0.1
0
0.1
0.2
0.3
0.4

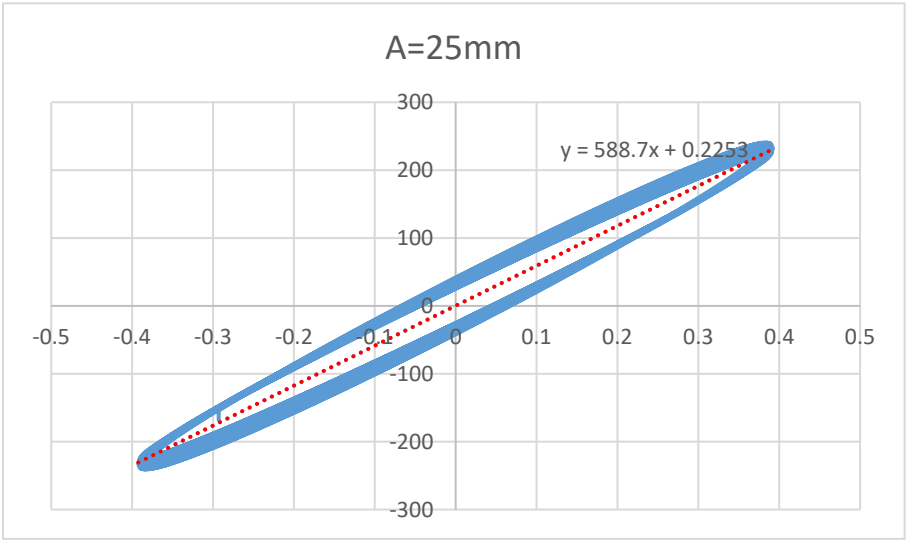
A=25mm
y = 588.7x + 0.2253
300
200
100
0
-100
-200
-300
-0.5
-0.4
-0.3
-0.2
-0.1
0
0.1
0.2
0.3
0.4
0.5

| Amplitude of motion (mm) | Damping Coefficient Obtained (N.s/m) | Medium Damping Coefficient (N.s/m) |
|---|---|---|
| 5.0 | 760.86 | 696.79 |
| 10.0 | 765.01 | |
| 15.0 | 658.74 | |
| 20.0 | 710.64 | |
| 25.0 | 588.70 | |

DAMPING DEVICE 20-5 – FREQUENCY: 2.5 HZ

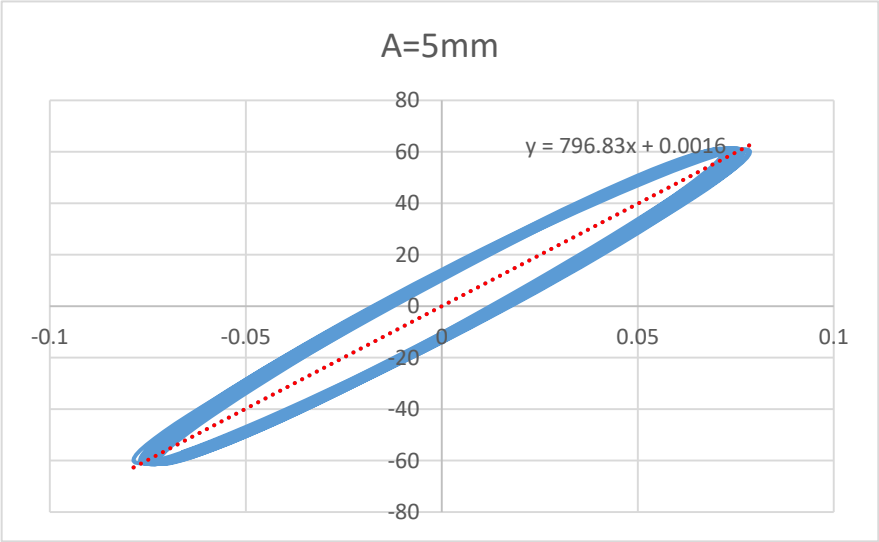


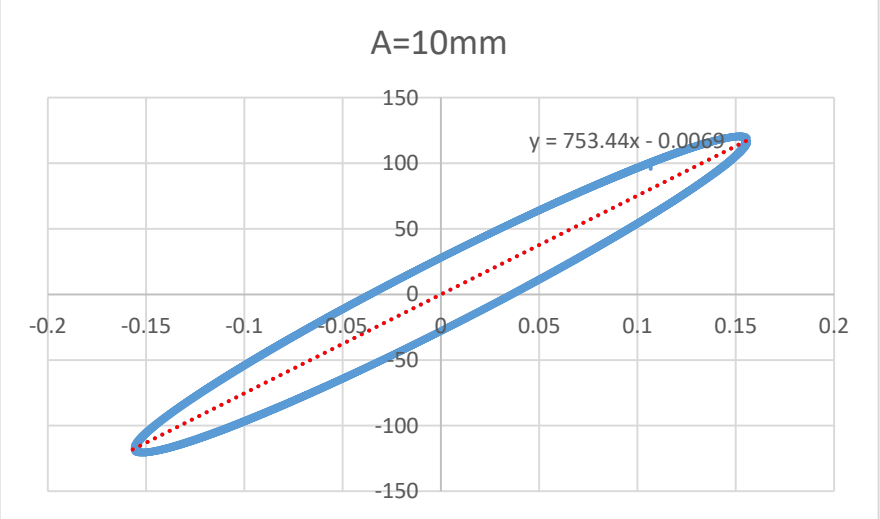

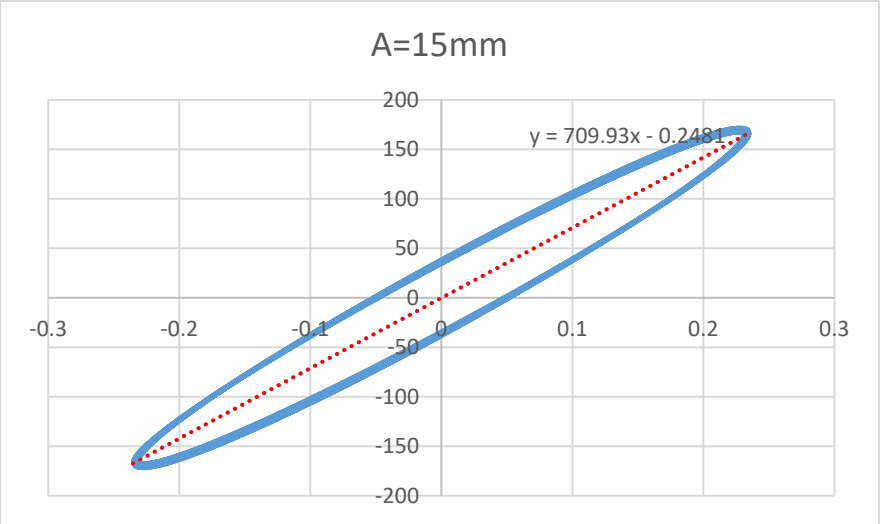


| Amplitude of motion (mm) | Damping Coefficient Obtained (N.s/m) | Medium Damping Coefficient (N.s/m) |
|---|---|---|
| 5.0 | 796.83 | 753.40 |
| 10.0 | 753.44 | |
| 15.0 | 709.93 | |

DAMPING DEVICE 25-30 – FREQUENCY: 2.5 HZ

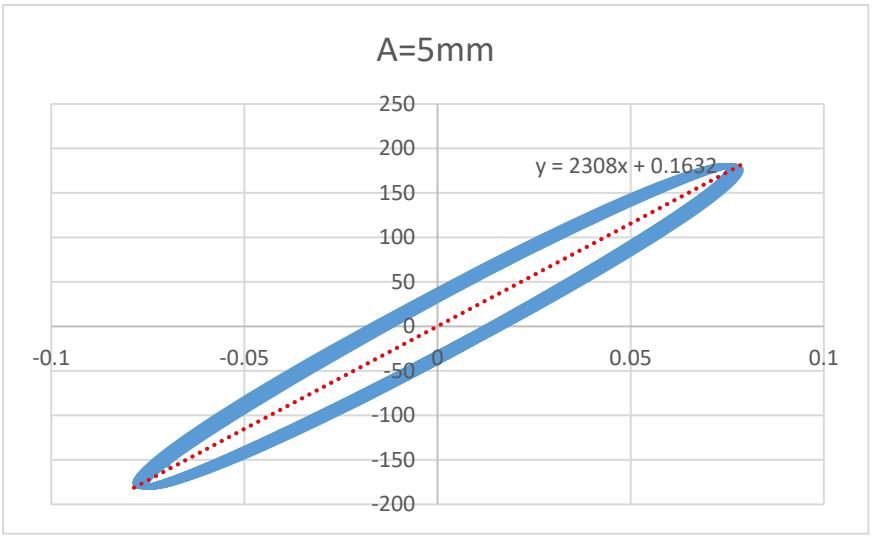

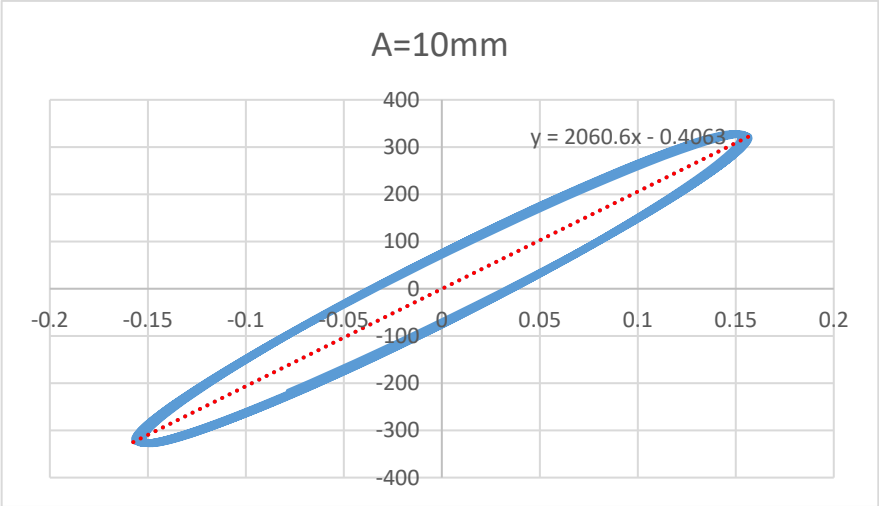
A=10mm
y = 2060.6x - 0.4063
400
300
200
100
0
-100
-200
-300
-400
-0.2
-0.15
-0.1
-0.05
0
0.05
0.1
0.15
0.2

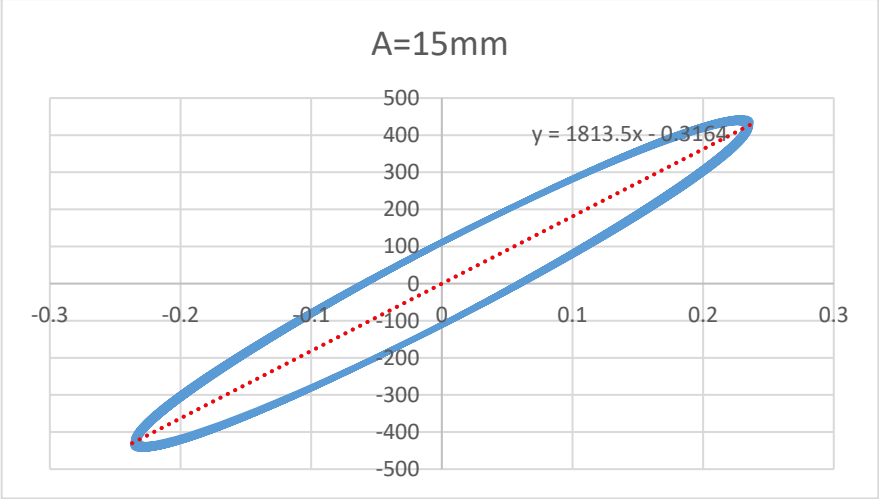
A=15mm
y = 1813.5x - 0.3164
500
400
300
200
100
0
-100
-200
-300
-400
-500
-0.3
-0.2
-0.1
0
0.1
0.2
0.3

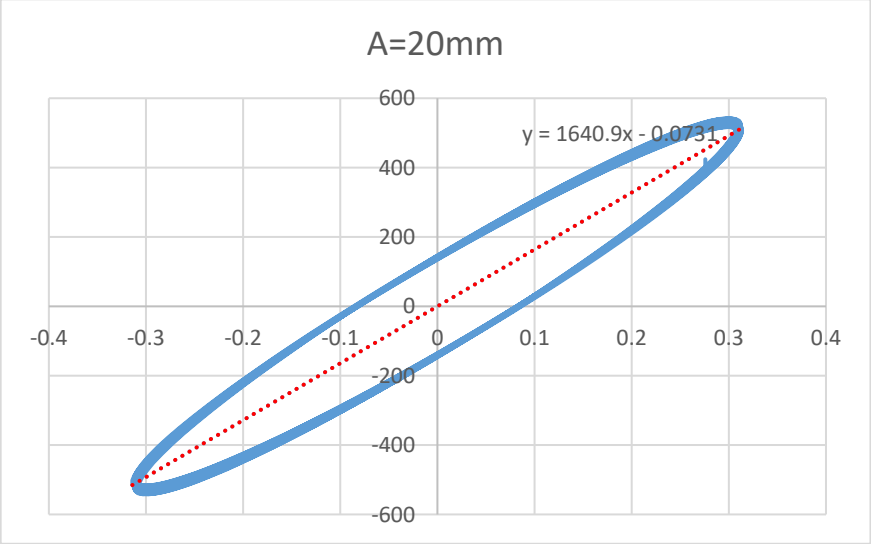
A=20mm
y = 1640.9x - 0.0731
600
400
200
0
-200
-400
-600
-0.4
-0.3
-0.2
-0.1
0
0.1
0.2
0.3
0.4

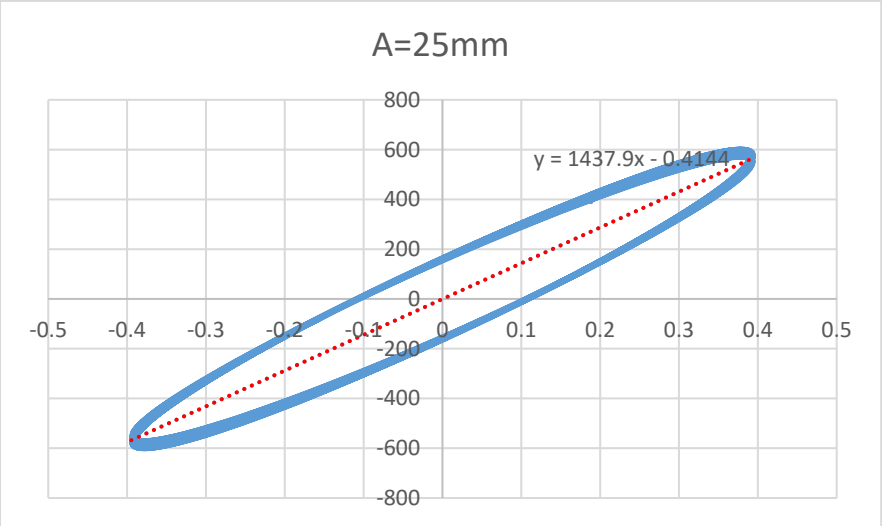


| Amplitude of motion (mm) | Damping Coefficient Obtained (N.s/m) | Medium Damping Coefficient (N.s/m) |
|---|---|---|
| 5.0 | 2308.00 | 1852.18 |
| 10.0 | 2060.60 | |
| 15.0 | 1813.50 | |
| 20.0 | 1640.90 | |
| 25.0 | 1437.90 | |

## ANNEX 2: DAMPING CHARACTERIZATION TESTS – DISPLACEMENT (MM – HORIZONTAL AXIS) VERSUS FORCE (N – VERTICAL AXIS) GRAPHICS

DAMPING DEVICE 19-5 – FREQUENCY: 2.5 HZ

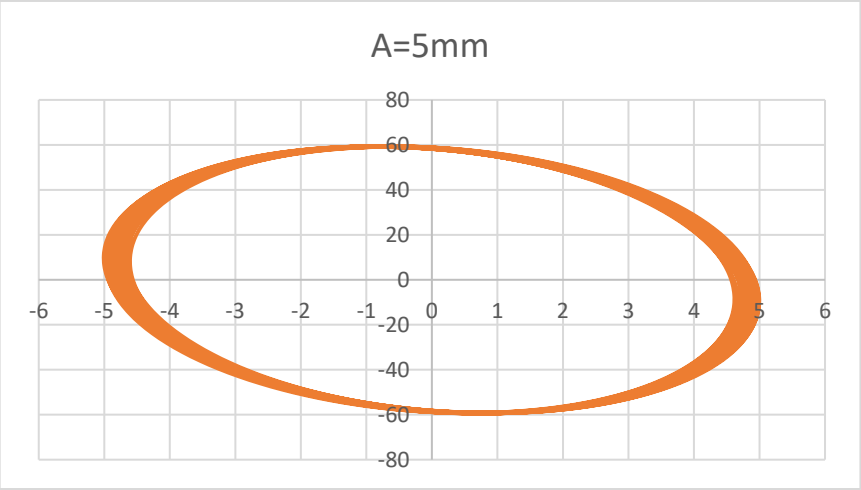


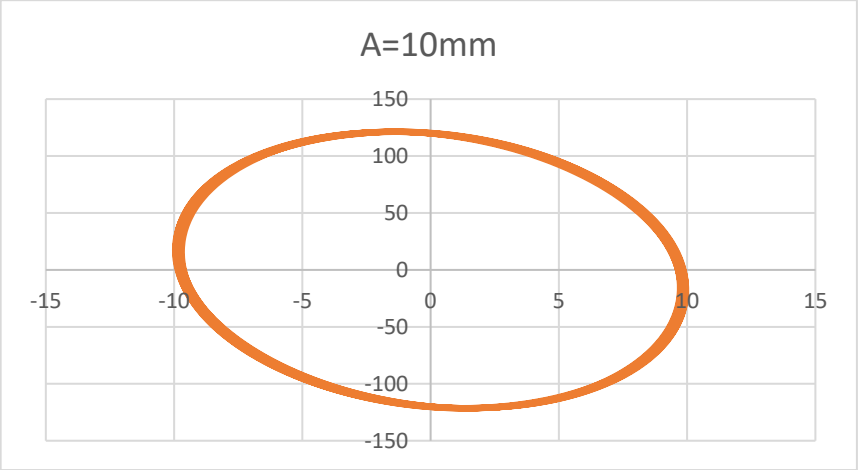


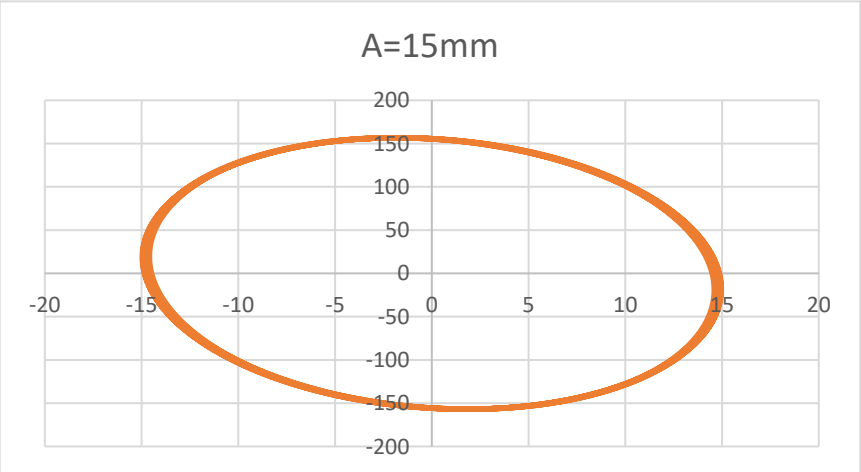

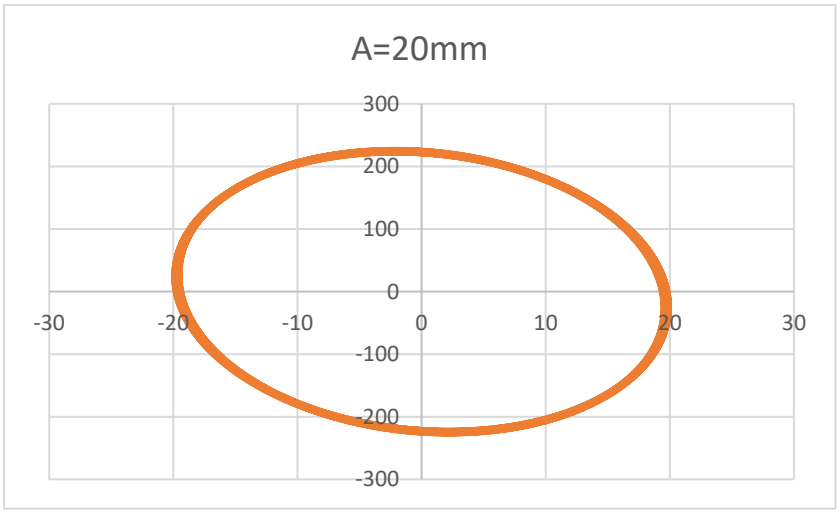


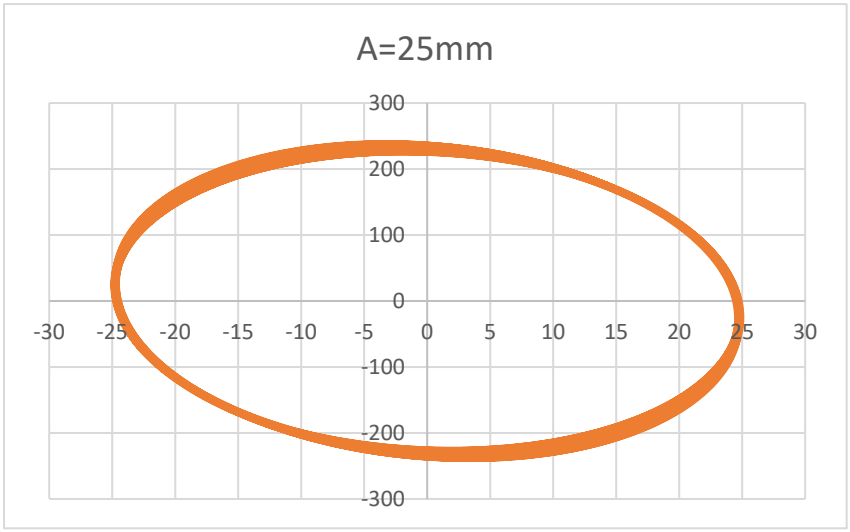


DAMPING DEVICE 20-5 – FREQUENCY: 2.5 HZ

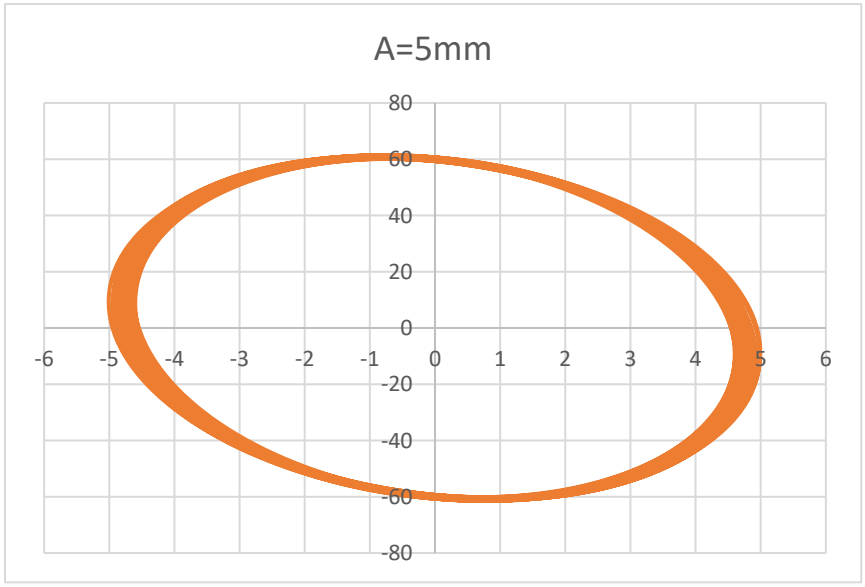

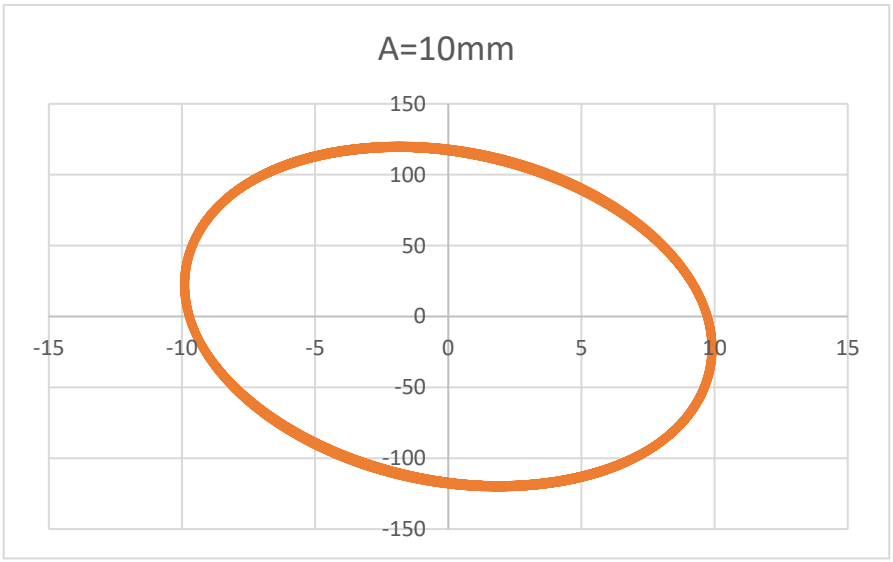


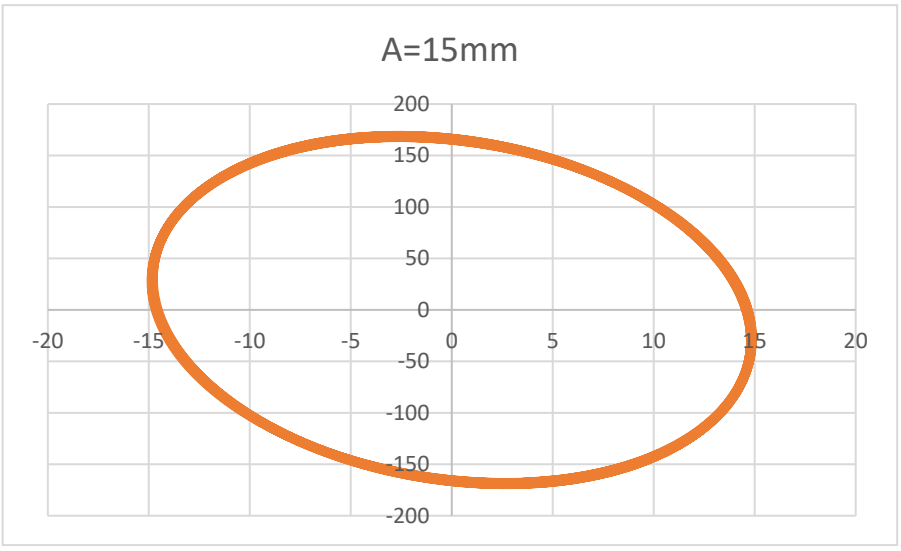


DAMPING DEVICE 25-30 – FREQUENCY: 2.5 HZ

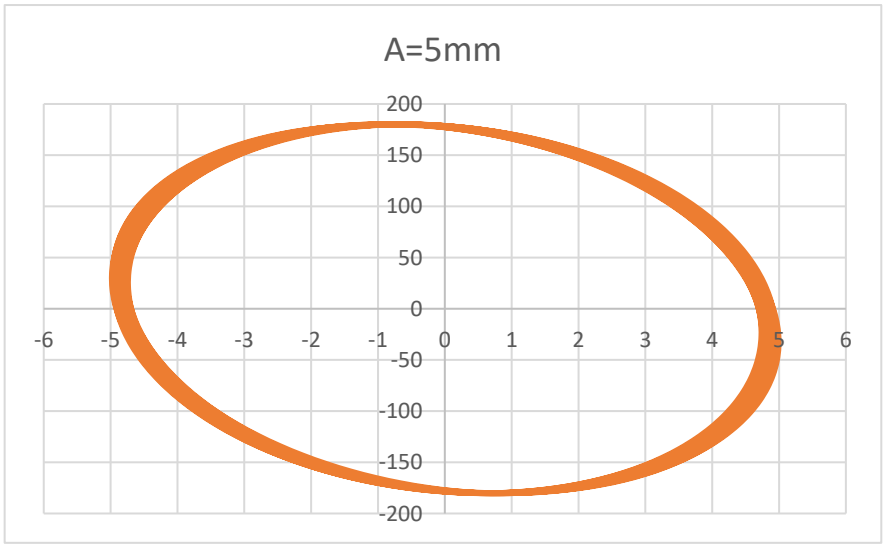

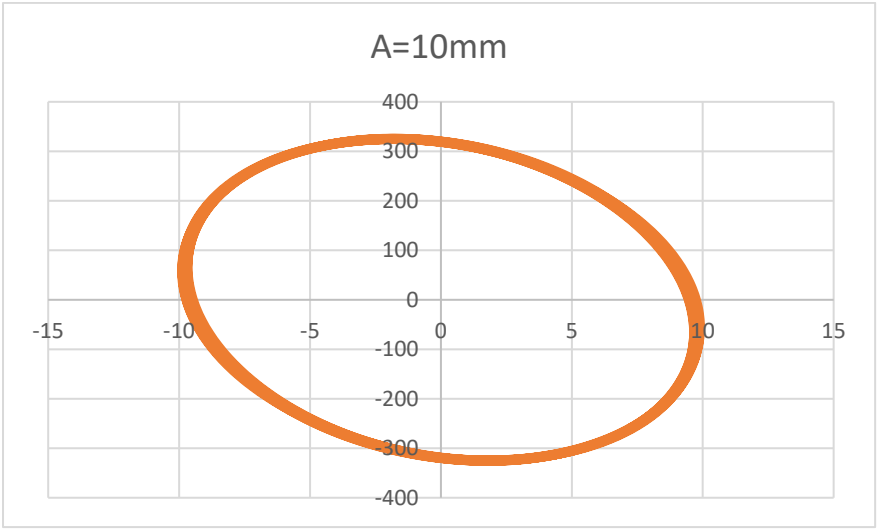
A=10mm
400
300
200
100
0
-100
-200
-300
-400
-15
-10
-5
0
5
10
15

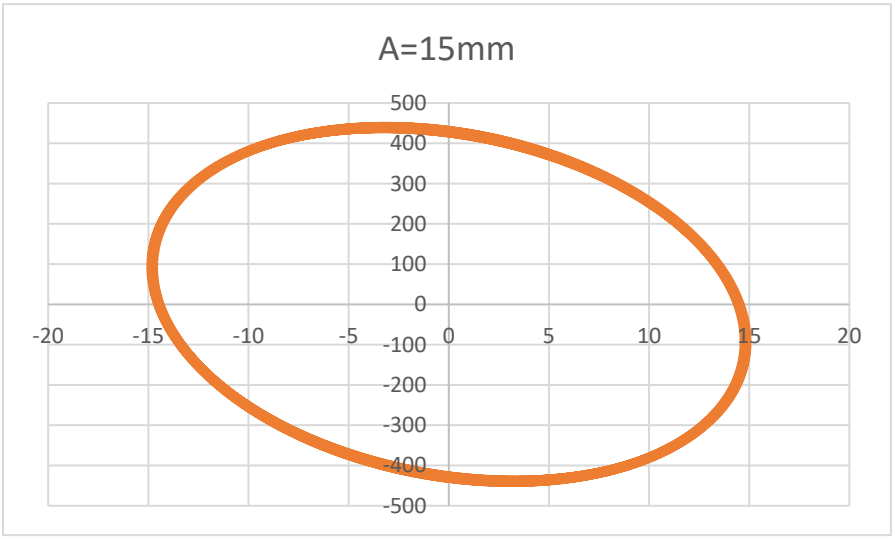
A=15mm
500
400
300
200
100
0
-100
-200
-300
-400
-500
-20
-15
-10
-5
0
5
10
15
20

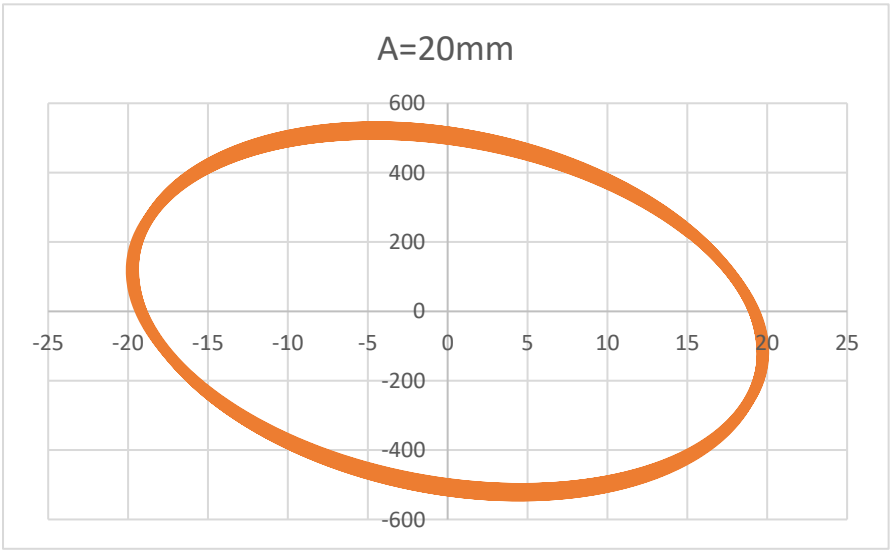
A=20mm
600
400
200
0
-200
-400
-600
-25
-20
-15
-10
-5
0
5
10
15
20
25

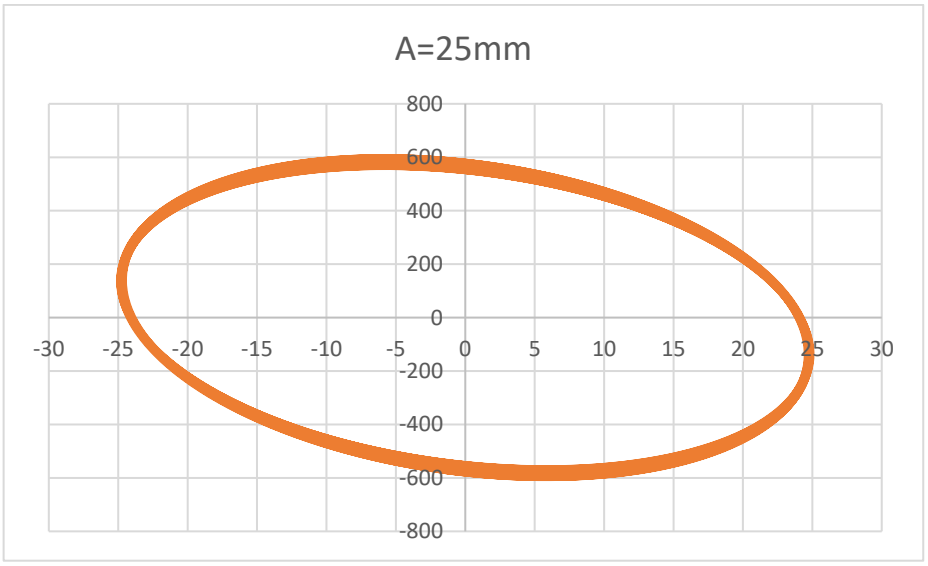
A=25mm
800
600
400
200
0
-200
-400
-600
-800
-30
-25
-20
-15
-10
-5
0
5
10
15
20
25
30

## ANNEX 3: SEISM TESTS RESULTS – TIME (S – HORIZONTAL AXIS) VERSUS ACCELERATION (M/S² - VERTICAL AXIS) GRAPHICS

SEISM 2

State Space Formulation

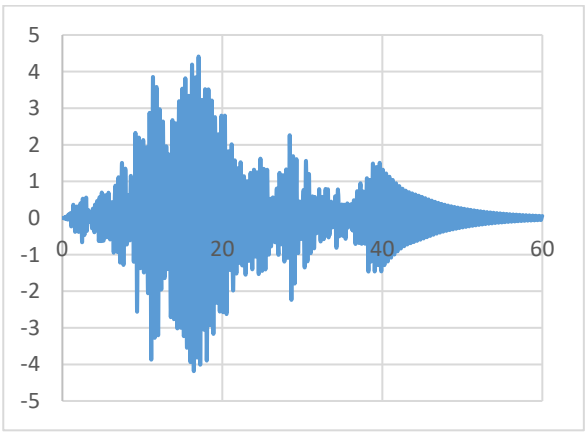


Un-damped structure

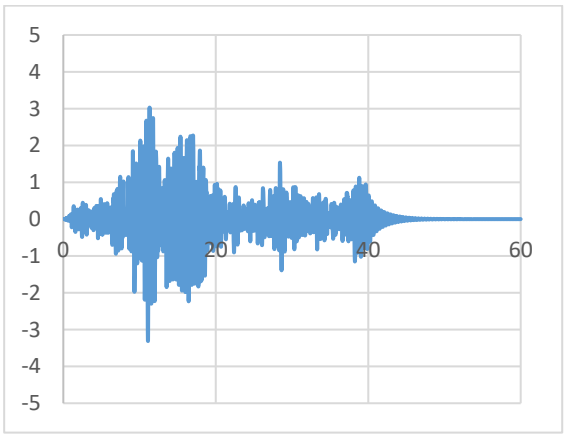


Damped structure

Simulation Tests

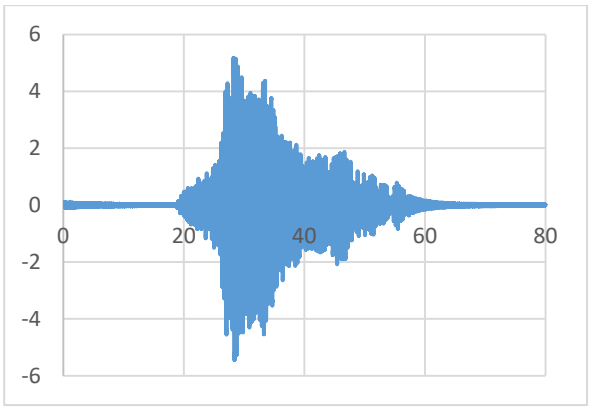


Un-damped structure

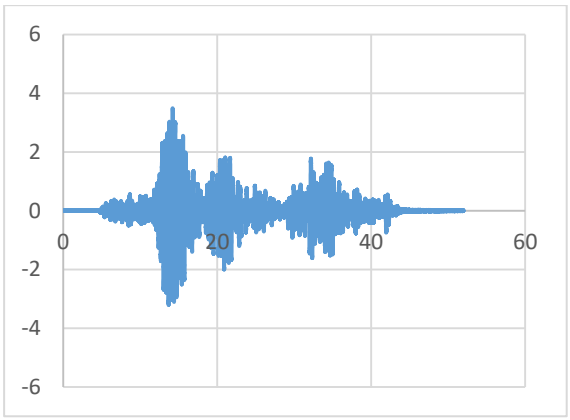


Damped structure

SEISM 3

State Space Formulation

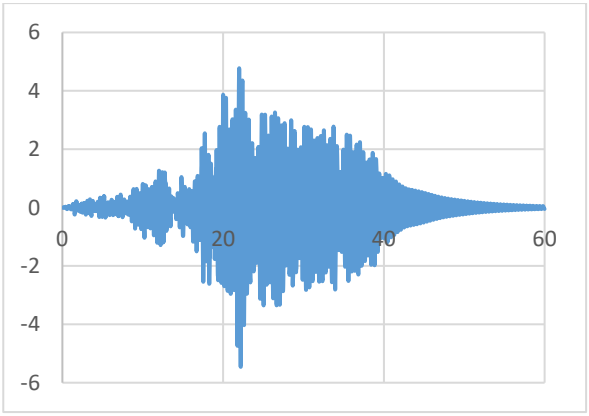


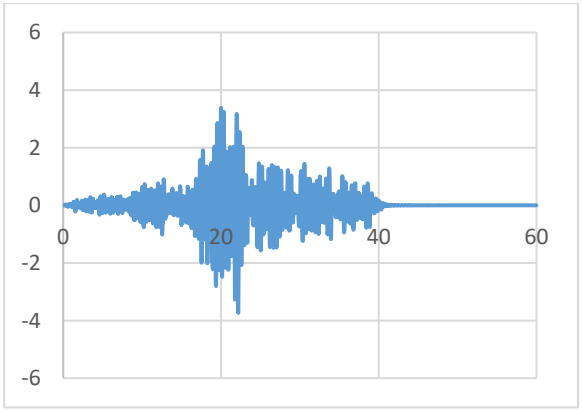

Un-damped structure

Damped structure

Simulation Tests

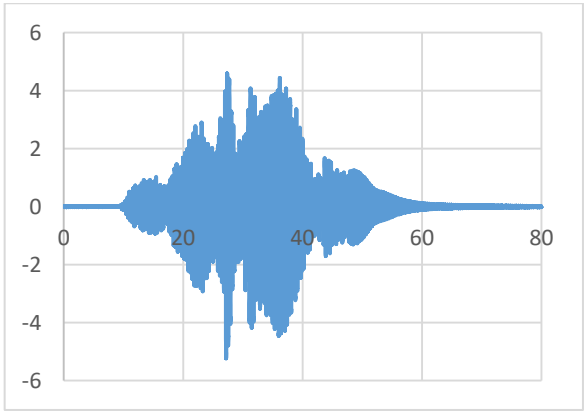


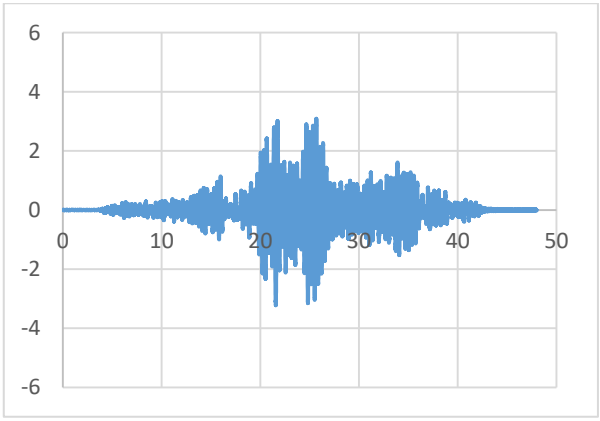


Un-damped structure

Damped structure

SEISM 4

State Space Formulation

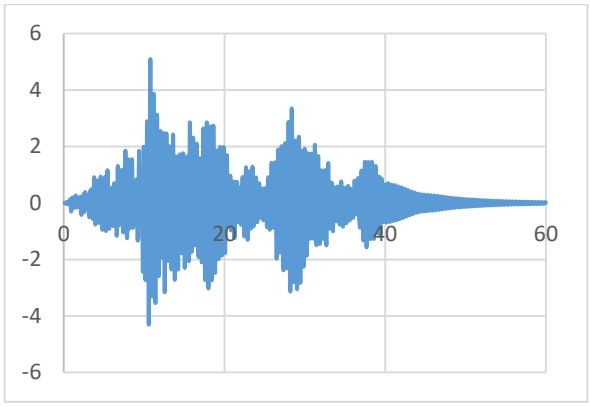


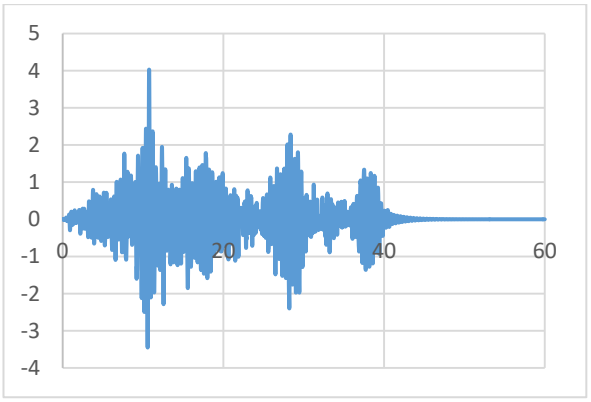


Un-damped structure

Damped structure

Simulation Tests

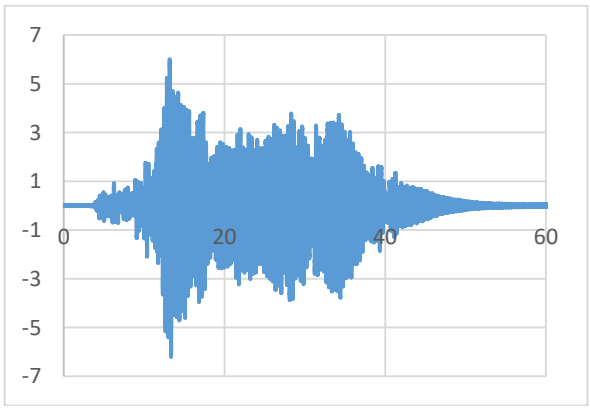


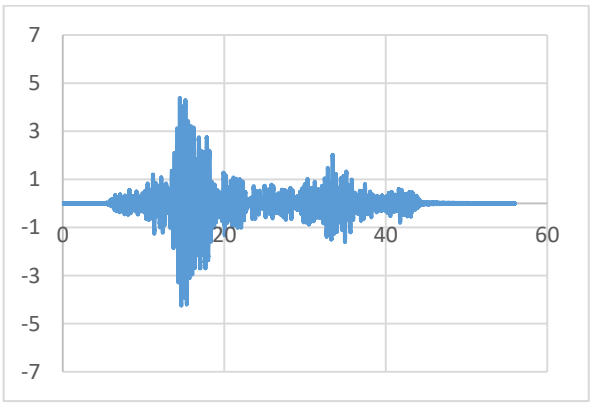


Un-damped structure

Damped structure

SEISM 5

State Space Formulation

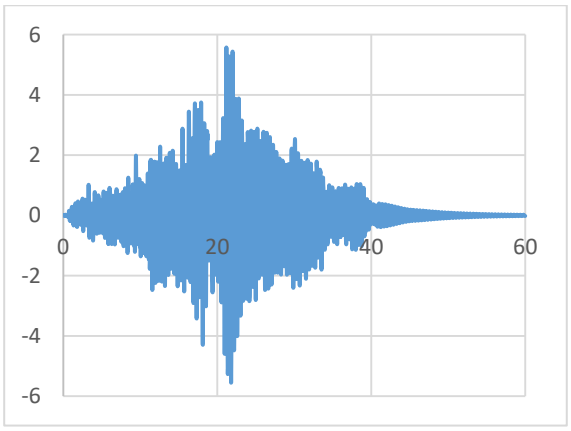


Un-damped structure

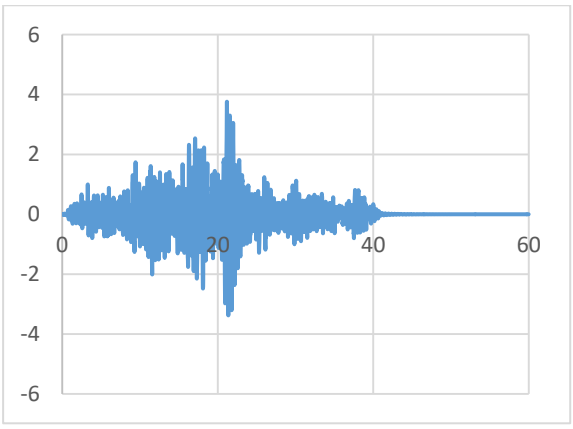


Damped structure

Simulation Tests

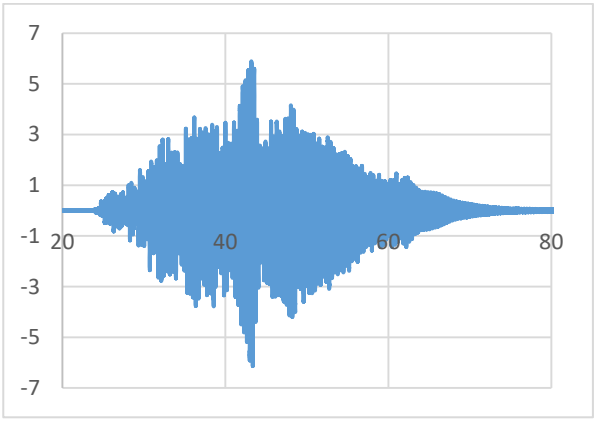


Un-damped structure

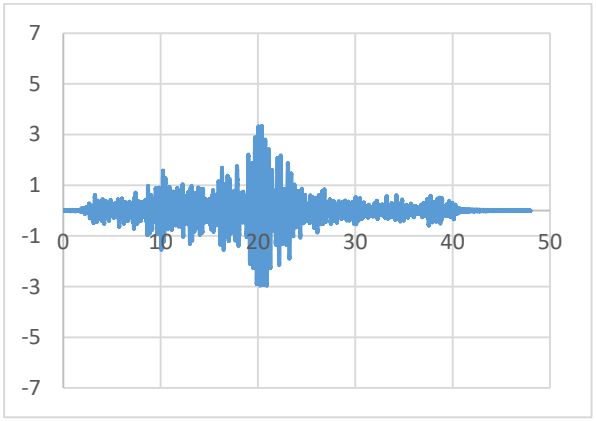


Damped structure

SEISM 6

State Space Formulation

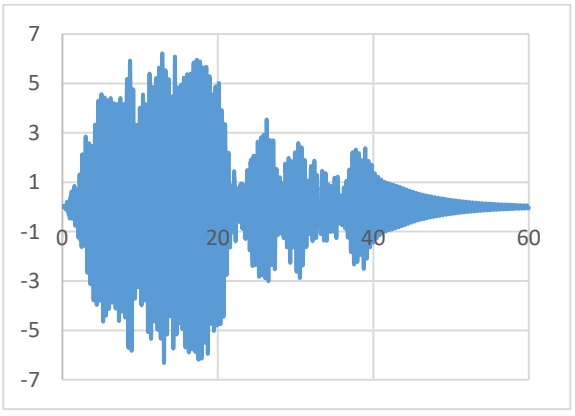


Un-damped structure

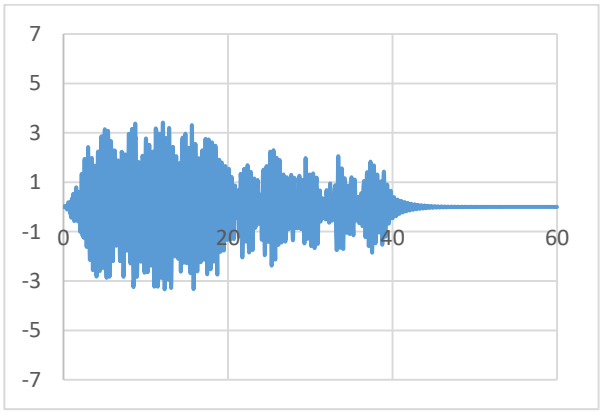


Damped structure

Simulation Tests

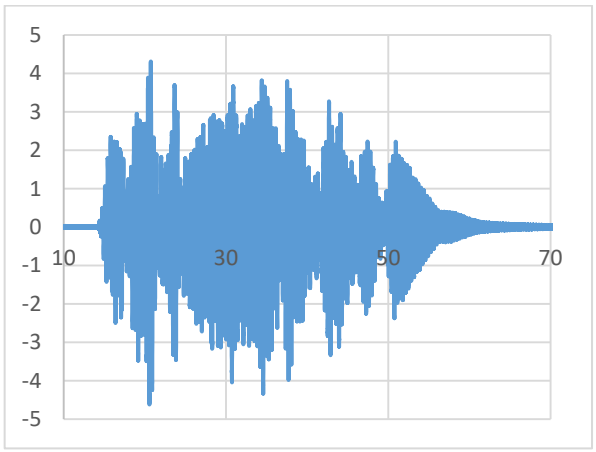


Un-damped structure

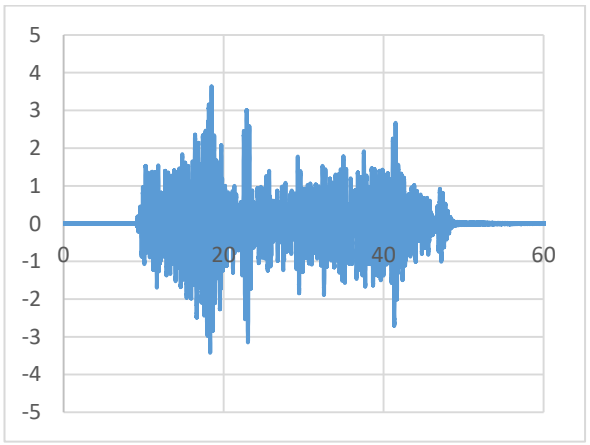


Damped structure

SEISM 7

State Space Formulation

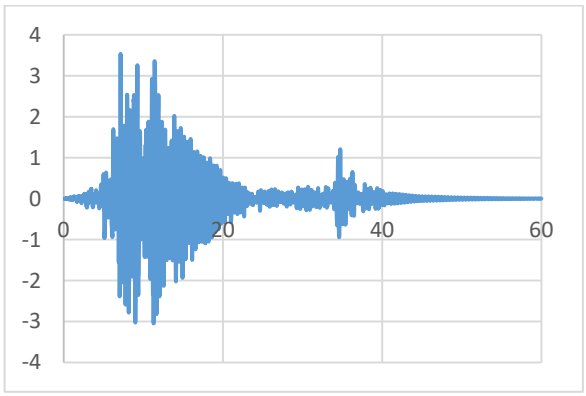


Un-damped structure

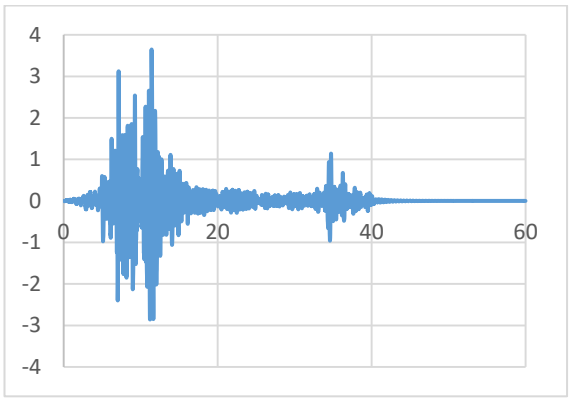


Damped structure

Simulation Tests

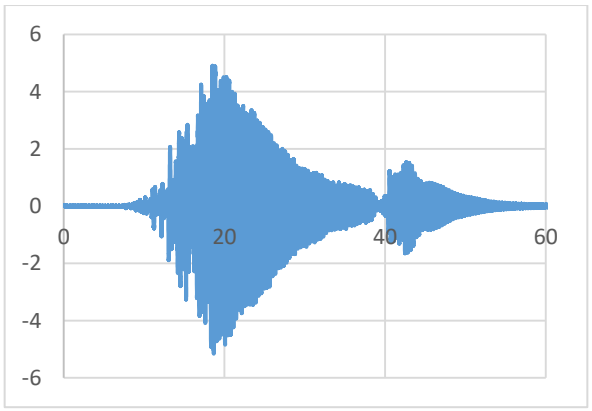


Un-damped structure

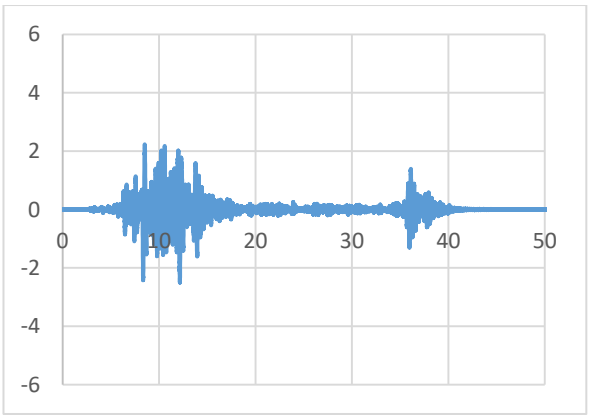


Damped structure

SEISM 8

State Space Formulation

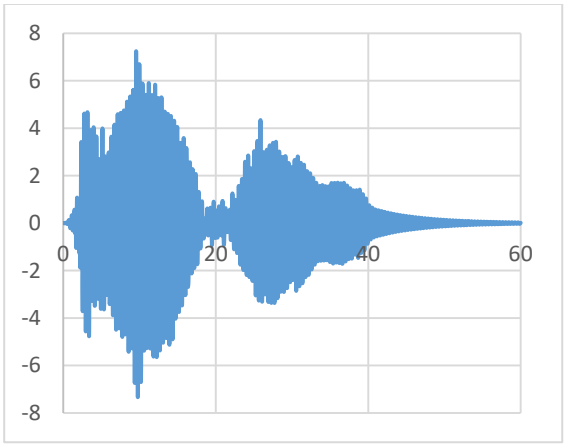


Un-damped structure

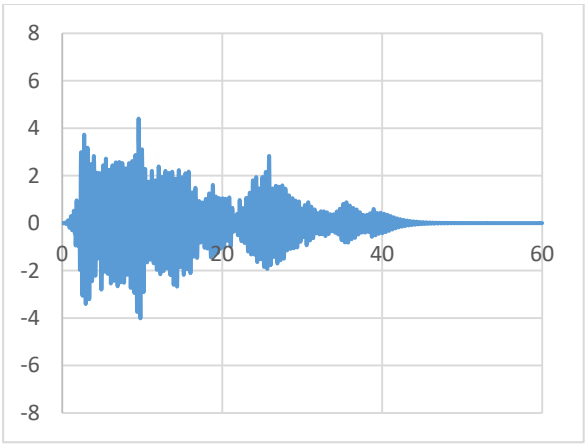


Damped structure

Simulation Tests

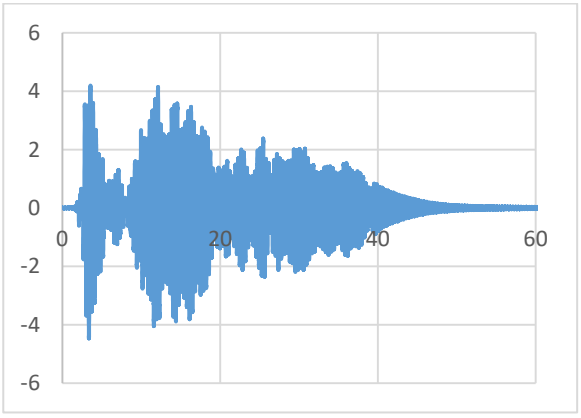


Un-damped structure

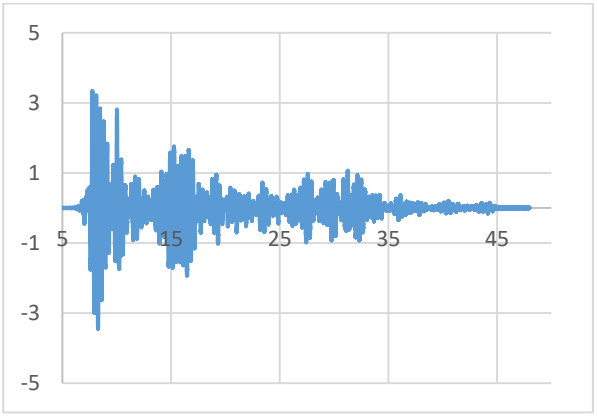


Damped structure

SEISM 9

State Space Formulation

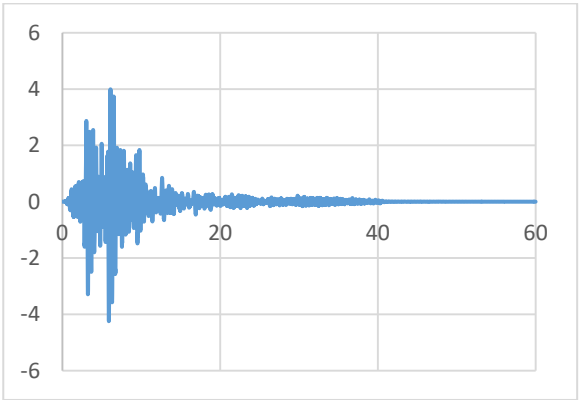


Un-damped structure

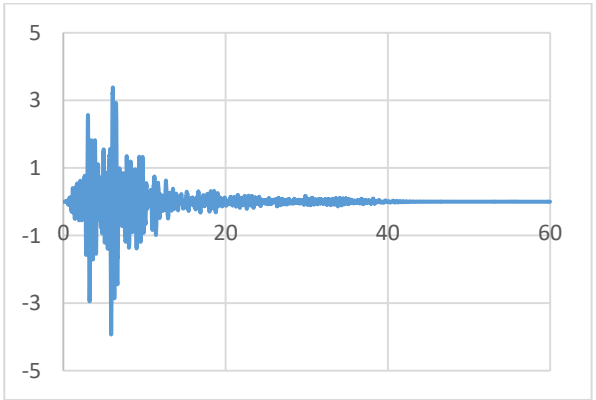


Damped structure

Simulation Tests

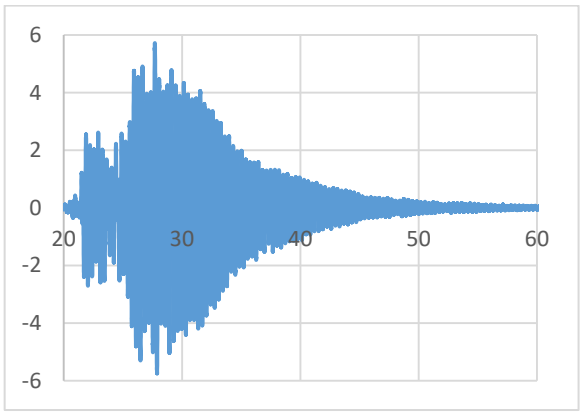


Un-damped structure

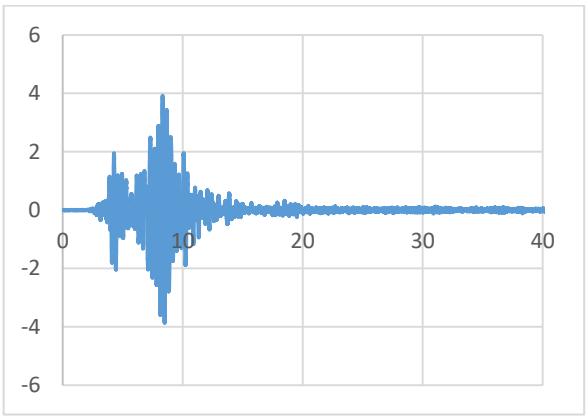


Damped structure

SEISM 10

State Space Formulation

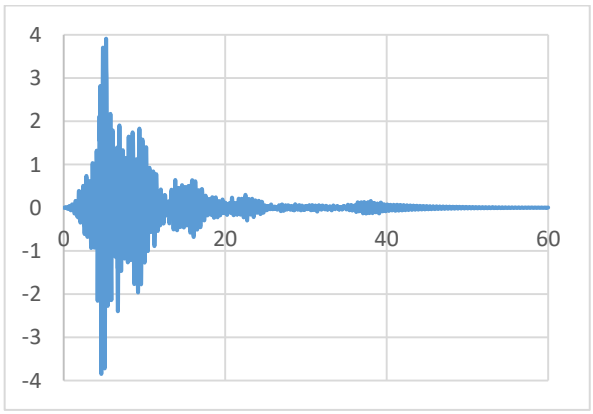


Un-damped structure

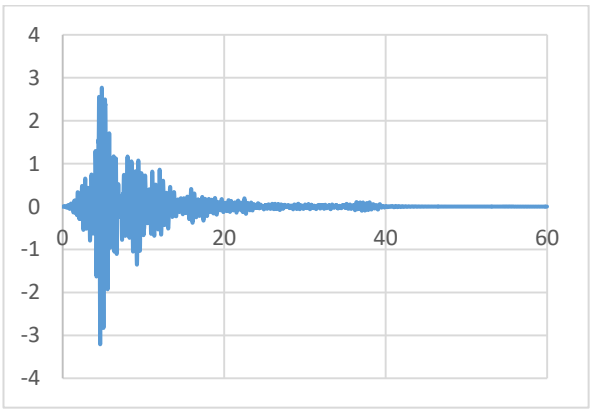


Damped structure

Simulation Tests

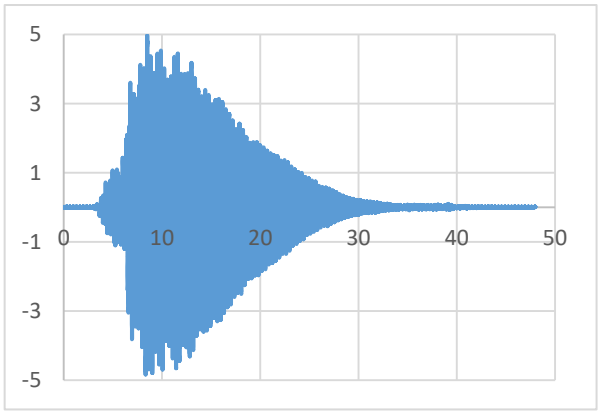


Un-damped structure

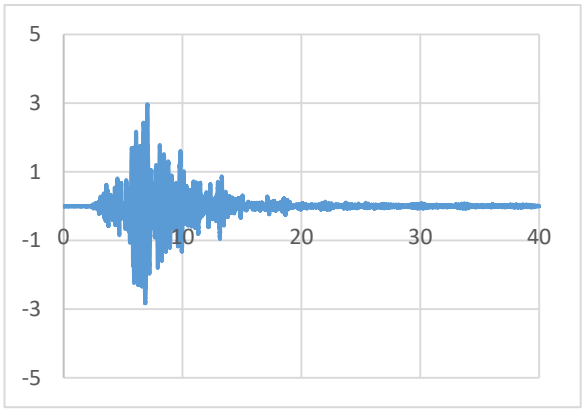


Damped structure

## ANNEX 4: CALCULUS PROCEDURE FOR THE RESPONSE DETERMINATION OF A 1-DOF STRUCTURE WITH A VARIABLE DAMPING NATURAL FACTOR

```
% 1 Degree of Freedom Model Response
% Natural Damping Variation
clear
%%% Initial data %%%
dt=0.01;    % time discretization
ngl=1;      % number of DOF
%%% Structure Data %%%
m1=1;
M=[m1]; % Mass Matrix
k=1000; % Stiffness of 1 floor
K=[k]; % Stiffness Matrix
O=K-K; % Null Matrix
I=K^0; % Identity Matrix
AM=O; %Null Damping Matrix
A=[O I ;-M^-1*K -M^-1*AM]; % State Matrix
[V,D]=eig(A);
Dd=abs(D);

for amortecimento=1:30 %Natural Damping Factor
for ns=1:10 % Seism order number
clear x;

AE=amortecimento*0.01;
c1=2*AE*m1*Dd(1,1);
C=[c1]; %Modal Damping Matrix

A1=[O I ;-M^-1*K -M^-1*C];  % State Matrix with not null damping
B=[0;M^-1*I]; %Input Matrix
E=expm(dt*A1);
II=[I O; O I];
G=A1^-1*(E-II)*B;

%%% Dynamic Action %%%
load sismo.dat
[dy,dx]=size(sismo);
t=(0:dt:(dy-1)*dt);
u(1,:)=(sismo(:,ns)*m1)'; % Seismic force at the first floor
x(ngl*2,1)=0; % Initial Condition of the State Vector

%%% Response Calculation
for i=1:(dy-1)
    x(:,i+1)= E*x(:,i)+G*u(:,i);
end
x=x';

result(amortecimento,ns)=max(abs(x(:,1)));

end
end

for amortecimento=1:30
media(amortecimento,1)=mean(result(amortecimento,1:10));
```

```
end
```

## ANNEX 5: CALCULUS PROCEDURE FOR THE RESPONSE DETERMINATION OF A 3-DOF STRUCTURE WITH A VARIABLE EXTRA DAMPING COEFFICIENT

```
% 3 Degrees of Freedom Model Response
% Force and acceleration analysis
clear
%%% Initial data %%%
dt=0.01;    % time discretization
ngl=3;      % number of DOF

%%% Structure data %%%
m1=1.055;
m2=1.055;
m3=1.055;
M=[m1 0 0; 0 m2 0; 0 0 m3]; % Mass Matrix
K=[3068.9 -1592.54 115.98; -1592.56 2928.94 -1457.24; 115.98 -1457.24
1346.16]; % Stiffness Matrix (flexible beams model)
O=K-K; % Null Matrix
I=K^0; % Identity Matrix
B=[0 0 0 1/m1 0 0; 0 0 0 0 1/m2 0; 0 0 0 0 0 1/m3]'; %Input Matrix
II=[I O; O I];
load sismo.dat
[dy,dx]=size(sismo);

for c=1:40 % Extra Damping Coefficient
  for ns=1:10 % Seism order number
    clear x;

AM=[2*c -c 0; -c 2*c -c; 0 -c c];
A=[O I ;-M^-1*K -M^-1*AM]; % State Matrix (Non-Classical Damping)
[V,D]=eig(A);
E=expm(dt*A);
G=A^-1*(E-II)*B;

%%% Dynamic Action %%%
t=(0:dt:(dy-1)*dt);
u(1,:)=(sismo(:,ns)*m1)'; % Seismic force at the first floor
u(2,:)=(sismo(:,ns)*m2)'; % % Seismic force at the second floor
u(3,:)=(sismo(:,ns)*m3)'; % % Seismic force at the third floor
x(ngl*2,1)=0; % Initial Condition of the State Vector

%%% Response Calculation
for i=1:(dy-1)
    x(:,i+1)= E*x(:,i)+G*u(:,i);
end
x=x';
result(c,ns)=max(abs(x(:,3)));

% Extra Damping Factor
FA1(c)=100*(-real(D(5,5))/((real(D(5,5)))^2+(imag(D(5,5)))^2)^0.5);
FA2(c)=100*(-real(D(3,3))/((real(D(3,3)))^2+(imag(D(3,3)))^2)^0.5);
FA3(c)=100*(-real(D(1,1))/((real(D(1,1)))^2+(imag(D(1,1)))^2)^0.5);

end
end
```

```
for c=1:20
media(c,1)=mean(result(c,1:10));
end
```

## ANNEX 6: CALCULUS PROCEDURE FOR THE "CONVERSION" OF A NON-CLASSICAL DAMPING MATRIX TO A CLASSICAL DAMPING MATRIX AND RESPECTIVE RESPONSE DETERMINATION

```
% 3 Degrees of Freedom Model Response
% Force and acceleration analysis
clear
%%% Initial data %%%
dt=0.01;    % time discretization
ngl=3;      % number of DOF

%%% Structure data %%%
m1=1.055;
m2=1.055;
m3=1.055;
M=[m1 0 0; 0 m2 0; 0 0 m3]; % Mass Matrix
K=[3068.9 -1592.54 115.98; -1592.56 2928.94 -1457.24; 115.98 -1457.24
1346.16]; % Stiffness Matrix (flexible beams model)
O=K-K; % Null Matrix
I=K^0; % Identity Matrix
B=[0 0 0 1/m1 0 0; 0 0 0 0 1/m2 0; 0 0 0 0 0 1/m3]'; %Input Matrix
II=[I O; O I];
load sismo.dat
[dy,dx]=size(sismo);

for c=1:40 % Extra Damping Coefficient
  for ns=1:10 % Seism order number
    clear x;

AM=[2*c -c 0; -c 2*c -c; 0 -c c];
A=[O I ;-M^-1*K -M^-1*AM]; % State Matrix (Non-Classical Damping)
[V,D]=eig(A);

% Extra Damping Factor and Damped Frequency
FA1(c)=(-real(D(5,5))/((real(D(5,5)))^2+(imag(D(5,5)))^2)^0.5);
FA2(c)=(-real(D(3,3))/((real(D(3,3)))^2+(imag(D(3,3)))^2)^0.5);
FA3(c)=(-real(D(1,1))/((real(D(1,1)))^2+(imag(D(1,1)))^2)^0.5);
w1(c)=((imag(D(5,5)))^2+(real(D(5,5)))^2)^0.5;
w2(c)=((imag(D(3,3)))^2+(real(D(3,3)))^2)^0.5;
w3(c)=((imag(D(1,1)))^2+(real(D(1,1)))^2)^0.5;

%%% Dynamic Action %%%

% Rayleigh Method
alpha(c)=-2*(FA1(c)*w2(c)-FA2(c)*w1(c))*w1(c)*w2(c)/(w1(c)^2-w2(c)^2);
beta(c)=-2*(FA1(c)*w1(c)-FA2(c)*w2(c))/((w2(c)^2)*(1-(w1(c)/w2(c))^2));
Cc=alpha(c)*M+beta(c)*K;
Ac=[O I ;-M^-1*K -M^-1*Cc]; % State Matrix (Classical Damping)
[Vc,Dc]=eig(Ac);
Ec=expm(dt*Ac);
Gc=Ac^-1*(Ec-II)*B;

t=(0:dt:(dy-1)*dt);
u(1,:)=(sismo(:,ns)*m1)'; % Seismic force at the first floor
u(2,:)=(sismo(:,ns)*m2)'; % % Seismic force at the second floor
u(3,:)=(sismo(:,ns)*m3)'; % % Seismic force at the third floor
x(ngl*2,1)=0; % Initial Condition of the State Vector
```

```
%%% Response Calculation
for i=1:(dy-1)
    x(:,i+1)= Ec*x(:,i)+Gc*u(:,i);
end
x=x';

result(c,ns)=max(abs(x(:,3)));


end
end

for c=1:40
media(c,1)=mean(result(c,1:10));

end
```